INTERFACIAL POLARIZATION IN MEMBRANES

AND ITS SIGNIFICANCE IN THE INDUCED

POLARIZATION OF GEOLOGIC MATERIALS

by

DONALD JAMES MARSHALL

S.B., Massachusetts Institute of Technology

(1954)

M.S., California Institute of Technology

(1955)

SUBMITTED IN PARTIAL FULFILLMENT
OF THE REQUIREMENTS FOR THE
DEGREE OF DOCTOR OF
PHILOSOPHY

at the

MASSACHUSETTS INSTITUTE OF TECHNOLOGY

June, 1959

Signature of Author_____
Department of Geology and Geophysics
May 20, 1959

Certified by...
Thesis Supervisor

Accepted by...
Chairman, Departmental Committee
on Graduate Students

TABLE OF CONTENTS

ABSTRACT

Title: Interfacial Polarization in Membranes and its Significance in the Induced Polarization of Geologic Materials.

Author: Donald James Marshall

Submitted in partial fulfillment of the requirements for the degree of Doctor of Philosophy at Massachusetts Institute of Technology

An investigation of the possible causes of background effects in the induced polarization method of geophysical prospecting has led us to the conclusion that the most important ones are electromagnetic coupling effects and polarization in materials other than the metallic conductors. This thesis is concerned with polarization in clay type materials.

Using the methods of steady state thermodynamics an analysis is made of the polarization effects due to electro-osmotic coupling, thermoelectric coupling and diffusion coupling. This analysis yields an expression for the maximum polarization effects due to each type of coupling, in terms of measurable parameters of the material. When the expressions are evaluated using values for these parameters, typical of geologic materials, it is found that diffusion coupling only is important.

In order to determine more about diffusion coupling polarization, in particular its time dependence, a kinetic model is introduced. The solution of the equations describing this model leads to an impedance behaviour which can account for a 100% frequency effect. The frequency dependence of the impedance is similar to that of a Warburg impedance which is typical of diffusion controlled reactions at metal electrodes.

Experimental investigations of the polarization effects in clays and ion exchange resins indicate that there are appreciable effects in these materials and, while the comparison with the theoretical results is not ideal, there is good correspondence between them.

Studies were made on natural rock samples also. Great difficulty was experienced, however, because of the presence of minor amounts of metallic minerals which in several cases were shown to exhibit large polarization effects which completely overwhelmed any possible membrane effects.

A comparison of the frequency behaviour of metallic electrodes and membranes indicates that there is no reason to expect significant differences between the two. The major circuit

element in each case is a Warburg impedance associated with diffusion phenomena. Differences in frequency behaviour among different rock types were observed in the natural samples but they did not allow one to distinguish the two phenomena. The magnitude of the polarization effect appears to be the best guide to this separation.

Thesis Supervisor: T.R. Madden
Title: Assistant Professor of Geophysics

ACKNOWLEDGMENTS

I cannot fully express my debt and gratitude to my thesis supervisor, Professor Madden. The original area of investigation was outlined by him as a part of a proposal for research sponsorship which he presented to the Raw Materials Division of the Atomic Energy Commission. Many of the ideas incorporated within this thesis originated during conversation with Professor Madden and it is certain that a large number of them were originally conceived by him. He has been a constant source of encouragement throughout this work.

I consider myself fortunate to have been able to study under Professor MacDonald for two years. While these studies were not related directly to the thesis area, they provided a strong background in thermodynamics and other subjects which has been invaluable to me.

Throughout all my undergraduate and graduate years at M.I.T., I have benefited greatly from the advice and assistance of Professor Shrock and Professor Hurley.

I would like to thank the M.I.T. Soil Technology Lab for the use of their Differential Thermal Analysis equipment. I have very much enjoyed working with Mr. Olsen and Dr. Martin of this laboratory and have benefited greatly from the opportunity to work with them and from the many formal and informal discussions which we have had about mutual problems of clays and clay structures.

I would like to thank Mrs. Shirley Fahlquist for checking the very tedious algebra of the kinetic model solution in Chapter III

The spectrochemical analyses were carried out by Dr. Dennen and Mr. Phil Andersen. I also obtained assistance in the heavy mineral analyses from W. Phinney.

Mr. Duane Uhri carried out the thermoelectric measurements whose results are listed in Chapter II.

John Annese and Ken Harper cheerfully performed the machining of the various items used in this research.

I would like to thank Miss Frank and Mrs. Sarver for the conscientious manner in which they performed the typing of the thesis and Mr. Earl Michaels for doing the drafting.

Translation of several Russian papers on induced polarization were made available by Bear Creek Mining Co.

Much of this work was performed during the year I was supported by a fellowship granted by Standard Oil Co. of California and I am extremely grateful for this assistance.

In addition, I received financial support on a research project sponsored by the Raw Materials Division of the Atomic Energy Commission.

I gratefully acknowledge the support of Nuclide Analysis Associates in the publication of the thesis.

My wife, Barbara, has been a constant source of encouragement during my entire graduate carrer and I gratefully acknowledge here confidence and devotion in this period.

LIST OF ILLUSTRATIONS

LIST OF TABLES

TABLE OF SYMBOLS

Chapter I

Introduction

The induced polarization method is presently one of the important methods of electrical prospecting used in geophysical work. The essence of this method is that many important mining geophysical targets are metallic conductors and exhibit a frequency dependent impedance. This property is detected by studying the transient behaviour of the voltages observed in the resistivity method of prespecting or by measuring the variations in apparent resistivity with frequency. These two methods are equivalent from a theoretical standpoint since the system is linear under normal field conditions.

When the targets become smaller or are at greater depths, their apparent induced polarization effects decrease and the question of the origin and influence of background effects arises. These background effects are thought to be due to electromagnetic coupling effects and to polarization in materials other than the metallic conductors. Among the materials which have been suspected of causing these background effects, the clays are the most important.

In 1956 the AEC began sponsorship of a research project in the MIT Department of Geology and Geophysics. The purpose of this project was to study the various background effects in more detail. The present research was carried out

under this project and is concerned with polarization in clays and other membranes. Three objectives were laid down at the initiation of this research.

The first objective was to experimentally study the effects in mineralized rocks and in rocks containing clays and altered material in order to get an idea of the magnitude of the effects to be expected and their correlation with the rock types. This is one phase of a program of induced polarization measurements on natural rock samples which has been undertaken in this laboratory. To date over 200 rock samples of many types have been studied.

The second objective was to study the physical chemical processes which might be responsible for the polarization effects in clays in an attempt to arrive at a satisfactory explanation of the phenomenon.

The third objective was to determine from the experimental and theoretical results whether any parameter is sufficiently diagnostic that a separation between clays and metallic conductors can be made on the basis of the induced polarization data alone. This, of course, is a most important objective once we have shown that significant background polarization effects are possible from these systems.

At about the same time that the present research was undertaken, Mr. H. Olsen of the MIT Soil Mechanics Department undertook a comprehensive study of the variation of several properties of clays with their consolidation histories. His

plans were to work with systems of pure clays in various electrolytes and various states of aggregation and study their permeability, compressibility, conductivity, and streaming potential as he compressed them from a slurry to a solid clay mass. Through conversations with him, we became interested in also studying the variations of their induced polarization properties during compression. It was felt that a model constructed from the results of this data and simultaneously satisfying the several parameters measured would be a quite good model and an important step towards the understanding of compacted clay systems. In this thesis, the results of some of the polarization measurements only will be presented. The detailed discussion of the possible structural models will be presented by Mr. Olsen in his Ph.D. thesis.

Most of the workers in induced polarization employ transient methods to study the phenomena. In the work at MIT, the phenomena has been primarily studied in the frequency domain. The methods are equivalent, theoretically, for under normal field conditions the system behaves linearly. There are certain practical advantages and disadvantages to each method, however. In the frequency domain approach, measurements are usually made at two or three frequencies only. The field equipment required to do this is much more compact than the equipment used in the transient methods so that it is possible to obtain a greater areal coverage. This advantage is

gained at the expense of losing details of the impedence spectra, since the transient analysis contains information over a range of frequencies. If it could be shown that the details of the frequency spectra are diagnostic, this added information would be a real advantage. At the present time, however, it has not been shown that the details of the frequency spectra are diagnostic of the material present. This is one of the objectives of the present research.

Regardless of whether one works in time or frequency it is useful to have an equivalent circuit description of the mineralized rock system which we are studying. This can be arrived at from qualitative considerations of the nature of the conduction mechanisms within the rock. (See Figure 1a)

Within the rock itself, current conduction takes place through the pore channels. If these channels are filled with pore fluid only, as is usually the case, the conduction through them is purely ionic and representable by a simple pure resistance. If however the path is partially or completely blocked by a metallic mineral, the conduction mechanism becomes more complicated. In the pore fluid part of the path it is still ionic. Within the metallic mineral it is electronic. This means that there is a transition between ionic and electronic conduction at the boundary of these two phases and this transition requires the charging and discharging of ions. This process introduces an additional barrier or impedance to current flow. The impedance arising at

ROCK MATRIX

METALLIC MINERAL GRAIN

POREPATH FILLED WITH FLUID
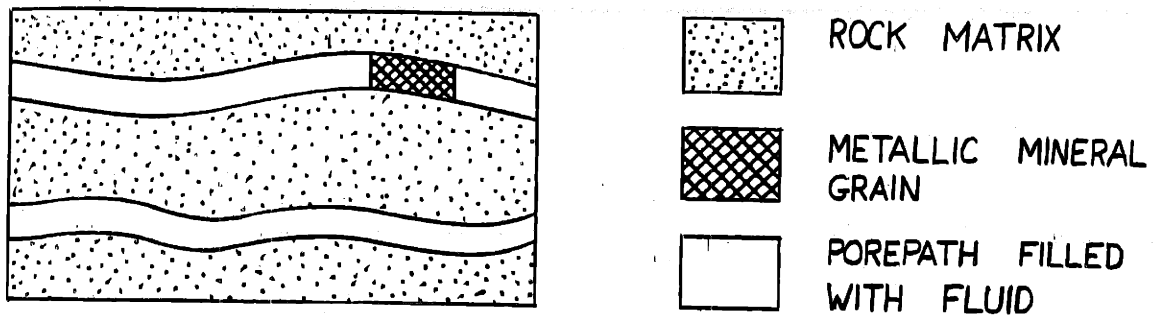
Figure 1.1a: Cross section of a Mineralized Rock showing a mineralized and an unmineralized pore path.

R_1 IONIC   PATH
R_2 IONIC   PATH

$Z' = Z /\!/ R_1$
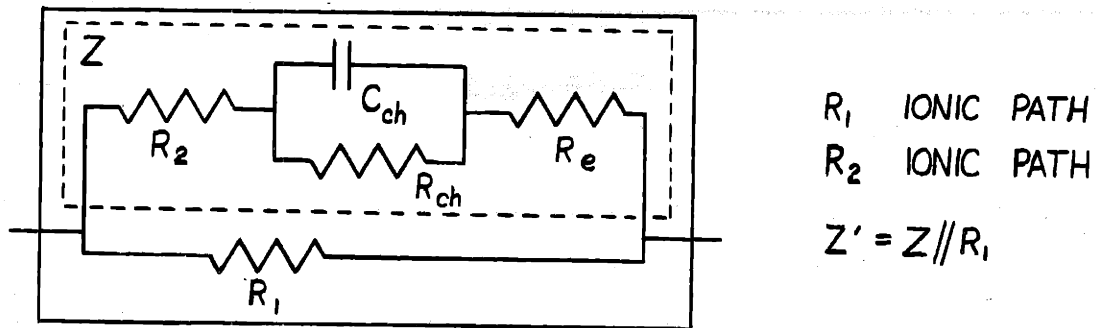
Figure 1.1b: Equivalent Circuit for the Cross Section shown in Figure 1.1a.

the boundary between an electrolyte and a metallic conductor has been the subject of intensive study by electrochemists who are interested in the same phenomena occurring at the surfaces of more conventional electrodes. (Grahame, 1952) Electrode impedances are large and may have a quite complicated frequency dependence but for our present purposes it is sufficient to represent them as a parallel resistance and capacitance. If we translate this verbal description into an equivalent circuit we obtain the result shown in Figure 1b.

The property of the system which is measured is the impedance or apparent resistivity at several frequencies when these resistivites are normalized to percentage changes from the D.C. resistivity, we obtain a parameter called the frequency effect.

$$\text{Frequency Effect} = \frac{Z'(o) - Z'(f)}{Z'(f)} \times 100$$

The parameter thus defined has a disadvantage in that it includes the effects of both the purely ionic paths and the blocked paths. Very conductive parallel ionic paths (R_1 small) will attenuate the polarization effects of the blocked paths. Such paths are very often present in field situations in the form of sheared and fractured zones. It would be desirable to eliminate their effect and this can be accomplished by a simple correction. If, instead of talking about impedances, we talk about conductivities we note that

the conductivities of the blocked and unblocked paths add.
The change in conductivity with frequency of the system is
therefore just the change in the conductivity of the blocked
paths.

$$\lambda'(f) - \lambda'(o) = \lambda(f) - \lambda(o)$$

$$= \frac{1}{Z(f)} - \frac{1}{Z(o)}$$

$$= \frac{Z(o) - Z(f)}{Z(o)\, Z(f)}$$

$$= \frac{Z'(o) - Z'(f)}{Z'(o)\, Z'(f)}$$

The quantity thus defined turns out to be a most useful diag-
nostic parameter for the interpretation of induced polariza-
tion measurements. Using typical values for the impedances
of the ionic paths and the electrode equivalent circuit we
find that

$$Z(o) >> Z(f)$$

so that the conductivity change becomes

$$\lambda'(f) - \lambda'(o) = \frac{1}{Z'(f)}$$

In practice this quantity is multiplied by a numerical factor
to give it convenient numerical values. The unit thus de-
fined is called the Metal Factor

$$\text{Metal Factor} = \frac{1}{Z'(f)} \times 2\pi \times 10^5 \quad (Z'(f) \text{ in ohm feet})$$

The metal factor concept was first introduced by
Mr. T. R. Madden (1958). Mr. Madden has discussed this con-
cept in much greater detail and includes many examples of its

usefulness. This brief review has been included here for convenient reference.

Some representative values for the metal factor are listed in Table 1.1. The values listed are derived from both field and laboratory studies.

Table 1.1

Typical Metal Factor Values At 10 Cycles Per Second

granite	2
basalt	2-20
slight sulfides	1-300
porphyry coppers	100-10,000
high magnetite	10-20,000
heavy sulfides	1000-no limit

Polarization Effects of Clays

Returning to our equivalent circuit description of a mineralized rock we now ask in what manner clays fit into this picture. Dry clay minerals are non-conductors like the remainder of the rock matrix and by themselves do not offer lower impedance paths for the current as the metallic conductors do. In order to understand their effect we must look further into their properties.

The clay minerals are silica alumina sheet structures. Usually some isomorphous substitution of Al for Si or Mg for Al occurs in the structure. The cation charge deficiency in-

troduced by this structural substitution is compensated for by adsorption of cations on the surface of the particle. In the presence of water these surface adsorbed ions may dissociate from the clay particle and go into solution and in so doing they form what is known as a diffuse layer. This diffuse layer is a zone of net charge extending into the solution with an exponential length of the order of 100 Angstroms, depending on the particular type of clay particle, the fluid, the temperature, and several other factors. The dissociated ions going into the solution leave behind a net charge of opposite sign on the surface of the particle so the equilibrium situation is one of balance between electrostatic attraction forces keeping the dissociated ions near the surface and thermal agitation tending to separate them from the surface. The diffuse layer concept has been excellently reviewed by Grahame (1947) for the case of metal electrodes. Its behaviour in colloidal systems of electrolytes is discussed by Kruyt (1952). Lambe (1958) has given an excellent review of its nature on clays with a qualitative discussion of the effects of all the important variables.

The diffuse layer is very important in determining the structural properties of clays, adsorption properties and others but we are most interested in its influence on the electrical properties. The dissociated cations increase the ionic concentration near the clay particle relative to that in the fluid at great distances from the particle. The con-

centration increase results in an increase in the specific conductivity within the diffuse layer. Even more important however it results in a change in transference properties (relative to the fluid) since the cation population outnumbers the anion population.

Since the conductive diffuse layer is so close to the surface, its conductance is often spoken of as a surface conductance. This property becomes quite important when the pore dimensions are small, approaching diffuse layer dimensions and also increases in importance as the particle size decreases since the effective surface area becomes larger.

It is to be emphasized that all materials form a diffuse layer to some degree. It is not a property peculiar to clays. Fine grained material of any kind might be expected to exhibit some degree of surface conductance and anomalous transference. The surface charges are usually negative on clays but they may be positive on other materials.

Since the diffuse layer contains a preponderance of either cations or anions, its transference properties are different from those of the pore fluid. In the case of clays this means that cations will carry a larger proportion of the current in the diffuse layer than they do in normal solution. Consider a geometrical arrangement which may be typical of a clay structure whereby we have clay particles in series with water (pore fluid) zones. When current is passed through such a system, cations are removed by the clays faster than

they are being supplied by the fluid zone. This situation
cannot be maintained and must result in an appropriate build-
up or decrease in concentration to make up for this differ-
ence in cation flux. We shall show in Chapter II that this
concentration gradient acts as an additional impedance. The
concentration buildup is larger at low frequencies than at
high frequencies because there is less time for it to occur
at the higher frequencies. This difference in the impedance
at high and low frequencies is a polarization effect.

In addition to the fact that the population of anions
and cations differs in the diffuse layer, there is also the
possibility of a difference in their mobilities above and be-
yond that which exists in normal solutions. In an ordinary
solution, cations and anions move under approximately the
same set of forces and differences in mobility are due to dif-
ferences in such things as ionic size. In the diffuse layer,
however, we have the possibility of some of the cations
moving right along the surface of the clay particle or at
least in close proximity to the surface and we must introduce
the possibility that the difference in the types of forces
acting upon them here leads to further differences in mobil-
ity. We shall see, in a later chapter, that transference dif-
ferences due to mobility differences are probably more impor-
tant than transference differences due to concentration dif-
ferences in causing polarization effects.

Similarly the phenomena of electroosmosis (Kruyt,1952)

depends on the diffuse layer properties, in particular the fact that a net charge is present in the diffuse layer zone. This net charge is swept along with a fluid flow and in so doing leads to the establishment of a potential gradient. These electroosmotic effects are possible sources of polarization also.

These and other types of polarization will be discussed in more detail in Chapter II.

Electrochemical Nature of Clays

Clays are but one of a large class of substances including ion exchange resins and membranes of various types which exhibit selective transference properties. The general term membrane is often used to describe this whole group and we will use this term throughout our discussion.

An excellent collection of papers on membrane phenomena appeared recently in a Discussion of the Faraday Society (1956). One finds on reading this and other material on this subject that virtually all the work done on membranes has been concerned with their steady state or static properties. Such phenomena as permeability, diffusion coefficients and diffusion potentials are dealt with primarily. Practically no work has been done on the polarization properties of these systems. We shall see however that ion exchange resins exhibit polarization properties and the theoretical model which we use to explain the effects in clays is also applicable to general membrane materials.

Previous Work

While this research was in progress, Vacquier, Holmes, Kintzinger, and LaVergne (1957) and Henkel and Van Nostrand (1957) published the results of their studies on polarization in clay systems.

Vacquier et al studied the polarization effects of a great number of mixtures of sand and clay. Their sample consisted of intimate mixtures of sand and clay which they produced in several different ways. An electrolyte was introduced into the mixture and transient measurements were made on the system. They used several clay types and many different electrolytes. Important polarization effects were found in many of the systems they studied. They professed, however, that a complete explanation of the polarization mechanism was not yet available. The general picture which they proposed is that the passage of current leads to the setting up of concentration cells in the clay-pore fluid system. The decay of these cells after the current source is removed sets up a diffusion potential which is responsible for the polarization voltages observed. As we shall see later, this qualitative picture is in general agreement with the mechanism which we propose. Further comments on some of the details of Vacquier's work will appear in the later discussion.

Henkel and Van Nostrand (1957) also recognized that, due to the selective transference properties of the clays, concentration cells would be set up. They compared the effect

to the concentration polarization occurring at metal electrode - solution interfaces. The basis of a mathematical treatment was introduced but they did not carry through the details. They observed the effect in pure clay masses by transient measurements.

Dahknov et al (1952) considered the problem of polarization in clays briefly and concluded that the effects were probably due to electroosmosis and were usually small.

Bleil (1953) attempted to study the problem of polarization in a media of varying electrolytic properties by using two different solutions of electrolyte separated by a membrane. His results were negative. We shall see, however, that this system is not the most suitable one for observing such effects for the frequency range, which varies inversely with the square of the system dimensions, is much too low. For the effects to lie in the frequency range from 10 cycles per second to 1000 cycles per second, the system dimensions must be of the order of .001 to .0001 cm.

The studies on polarization effects in artificial membranes are even more limited.

Juda and McRae (1953) observed polarization effects in a phenol sulfonic polymer. The specific conductivity of this material was about .14 mho/cm. The effects were measured at fairly high frequencies, 1 KC to 20 KC.

Albrink and Fuoss (1949) also made measurements on a synthetic membrane and noticed polarization effects between

100 cps and 20 KC. I believe the impedance of their membrane was so high, however, that much of the effect that they were observing was due to simple dielectric properties.

Neither of the last mentioned investigators offered an explanation for the phenomena.

Thus while polarization effects in clays and synthetic membranes have been observed in a few cases, very little progress has been made towards explaining the phenomena. It seems worthwhile to study these phenomena more thoroughly both from the standpoint of their geophysical importance and from the standpoint of their possible applications in the studies on synthetic membranes.

Organization

In chapter II of this thesis the various polarization mechanisms will be discussed and, in particular, we will discuss those mechanisms which are involved with the coupling of flows. The methods of steady state thermodynamics will be used to discuss the magnitudes of the polarization effect due to these coupling processes.

Coupling between current flow and matter flow turns out to be quite important and in order to further investigate this mechanism, a kinetic model approach will be introduced in Chapter III.

In Chapter IV, the results of experimental investigations on clays and ion exchange resins will be presented and compared with the theoretical results of Chapter III.

In Chapter V, the measured polarization properties of certain groups of anomalous samples are presented. In addition, the methods used for the mineralogical analysis of these samples are discussed.

A summary of the results is presented in Chapter VI. Also a discussion of the possibility of discriminating between the polarization effects of different types of materials by electrical measurements is included.

Chapter II

Polarization Mechanisms

In section I of this chapter, the various types of polarization mechanisms are discussed in a qualitative manner, with primary consideration being given to polarization effects due to coupling of flows.

The analysis of these mechanisms is discussed in section II. There are three general methods of attacking problems in electrochemistry such as these, classical thermodynamics, steady state thermodynamics, and kinetic models. Classical thermodynamics is of little use in the discussion of polarization processes for these processes are (in essence) irreversible. The methods of steady state thermodynamics prove to be quite useful in studying some aspects of the behaviour of these systems. Kinetic models must be resorted to, however, when the details of the frequency behaviour are desired.

Section I: Polarization Mechanisms

There are numerous processes which are capable of causing polarization in electrolyte systems including dielectric effects, electrode polarization phenomena, and coupling phenomena.

The dielectric effects due to the normal dielectric properties of the solvent become important only at frequencies greater than 10,000 cps. Similarly, the Debye-Falkenhagen effect due to relaxation effects in the ionic atmosphere do not become important until frequencies greater than a megacycle (Glasstone, 1954). The interfacial polarization mechanisms due to coupling phenomena and electrode phenomena, however, are important in the frequency range from 10,000 cps to D.C. This is the frequency range of practical interest in geophysical applications of induced polarization.

The most well known of the interfacial phenomena is that occurring at the interface between metal electrodes and electrolytes. Current flow across this boundary involves a transition from ionic to electronic conduction and this in turn requires the charging and discharging of ions, a process which is hindered by activation energy barriers at the surface of the metal. These energy barriers are equivalent electrically to added impedances. This surface also has associated with it a capacitance due to a layer of ions which are strongly adsorbed. This layer of ions is called the fixed

layer. Its capacitance acts in parallel with the activation
energy barrier and therefore the total impedance decreases
with increasing frequencies. The mechanism is actually much
more complicated than this simple picture and has been dis-
cussed in detail by Madden (1959). In addition he has
pointed out its practical importance in the induced polariza-
tion of geologic materials. This is the most important polar-
ization mechanism in these materials both because the magni-
tude of the effect is so large and also because it is associ-
ated with the primary targets of mining geophysical explora-
tion programs, that is the metallic ore bodies.

Another very interesting and important class of polar-
ization mechanisms arise because of the coupling effects
existing between current flow and other flows in electrolyte
systems. The flows which may be coupled to the current flow
are heat flow, solvent flow, and diffusion flow. All of
these may be responsible for polarization.

The best known and understood of these coupling pro-
cesses is that associated with the solvent coupling. This
effect is called electroosmosis. Ions in solution are sol-
vated. Because of this it is possible for a net water movement
to accompany the flow of current in the system. This fluid
(water) is not being continually supplied or removed so its
flow cannot be continued indefinitely. Eventually what will
happen is that a pressure gradient will build up across the
system of such a magnitude and in such a direction as to stop

any further flow of fluid. In addition, this induced pressure gradient will act on the migrating ions in such a way as to decrease the current flow. The net result is that as this steady state builds up the impedance of the system increases. The steady state when the pressure gradient has built up to its final value is the D.C. limit of the impedance. The impedance when the pressure gradient is zero is the high frequency impedance of the system. The difference is due to the polarization effects caused by the induced pressure gradient.

This mechanism of polarization has been mentioned by Dakhnov et al (1952) and Vacquier et al (1957) as a possible but unimportant cause of induced polarization in geologic materials.

The case of thermal coupling is completely analogous to that for electroosmotic coupling. The flow of current through a system tends to produce a net heat flow. Since heat is not being supplied at the sources, this flow will not continue indefinitely because in time a thermal gradient will be set up to oppose further heat flow. This temperature gradient will also tend to decrease the current flow and thus increase the impedance. It must be mentioned in connection with this effect that even though heat as such is not being supplied, electrical energy is being supplied and this in

turn is partially converted to heat because of the dissipa-
tion in the resistance of the solution. However, this supply
of heat is added uniformly to all parts of the system at once
and results in a uniform increase of temperature. The flow
of heat associated with the ionic current flow is superim-
posed on this effect.

The molecular description of the origin of the ther-
mal electric coupling requires the introduction of a quantity
called the heat of transport. This quantity has been dis-
cussed by Denbigh (1951) and the kinetic interpretation of
the heat of transport is discussed. These details are not of
paramount importance in the present discussion, however.

To our knowledge, this effect has not been previously
considered as a polarization mechanism in geologic materials.

In both of these coupling processes, we have talked
about polarization being a maximum at the steady state where
the induced flow has been reduced to zero. This state is the
ultimate steady state and may require such a long time to be
attained that it is of little practical significance. In
some situations where the media is not completely homogeneous,
we may have steady state equilibrium of a different type set
up between the zones of different properties in the non-homo-
genous media. Thus if the media were made up of a great
number of small zones of alternating properties (electro-
osmotic or thermoelectric properties), an intermediate steady
state would be established in which the induced flows,

instead of being zero, become equal in adjacent zones, though a slight unbalance exists when a great number of zones are considered. This type of steady state which we call a quasi-steady state to distinguish it from the ultimate steady state will be established in a much shorter time, since only small zones are involved instead of the whole media.

To make these ideas a little clearer by a specific example we consider the case of electroosmotic coupling in a region consisting of a sandstone and a shale in contact. We assume that the shale has a simple structure consisting of fluid zones of relatively large area in series with zones of parallel closely spaced clay particles. Pressure gradients will be induced across the clay zones during current flow because of the strong electroosmotic coupling in these zones. The fluid zones have a smaller coupling and as a result gradients in the opposite direction will be induced across them. On this scale the steady state for an applied current flow is arrived at when the gradients induced across the clay zones slow the fluid flow sufficiently that it is equal to the fluid flow in the water zone where a pressure gradient is acting to speed it up. The dimensions over which this effect takes place are of the order of the length of the clay particles which may be .001 cm or less and the time scale is correspondingly short of the order of seconds. In the overall shale stratum there may still be a greater induced fluid flow than

in the adjoining sand. Eventually this will cause a net
pressure to accumulate across these two strata, opposing the
flow in the shale and helping it in the sand until the two
flows are equal. It takes a much longer time for this steady
state to be arrived at because the dimensions involved are
now of the order of several feet. The time scale for this
steady state may be as long as 10^9 seconds. The latter
steady state is the ultimate steady state while the former is
a quasi-steady state.

We now proceed to a discussion of the polarization
effects due to diffusion coupling. The reason we have in-
serted this discussion of the ultimate steady state and the
quasi-steady state before discussing the coupling due to dif-
fusion is that the quasi-steady state situation is most impor-
tant in the diffusion coupling process.

In diffusion coupling we consider the matter flow as-
sociated with the current carrying ions. If we argued in a
manner analogous to that used in the previous examples of the
ultimate steady state we would say that eventually the flow
of these ions goes to zero. We might be tempted to conclude
from this that the current also becomes zero and an infinite
polarization effect is possible. However, this need not be
the case.   Somewhere at the extremes of our system, there
must be two electrodes through which we are supplying current.
The reactions occurring at these electrodes produce ions
which may be different from those carrying current through

the bulk of our system. For convenience let us label the current carrying ions in the system at the time we initially apply the current as A and let us label the ions produced in the electrode reaction as B. Since no source for A is present, there flow will eventually go to zero. However, when this happens, ions of type B will take over carrying the current in the system. The current will not become zero. Clearly the ultimate steady state is difficult to analyze and it can be shown that it is of no practical importance because the time scale involved is so long. (This will be discussed in Section III of this chapter).

The quasi-steady state which in this case involves equal effective transference in all zones may be very important however. In clays and shales in particular, we may expect to have small zones of alternating transference properties with the regions between closely spaced clay particles being highly selective to cations and other zones being essentially simple pore fluid zones with no selectivity. In the quasi-steady state, the anion transference in all the zones would be required to approach zero. This leads to effects of finite but very important magnitudes.

Polarization due to the selective cationic transference properties of clays has been recognized by Vacquier et al (1957) and Henkel and Van Nostrand (1957) as an important cause of polarization in clays and shales.

All of these processes of polarization due to coupling

involve the concept of energy storage in the induced gradients or generalized forces. In the time domain we can picture these gradients being built up when a current step is applied to the system. These gradients then dissipate when the current is reduced to zero. If the system were purely resistive we would observe a voltage when the current step is applied and this voltage would immediately drop to zero when the current is turned off. Actually the system is not purely resistive and what is observed is that the voltage does not drop immediately to zero when the current goes to zero. The reason that it doesn't is that during the dissipation of the induced gradients, a voltage caused by the inverse coupling to that which induced them is present. Thus if a concentration gradient is induced, its dissipation will involve the setting up of diffusion potentials. Similarly a streaming potential will be set up in the case of an induced pressure gradient which is allowed to relax.

If we plotted curves of voltage versus time for these processes, they would be similar to the charging and discharging curves for an RC circuit. The process is analogous to the charging and discharging of a capacitor. The capacitor stores electrostatic energy while in these processes energy is stored in other forms.

Section II: Analysis of Polarization Mechanisms

In the previous section we have described the general behaviour of a system in which current flow is taking place and discussed the buildup of polarization due to coupling between current flow and other flows. In this section we wish to analyze these effects quantitatively. The most suitable approach to this problem is to use the methods of steady state thermodynamics. These methods have been discussed by several authors (Denbigh, 1951; Staverman, 1952; DeGroot, 1952.) The methods are suitable for the description of a system in which several flows are taking place simultaneously. The types of flows in which we are interested are heat flow, solvent flow, matter flow, and current flow. The classical physical laws governing these flows are

J heat	$=$	$-K\nabla T$	Fourier	2.2.1
J solvent	$=$	$-k\nabla P$	Darcy	2.2.2
J matter	$=$	$-D\nabla C$	Fick	2.2.3
J current	$=$	$-\lambda\nabla\Phi$	Ohm	2.2.4

The form of all these laws is the same, the flow being proportional to a generalized conductivity and to a gradient of some potential which may be regarded as a generalized force.

The first postulate of steady state thermodynamics is that the classical description is incomplete and actually each of these flows is a linear combination of all the generalized forces. In matrix notation this statement becomes

$$J_i = L_{ij}X_j \qquad\qquad 2.2.5$$

where J_i is the flow, X_i is the generalized force, and L_{ij} is a generalized conductivity matrix. This first postulate involves two conditions, one of linearity and one of the existence of the coupling implied by the presence of the off-diagonal terms. The condition of linearity means that we are restricted to small deviations from an equilibrium situation. In practice a region in which this assumption is correct can always be found but the extent of this region must be determined in any given case. The presence of the coupling is the most interesting aspect as far as polarization is concerned and its existence can be readily demonstrated in several cases. We have discussed some of these qualitatively in section I of this chapter (i.e., electroosmosis, thermal electric, etc.)

The second postulate of steady state thermodynamics is that if the forces and flows in 2.2.5 are chosen in such a way that their product gives the rate of entropy production within the system then the matrix, L_{ij}, is symmetric.

$$\text{If } \frac{dS}{dt} = L_{ij} X_j X_i$$

$$\text{then} \quad L_{ij} = L_{ji} \qquad 2.2.6$$

The proof of this second postulate is rather involved and will not be discussed. A discussion can be found in DeGroot (1952). The symmetry has been verified experimentally for the case of streaming potential effects by Bull (1935).

For the general system which we wish to discuss, the

forces and flows in the matrix equation 2.2.5 are

	Flows		Forces	
Matter flow, non-ionic,	moles/cm.sec.	J_1	$-\nabla\mu$	2.2.7
Matter flow, ionic	moles/cm.sec.	J_2	$-[\nabla\mu\ Fz\nabla V]$	2.2.8
Solvent flow	cm./sec.	J_3	$-\nabla P$	2.2.9
Heat flow	calories/cm²sec.	J_4	$-\dfrac{\nabla T}{T}$	2.2.10

In writing the forces in this form, we have essentially adopted them as given by Eckart (1940). Denbigh (1951) has the same form except for the presence of a term $-\dfrac{\mu}{T}\nabla T$ in the matter flow force. This form may be correct but it is inconvenient to use for, since μ_i has an undetermined constant, it would probably be necessary to choose constants L_{ij} which depended on the standard state chosen.

Current flow is not included explicitly but in electrolyte solutions it is a linear comination of cationic and anionic matter flows.

$$I = F(J_1 - J_2) \qquad 2.2.10a$$

We have discussed previously how the buildup of counterpressures affects the current flow. During this buildup the equations, 2.2.5 apply at all times. We are handicapped in applying them, however, since we do not usually know all the forces. Ordinarily one force, for example a potential gradient, is maintained constant across a system by some external means. The induced forces change continuously after this potential gradient is applied until finally the system reaches a steady state, and they remain constant thereafter.

From our previous discussion we recall that this steady state is the situation of minimum current flow and hence maximum polarization. We also recall that certain subsidiary conditions relating to the vanishing of the induced flows apply at this time. It turns out that there are enough of these subsidiary conditions to allow us to solve for all the induced forces in terms of the applied force and in turn this means that we can express the current flow in this state in terms of the applied potential gradient only. The constant relating them is the steady state conductivity of the system. The initial or high frequency conductivity is easily found and the ratio of these two is the maximum polarization effect.

Section IIa. Electroosmotic Coupling

Let us consider the specific example of streaming potential coupling to illustrate these steps in more detail. In this analysis and the succeeding ones we will study the coupling between electrical potential and one induced force and we will assume that only one induced force, in this case the pressure, is important and set all the others to zero. In a real system this will not be the case but since we are primarily interested in determining the order of magnitude of the coupling it is a satisfactory assumption. We shall also consider systems of a single uni-univalent electrolyte in water unless otherwise specified. The geometry will be assumed to be one dimensional.

The relevant equations for the discussion of electro-osmotic coupling are (from 2.2.5 with $\nabla T, \nabla u = 0$)

$$J_1 = L_{11}F\nabla\Phi + L_{12}F\nabla\Phi - L_{13}\nabla P$$

$$J_2 = L_{21}F\nabla\Phi + L_{22}F\nabla\Phi - L_{23}\nabla P$$

$$J_3 = L_{31}F\nabla\Phi + L_{23}F\nabla\Phi - L_{33}\nabla P$$

The electric current is $I = F(J_1 - J_2)$

$$I = F^2\nabla\Phi(-L_{11}-L_{22} + L_{12}+L_{21}) + F\nabla P(L_{23}-L_{13})$$

so that the final system of equations is

$$I = F^2\nabla\Phi(-L_{11}-L_{22} + L_{12}+L_{21}) + F\nabla P(L_{23}-L_{13}) \qquad 2.2.11$$

$$J_3 = (L_{32}-L_{31})F\nabla\Phi = L_{33}\nabla P \qquad 2.2.12$$

The steady state condition for an applied potential gradient is that J_3, the solvent flow, vanishes. When this state is attained, the pressure gradient is found to be

$$\left(\frac{\nabla P}{\nabla\Phi}\right)_{J_3 = 0} = \frac{(L_{33}-L_{31})F}{L_{33}}$$

Therefore the current flow in this state is

$$I = \left[F^2(-L_{11}-L_{22}+L_{12}+L_{21}) + \frac{F^2(L_{23}-L_{13})(L_{32}-L_{31})}{L_{33}}\right]\nabla\Phi$$

$$= -\lambda d.c. \nabla\Phi$$

$$\lambda_{d.c.} = F^2(L_{11}+L_{22}-L_{12}-L_{21})+F^2\frac{(L_{13}-L_{23})(L_{32}-L_{31})}{L_{33}} \quad 2.2.13$$

The high frequency conductivity is obtained directly from 2.2.11 with $\nabla P=0$

$$I = F^2(-L_{11}-L_{22}+L_{12}+L_{21})\nabla\Phi$$

$$\lambda_{a.c.} = L_{11}+L_{22}-L_{12}-L_{21} \qquad 2.2.14$$

The maximum polarization effect is the ratio of these conductivities.

$$\frac{\lambda a.c.}{\lambda d.c.} = \frac{1}{1 - \frac{F^2(L_{23} - L_{13})^2}{L_{33}\lambda a.c.}}$$

2.2.15

The maximum frequency effects can be predicted if we know the values of the coefficients L_{23}, L_{13}, L_{33}. The coefficient L_{33} is just the permeability of the medium, $\left(\frac{J_3}{\nabla P}\right)_{\nabla \Phi = 0}$. The coupling is almost always so small that this is equal to $\left(\frac{J_3}{\nabla P}\right)_{I = 0}$ which is the commonly measured permeability coefficient. The other coefficients are related to the experimentally measureable quantities of streaming potential and electroosmotic coefficient. The streaming potential is defined as the potential gradient induced across the sample by an applied pressure gradient. The steady state condition for an applied pressure gradient is zero current flow and using this condition we can find the streaming potential from 2.2.11

$$S = \left(\frac{\nabla \Phi}{\nabla P}\right)_{I = 0} = \frac{F(L_{23} - L_{13})}{\lambda a.c.}$$

2.2.16

We note that S involves the same combination of the unknown coefficients L_{23}, L_{13} as 2.2.15 does. Therefore substituting 2.2.16 into 2.2.15 we find

$$\frac{\lambda a.c.}{\lambda d.c.} = \frac{1}{1 - S^2 \frac{\lambda a.c.}{L_{33}}}$$

2.2.17

A considerable number of streaming potential measurements have been made in geologic materials, primarily clays, and some representative values are listed in Table II. The data of Casagrande and Kermabon were reviewed in a previous project report (Madden et al, 1957). Since that time, Olsen

TABLE 2.1

Electroosmotic Polarization Parameters for Geologic Materials

Material	L_{33} $\dfrac{m^4}{Sec.\ newton}$	$\lambda_{a.c.}$ $\dfrac{mho}{m}$	$\lambda_{a.c.}$	Max. % effect
qtz. sandstone	3.8×10^{-14}	1.9×10^{-3}	1.5×10^{-10}	.03
limestone	1.9×10^{-15}	1.3×10^{-3}	2.6×10^{-11}	.03
qtz. sandstone	1.7×10^{-11}	5.3×10^{-3}	4.6×10^{-10}	.0002
red sandstone	2.7×10^{-14}	1.9×10^{-3}	1.0×10^{-10}	.02
shale	3.0×10^{-16}	1.7×10^{-3}	1.7×10^{-11}	.005

Above data by Kermabon (1956)

Material			$\lambda_{a.c.}$	
London Clay			$.58 \times 10^{-8}$	
Boston Blue Clay			$.51 \times 10^{-8}$	
Commercial Kaolin			$.57 \times 10^{-8}$	
clayey silt			$.50 \times 10^{-8}$	
rock flour			$.45 \times 10^{-8}$	
red marl			$.07 - .26 \times 10^{-8}$	
Na Bentonite			$.20 \times 10^{-8}$	
Na Bentonite			1.20×10^{-8}	
mica powder			$.69 \times 10^{-8}$	
fine sand			$.41 \times 10^{-8}$	
quartz powder			$.45 \times 10^{-8}$	
quartz powder			$.68 \times 10^{-8}$	

Above data by Casagrande (1952)

Material	L_{33}	$\lambda_{a.c.}$	$\lambda_{a.c.}$	Max. % effect
Kaolinite, dispersed	6.97×10^{-14}	.0176	$.54 \times 10^{-8}$	2.0
Kaolinite, nat. flocc.	1.64×10^{-13}	.002	$.034 \times 10^{-8}$	.02
Na Kaolinite, .1N	$.9 \times 10^{-13}$	.158		.001

Above data by Olsen (1959)

has made measurements on several clay systems including kaolinites, illites, and micas.

The polarization due to electroosmotic coupling in these materials is quite small and nearly always negligible.

Check on Assumptions:

In deriving 2.2.11 and 2.2.12 we have assumed that $\nabla \mu_i = 0$. Actually we should only assume that the contribution to $\nabla \mu_i$ from ∇T and ∇concentration are zero. ∇u_i still has a contribution from the term depending on P given by

$$\nabla \mu_i = \frac{\partial \mu_i}{\partial P} \nabla P = V_i \nabla P \qquad 2.2.18$$

We must therefore show that V_i is small compared with $\frac{L_{13}}{L_{11}}$ for this assumption to be upheld. V_i is on the order of 100 c.c./mole

$$L_{11} = \frac{\rho_0 D}{RT} \; ; \; L_{13} = \frac{S \lambda a.c.}{F}$$

$$\frac{L_{13}}{L_{11}} = S F$$

$$S = \frac{30mv}{atm.} = \frac{30 \times 10^{-8} \text{ volt}}{M.K.S.}$$

$$\frac{V_i}{S F} = \frac{10^{-4}}{3 \times 10^{-7}} \times 10^5 = 3 \times 10^{-3}$$

Therefore the assumption is valid.

Section 11.b. Thermal Coupling

The two flows which must be considered in this case are heat flow and current flow. From 2.2.7, 2.2.8, 2.2.10 we have

$$\begin{pmatrix} J_p \\ J_n \\ J_q \end{pmatrix} = \begin{bmatrix} L_{11} & L_{12} & L_{14} \\ L_{21} & L_{22} & L_{24} \\ L_{41} & L_{42} & L_{44} \end{bmatrix} \begin{pmatrix} -\nabla u_p - FZ_p \nabla \Phi \\ -\nabla u_n + FZ_n \nabla \Phi \\ -\nabla T/T \end{pmatrix} \qquad 2.2.19$$

Now the chemical potential is a function of the temperature and the composition

$$\nabla \mu_j = \frac{\partial \mu_j}{\partial T} \nabla T + \frac{\partial \mu_j}{\partial c_i} \nabla c_i \qquad 2.2.20$$

so that in general it would be necessary to consider concentration gradients also. However, the time constant for diffusion is much longer than that for heat flow so that for short time intervals we can neglect concentration changes and we have

$$\nabla u_i = \frac{\partial u_i}{\partial T} \nabla T = S_i \nabla T \qquad 2.2.21$$

where S_i is the partial molar entropy of the i th component. Thus we have

$$\begin{bmatrix} J_p \\ J_n \\ J_q \end{bmatrix} = \begin{bmatrix} L_{11} & L_{12} & L_{14} \\ L_{21} & L_{22} & L_{24} \\ L_{41} & L_{42} & L_{44} \end{bmatrix} \begin{pmatrix} -TS_p \frac{\nabla T}{T} - FZ_p \nabla \Phi \\ -TS_n \frac{\nabla T}{T} + FZ_n \nabla \Phi \\ -\frac{\nabla T}{T} \end{pmatrix} \quad 2.2.22$$

The electric current is $I = F(Z_p J_p - Z_n J_n)$

$$I = F^2 \nabla \Phi \left\{ -L_{11} Z_p^2 + 2L_{21} Z_p Z_n - L_{22} Z_n^2 \right\}$$

$$+ F\frac{\nabla T}{T} \left\{ TS_p [L_{21} Z_n - L_{11} Z_p] + TS_n [L_{22} Z_n - L_{12} Z_p] + L_{24} Z_n - L_{14} Z_p \right\} \quad 2.2.23$$

and the heat flow is found to be

$$J_q = F\nabla \Phi \left\{ L_{42} Z_n - L_{41} Z_p \right\} + \frac{\nabla T}{T} \left\{ -L_{41} TS_p - L_{42} TS_n - L_{44} \right\} \qquad 2.2.24$$

In this case we see that the cross terms are not the same. Therefore a single measurement of one or the other of the cross effects is not sufficient, as it was in the case of electroosmotic coupling, to evaluate the polarization effects. Both of the cross terms would have to be measured.

The algebra is somewhat simplified by the introduction of the following quantities.

The heat of transport is defined as that part of the heat flow which is caused by non-thermal forces.

$$Q_i = \text{heat of transport}$$

$$Q_p J_p + Q_n J_n = F\nabla\Phi\left\{L_{42}Z_n - L_{41}Z_p\right\} \qquad 2.2.25$$

Denbigh (1951) has discussed molecular models of the heat of transport, but these are not of paramount importance in the present discussion.

The transference numbers are defined as the fractional part of the total current which is carried by the individual ion flows.

$$t^+ = \left(\frac{FZ_p J_p}{I}\right)\nabla T = 0 = \frac{F^2 Z_p}{\lambda a.c.}(L_{11}Z_p - L_{12}Z_n) \qquad 2.2.26$$

$$t^- = \left(\frac{FZ_n J_n}{I}\right)\nabla T = 0 = \frac{F^2 Z_n}{\lambda a.c.}(L_{22}Z_n - L_{21}Z_p) \qquad 2.2.27$$

Using these definitions we find

$$\frac{Q_p t^+ \lambda}{F Z_p} = L_{41}FZ_p; \quad \frac{Q_n t^- \lambda a.c.}{F Z_n} = FL_{42}Z_n$$

$$I = -\lambda a.c.\nabla\Phi + \frac{F\nabla T}{T}\left\{\frac{t^+ \lambda a.c.}{F^2 Z_p}\left[-Q_p - TS_p\right] + \frac{t^- \lambda a.c.}{F^2 Z_n}\left[Q_n + TS_n\right]\right\}$$

$$2.2.28$$

$$J_q = F\nabla\Phi\left\{\frac{Q_n t^- \lambda a.c.}{F^2 Z_n} - \frac{Q_p t^+ \lambda a.c.}{F^2 Z_p}\right\} - K\nabla T \qquad 2.2.29$$

The steady state condition for an applied electric field is that the heat flow be zero. The temperature gradient set up is found to be

$$\nabla T = \frac{\lambda a.c.\nabla\Phi}{FK}\left\{\frac{Q_n t^-}{Z_n} - \frac{Q_p t^+}{Z_p}\right\}$$

and in this state the current is

$$I = -\lambda a.c.\nabla\Phi \left\{ 1 - \frac{\lambda a.c.}{F^2 TK}\left[\frac{t^+}{Z_p}(-Q_p - TS_p) + \frac{t^-}{Z_n}(Q_n + TS_n)\right]\left[\frac{Q_n t^-}{Z_n} - \frac{Q_p t^+}{Z_p}\right]\right\}$$

$$\lambda d.c. = \lambda a.c.\left\{1 - \frac{\lambda a.c.}{F^2 TK}\left[\frac{t^+}{Z_p}(-Q_p - TS_p) + \frac{t^-}{Z_p}(Q_n + TS_n)\right]\left[\frac{Q_n t^-}{Z_n} - \frac{Q_p t^+}{Z_p}\right]\right\}$$

$$2.2.30$$

so that the expression for the maximum polarization effect is

$$\text{Max. Effect} = \frac{1}{1 - \frac{\lambda a.c.}{F^2 TK}\left[\frac{t^+}{Z_p}(-Q_p - TS_p) + \frac{t^-}{Z_n}(Q_n + TS_n)\right]\left[\frac{Q_n t^-}{Z_n} - \frac{Q_p t^+}{Z_p}\right]}$$

$$2.2.31$$

In addition to the fact that both of the cross terms must be measured, the experimental study of the cross terms is exceedingly difficult. Presumably one might go about this by first setting up a temperature gradient across the system of interest and then measuring the potential induced with an appropriate set of electrodes. This is not straight-forward, however, for the potential measuring electrodes must be at different temperatures and this introduces the need for a correction since the single electrode potentials, which depend on temperature, are no longer the same and do not cancel. This correction can not be made, however, since it involves the arbitrary constant in the single electrode potential. This constant is indeterminate and its temperature dependence also of course.

Uhri (1958) has made measurements using a system whereby the thermal potential of a sample is bucked out by the thermal potential of a water column and in this manner

the difference in thermal electric effects can be determined unambiguously. It is likely that these values are within an order of magnitude of the desired constant and are therefore suitable for an order of magnitude estimate of the importance of the effect. (Wagner, 1930) has certain theoretical reasons for setting the thermal effect off LiCl equal to zero and he compares other salts with this one.

The quantity which Uhri measures is the potential gradient induced by a thermal gradient. We let this coefficient be β

$$\beta = \left(\frac{\nabla\Phi}{\nabla T}\right) I = 0 \qquad\qquad 2.2.32$$

$$\beta = \frac{1}{FT}\left\{\frac{t^+}{Z_p}[-Q_p - TS_p] + \frac{t^-}{Z_n}[Q_n + TS_n]\right\} \qquad 2.2.33$$

The heats of transport Q_p, Q_n are of the order of 5 Kcal/mole (Denbigh, 1951). The partial molar entropy of K^+ in solution is 24 entropy units/mole. Therefore TS

$$Q_p - TS_p = \frac{.3\times10^{-3}\times300\times96,500}{.9.65 \text{ K cal/mole}}$$

so these cross terms are of the same order of magnitude.

In Table 2.2 are listed some of Uhri's results for β and the maximum effect computed using this value.

TABLE 2.2

Sample	mv/deg.C	Freq. effect
Sandstone with clay	.3	.000003%
Sandstone	.48	.00003%
Shale	.33	.00004%
Limestone	.27	.0000002%

Clearly this effect is of no importance in these types of material.

Even though this effect is of no importance in geophysical induced polarization work, it is of interest theoretically and practically for materials with large percentage effects can be found and these are being considered for energy conversion devices. Uhri is continuing with this study.

Section II.c: Diffusion Coupling in Uncharged Membrane

We now consider the more complicated situation existing when we have coupling between current flow and flow of the ionic species present. This type of coupling is very direct since the current is carried by the diffusing ions. The flow equations describing this situation are

$$J_p = L_{11}\nabla\mu_p - L_{11}FZ_p\nabla\Phi \qquad 2.2.34$$

$$J_n = L_{22}\nabla\mu_n - L_{22}FZ_n\nabla\Phi \qquad 2.2.35$$

where we have neglected not only ∇P, ∇T but also all the off-diagonal terms. This is permissible because the primary coupling is so important in this case. The L_{ii} can be expressed in terms of more familiar electrochemical quantities.

The chemical potential can be written in terms of the concentration and the activity coefficients as

$$\mu_i = RT \ln f_i C_i \quad (f_i = \text{activity coeffi-} \\ \text{cient, Glasstone, 1954})$$

so that

$$\nabla\mu_i = \frac{RT}{C_i} \nabla C_i \qquad 2.2.36$$

assuming small enough concentration gradients so that fi

remains constant.

The diffusion coefficient of the ith species is de-

fined as

$$D_i = -\left(\frac{J_i}{\nabla C_i}\right)_{\nabla\Phi=0} = \frac{L_{ii}RT}{C_i}$$

2.2.37

Using Einstein's relation we find the mobility in terms of the

diffusion coefficients

$$U_i = \frac{D_iF}{RT} = \frac{FL_{ii}}{C_i}$$

2.2.38

The ratio of the mobilities of the cations and anions

is a very useful parameter. We denote this by

$$\sigma = \frac{U_n}{U_p}$$

2.2.39

Introducing these quantities into 2.2.34 and 2.2.35 we

obtain

$$J_p = Up \ Z_p \ E - D\frac{\partial p}{\partial x}$$

2.2.40

$$J_n = U\sigma p \ Z_n E - D\sigma\frac{\partial n}{\partial x}$$

2.2.41

As we discussed in Section I of this chapter, the

ultimate steady state of zero flow of these ionic species is

of little interest but an intermediate quasi-steady state in

which the flow of the ionic species in adjacent zones is equal

may be very important. This equality cannot be brought about

by simply having different electric fields in the two zones

but instead requires that concentration gradients be set up

also. The quasi-steady state picture is shown in Figure 2.1
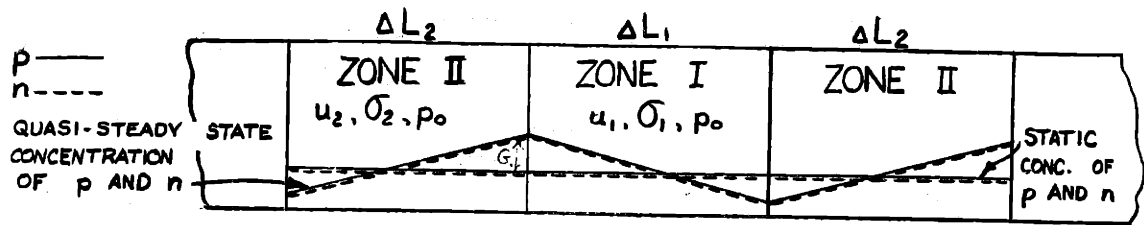
Figure 2.1 Model used in Quasi-Steady State Analysis of Diffusion Polarization in Membranes.

We have shown the concentrations of p and n equal throughout a given zone. This must be so because any unbalance will be a source for a large electric field which will tend to restore the balance. Actually a very slight unbalance does exist but it is important only for the additional electric field which it creates and not important in so far as differences in the diffusion forces are concerned. (Note: In charged membranes the total positive charge equals the total negative charge, but the concentration of the mobile ions which equations 2.2.40, 2.2.41 apply are unequal. Charged membranes will be discussed in chapter III)

At the boundary between the two zones we must have equality of the concentrations of p and n. Otherwise, an infinite gradient would exist in these quantities and we have seen that these gradients act as generalized forces. The final condition which is applied is that the total applied voltage across the zone pair is given by

$$V = -E_1 \Delta L_1 - E_2 \Delta L_2 \qquad\qquad 2.2.42$$

In this assumption we neglect the voltage drop occurring across the diffuse layer existing at the boundary. Such a

diffuse layer is present because the electric field appears to be discontinuous at this boundary and the source for this discontinuity in E is the charge associated with the diffuse layer. Actually, as we shall show later, there is reason to believe that E is continuous at this boundary when we look at the details of the diffuse layer zone. The total difference between E in the two zones is brought about by a rapid but continuous variation of E in the diffuse layer. If this holds, E in the diffuse layer always lies between the two extremes represented by its value in the separate zones. Therefore the voltage drop across the diffuse layer is always less than the larger of these two values multiplied by the thickness of the diffuse layer. Since E usually does not change by orders of magnitude, we see that the assumption above will be valid if the zone length is much greater than the diffuse layer length, which is the usual case. When these conditions are applied, we can solve for the concentration change at the boundary and for the electric field in each media and we find

$$G = \frac{U_{p_0}(\sigma_1 - \sigma_2) \; V \; Z_p Z_n}{D_1 \left[\sigma_2 + \sigma_1 + \sigma_2 \frac{B}{A}\right](Z_n + Z_p)} \qquad 2.2.43$$

$$E_1 = \frac{V}{\Delta L_1}\left\{\frac{1}{\sigma_2 + \sigma_1 + \frac{\sigma_2 A}{B} + \sigma_1 \frac{B}{A}}\right\}\left\{\frac{\sigma_2 Z_n + \sigma_1 Z_p + \sigma_2 \frac{A}{B}(Z_n + Z_p)}{\left(Z_n + Z_p\right)}\right\} \qquad 2.2.44$$

$$E_2 = \frac{-V}{\Delta L_2} \left\{ \frac{\sigma_2 Z_p + \sigma_1 Z_n + \sigma_1 \frac{B}{A}(Z_n + Z_p)}{\sigma_2 + \sigma_1 + \sigma_2 \frac{A}{B} + \sigma_1 \frac{B}{A}(Z_n + Z_p)} \right\} \qquad 2.2.45$$

where we have introduced the parameters

$$A = \frac{\Delta L_1}{\Delta L_2}; \qquad B = \frac{D_1}{D_2}; \qquad \theta = \frac{\sigma + 1}{\sigma} \qquad 2.2.46$$

The low frequency impedance is found to be

$$Z_{D.C.} = \frac{\Delta L_1 \left\{ \sigma_1 + \sigma_2 + A\frac{\sigma_2}{B} + \frac{B\sigma_1}{A} \right\}}{U_{P_0} Z_p F \left\{ \sigma_1 \sigma_2 \theta_2 + \frac{A}{B}\sigma_1 \sigma_2 \theta_1 \right\}} \qquad 2.2.47$$

At the high frequency limit in this system, no con-
centration gradients exist and the two unknowns are the
electric fields in each zone. The boundary condition is
this case are equality of total current and the condition,
2.2.42, on the total voltage across the zone. When these
conditions are applied we find

$$E_1 = \frac{-V}{\Delta L_1 \left[1 + \frac{B\sigma_1 \theta_1}{A\sigma_2 \theta_2} \right]} \qquad 2.2.48$$

The high frequency impedance is

$$Z_{a.c.} = \frac{\Delta L_1 \left[1 + \frac{B\sigma_1 \theta_1}{A\sigma_2 \theta_2} \right]}{U_{P_0} Z_p F \sigma_1 \theta_1} \qquad 2.2.49$$

Therefore the maximum frequency effect is

$$Z_{D.C.} = \frac{\theta_1 \left\{ \sigma_2 + \sigma_1 + \frac{A}{B}\sigma_2 + \frac{B}{A}\sigma_1 \right\}}{\sigma_2 \left\{ \theta_2 + \frac{A}{B}\theta_1 \right\} \left\{ 1 + \frac{B\sigma_1 \theta_1}{A\sigma_2 \theta_2} \right\}} \qquad 2.2.50$$

This expression has been evaluated for several
values of A, B, σ_2, assuming that $\sigma_1 = 1$ and the results are
shown in Figure 2.2. In Figure 2.2, the variable is the
apparent transference number for the series combination of
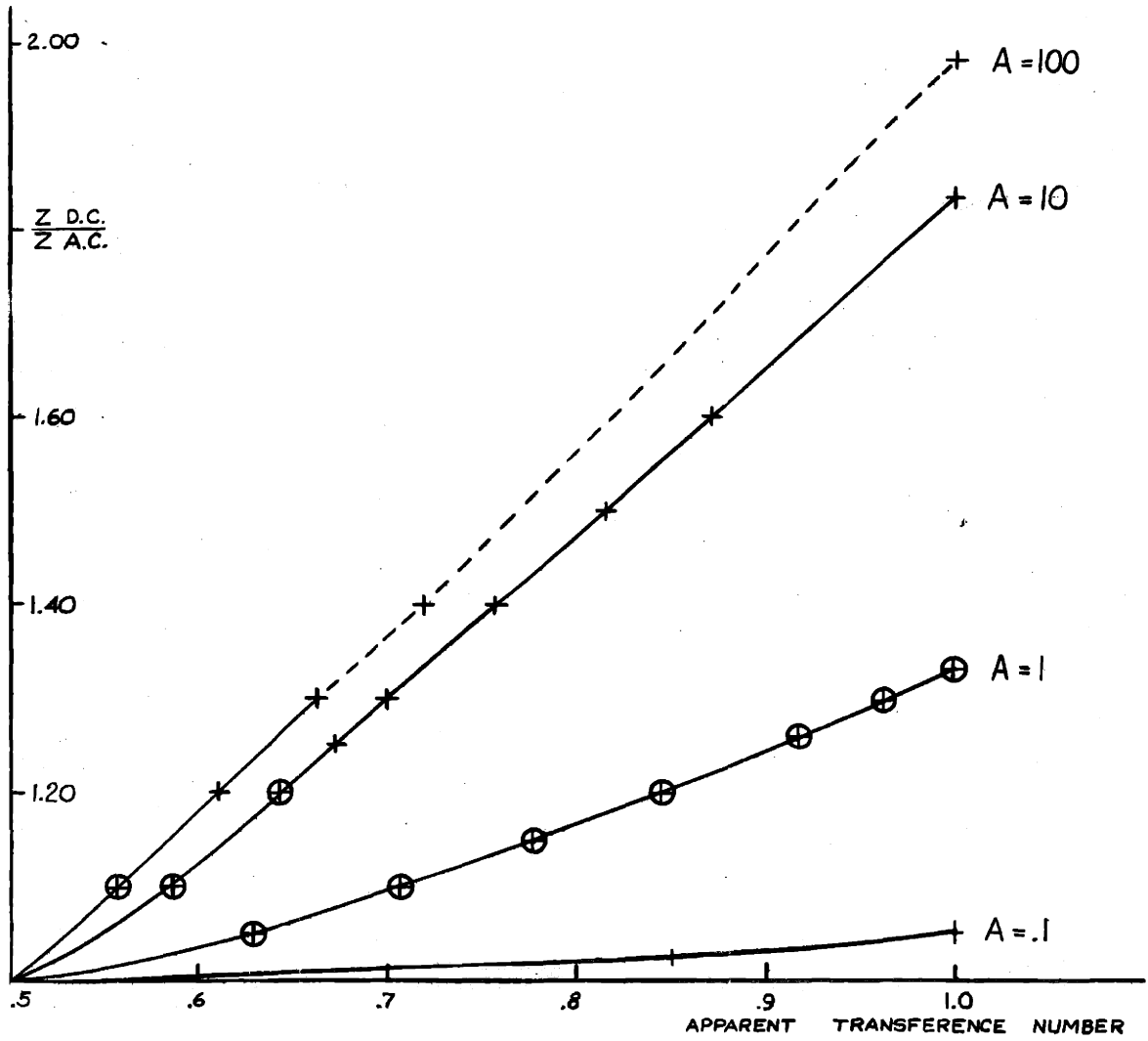
FIG. 2.2   MAXIMUM   POLARIZATION   EFFECTS   OF   MEMBRANE   MODEL

zones rather than the transference number of the selective zone. This apparent transference number was obtained in the following manner.

Assume that a concentration gradient is maintained across the zone pair as shown in Figure 2.3.
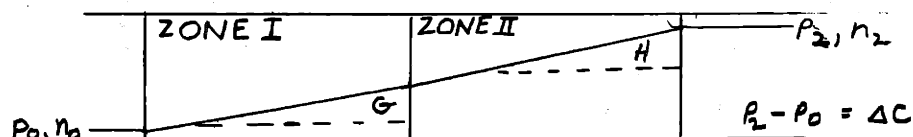
Figure 2.3. Membrane Model Assumed in Evaluation of Apparent Transference Number

Diffusion will occur and diffusion potentials will be set up across the zones. When these are set up the two ions diffuse at the same rate given by

$$J_{p_1} = J_{n_1} = \overline{D} \left(\frac{\partial p}{\partial x} \right)_1 \qquad 2.2.51$$

where

$$\overline{D} = D_1/\theta_1 \qquad 2.2.52$$

In order to solve for the concentration gradient across each zone we equate the flow in the separate zones and use the condition that the sum of the concentration differences in the two zones equals the overall concentration difference.

$$J_{p_1} = \frac{D_1 G}{\theta_1 \Delta L_1} = J_{p_2} = \frac{D_2}{\theta_2} \frac{H}{\Delta L_2} \qquad 2.2.53$$

$$G + H = \Delta C \qquad 2.2.54$$

Carrying this out we find

$$H = \Delta C \ \frac{B\theta_2}{A\theta_1 + B\theta_2} \qquad 2.2.55$$

If we assume that $\sigma_1 = 1$ the total voltage developed is developed across zone II. This voltage will be less than that developed if zone II only were present because the

total concentration change does not occur across this zone. Therefore the apparent transference properties are those of zone II attenuated by the ratio of the concentration across zone II to the total concentration change.

$$\frac{t_2^+ \text{ apparent}}{t_2^+} = \frac{H}{\Delta C} = \frac{\theta_2 B}{A\,\theta_1 + B\,\theta_2} \qquad 2.2.56$$

We have chosen the apparent transference numbers as an independent variable because this quantity is available from direct measurements of the diffusion potential for rock samples (Madden et al 1957). Of course the apparent transference number obtained depends upon our choice of the transference properties of the zone in series with the selective zone and on the absence of parallel paths. In addition there are hypothetical situations in which the possibility of large polarization effects would not be revealed by steady state measurements of transference numbers. For example one might have anion selective zones in series with cation selective zones. Diffusion potentials of opposing signs would be set up in adjacent zones and would tend to cancel. Thus the apparent transference properties of the media would tend to be nonselective even though it would be possible for the system to have a very large quasi-steady state polarization effect.

In Table 2.3 are listed some apparent transference numbers obtained from measurements on actual rock samples and the maximum possible effects due to diffusion polarization

which they predict. It is seen that quite appreciable effects are possible from this type of coupling in geologic materials.

TABLE 2.3

MEASURED TRANSFERENCE VALUES AND POSSIBLE POLARIZATION EFFECTS

Sample	t^+ (apparent)	Max.% freq.eff.
tuff	.51	1
tuff	.72	40
tremolite l.s.	.87	72
S.S., med. gr.	.48	1
S.S., med. gr.	.49	1
S.S., fine grained	.89	78
dirty S.S.	.60	20

So far, the geometry assumed has been quite simple. In particular, parallel paths have not been allowed for in the model though they are undoubtedly present in natural systems. These parallel paths will have the effect of attenuating the maximum frequency effect. They will also affect the transference values, causing smaller apparent transference numbers to be observed. To some extent these effects are self-compensating.

It is interesting to note that the maximum frequency effect is independent of the valencies of the ions. It can also be shown rather easily that the corresponding result in the time domain is that the millivolt/volt parameter measured immediately after the current is turned off, is also independent of valency.

Section III. Time Response of Polarization Mechanisms

So far using steady state thermodynamic methods we have succeeded in describing the maximum frequency effects for the various coupling processes. The next problem of importance which we consider is the description of the time behaviour of these processes.

First consider the case of electroosmotic coupling. A variety of physical situations can be imagined with greatly different frequency responses. If the pressure is built up in a zone enclosed by an impermeable boundary, the pressure build up will be essentially at the speed of transmission of a fluid pressure pulse and will depend on such things as whether or not the zone is saturated. The solution of this problem would involve the study of wave propagation within the system. In order to study this propagation one would have to go one step beyond the flow equations and set up the differential equations of motion for the fluid taking into account the electrical forces.

Another possibility is that the pressure is due to a hydraulic head (gravity head) being built up. The increase of pressure in this case is brought about by a column of water being built up. The pressure is related to the height of the column of water by the relation

$$\Delta P = \rho g \Delta L \qquad\qquad 2.3.1$$

The volume of water flowing over a given time interval must be equal to the volume of voids in the column so that

$$\rho C \Delta L = \int_0^t J_3 dt \qquad 2.3.2$$

where C is the porosity of the media. We find

$$\Delta P = \frac{g}{C} \int_0^t J_3 dt \qquad 2.3.3$$

$$\Delta P = \frac{g}{C \Delta L} \int_0^t J_3 dt \qquad 2.3.4$$

and therefore we have

$$J_3 = F(L_{23}-L_{13})\nabla\Phi - \frac{L_{33}g}{C \Delta L} \int_0^t J_3 dt \qquad 2.3.5$$

When this equation is integrated we obtain

$$J_3 = F(L_{23}-L_{13})\nabla\Phi \ e^{\frac{-L_{33}g}{C \Delta L} t} \qquad 2.3.6$$

Therefore the time constant for this process is

$$\mathcal{T} = \frac{C \Delta L}{L_{33}g} \qquad 2.3.7$$

Assume that the porosity, C, is 1% so C is .01. The value
of g in mks units is 9.8 meters/sec^2. The permeability, L_{33},
is of the order of 10^{-12} mks units so that the time constant
is

$$\mathcal{T} = 10^9 \Delta L \qquad 2.3.8$$

$\mathcal{T}$ is in seconds when the zone length, ΔL, is in meters.
This time scale is impossibly long, even in zones with the
dimensions of individual clay particles (10^{-5} meters), and is
of no importance in ordinary geophysical studies.

We can tell even less about the time behaviour for the
diffusion coupling case because of the strong tie-up between
$\nabla\Phi$ and the concentration. Following an argument similar to
the previous one we have

$$\Delta p \ \alpha \ \int J_p dt \qquad 2.3.9$$

so that the concentration gradient is

$$\nabla p \; \alpha \; \frac{\int Jpdt}{\Delta L} \qquad\qquad 2.3.10$$

Substituting this into 2.2.34 we have

$$Jp = k_1 \nabla \Phi + \frac{k_2}{\Delta L} \int Jpdt \qquad\qquad 2.3.11$$

But we know that $\nabla \Phi$ will change as p builds up because a
diffusion potential must be set up. Because of this inter-
dependence we cannot simply decouple the flow equations for
p and n and then integrate them. Instead it will be necessary
to resort to a kinetic model approach in which we convert the
flow equations, 2.2.34, 2.2.35, to differential equations and
bring in explicitly the dependence of E on p and n through
Poisson's equation. This approach will be discussed in detail
in the next chapter.

A dimensional analysis can be made of the diffusion
coupling case to obtain an order of magnitude estimate of the
time constant. The probable factors of importance in deter-
mining the time constant are the diffusion coefficients, the
concentration, and the zone length. Listing these quantities
and their dimensions we have

Diffusion coefficient $\quad$ D $\quad$ $L^2 T^{-1}$

Zone lengths $\quad$ L_a, L_b $\quad$ L

Concentration $\quad$ p $\quad$ $moles/L^3$

Time constant $\quad$ τ $\quad$ T

A dimensionless quantity is

$$\frac{D}{L_A L_B} f\left(\frac{L_A}{L_B}\right) \qquad\qquad 2.3.12$$

so that if we have correctly chosen the parameters of importance,

$$\Upsilon \quad \alpha \ \frac{L_A L_B}{D} \ f\left(\frac{L_A}{L_B}\right)$$

The value for D in solution is of the order of 10^{-5} cm^2/sec. so that

$$\Upsilon \simeq 10^9 L_A L_B \qquad\qquad 2.3.13$$

where L_A, L_B are in meters.

For Υ to be 1 second, we find that L_A, L_B must be of the order of 3×10^{-3} cm. This is typical of the lengths of individual clay particles. This time analysis shows why the quasi steady state only can be important in these materials for the time scale when any appreciable zone length is involved is much too long to be of practical importance.

Summary

Using the methods of steady state thermodynamics we have been able to analyse the polarization processes due to coupling of flows and estimated the maximum frequency effects due to these processes.

In geologic materials, electroosmotic and electro-thermal coupling are not important but diffusion coupling can be very important leading to frequency effects of 100% or more.

The details of the time buildup could not be obtained from the steady state analysis of the diffusion coupling and therefore we find it necessary to introduce a kinetic model to

study this behaviour. This will be done in the next

chapter.

Chapter III

A Kinetic Model for Polarization Due to Diffusion
Coupling in Membranes

In the previous chapter we applied the steady
state thermodynamic approach to the problem of describing
polarization phenomena. With this approach we were able
to make estimates of the maximum effects due to the various
coupling processes. Consideration of the parameters
involved has shown that thermal and solvent coupling are
not important polarization mechanisms in geologic materials
but that diffusion coupling can be important in systems
like clays with very selective transport properties. The
details of the time behaviour of the polarization buildup
in diffusion coupling could not be obtained from the steady
state analysis, however, and therefore in this chapter
we resort to a kinetic model approach to the problem.

With this model we will attempt to study in more
detail the impedance characteristics of the quasi-steady
state which exists when current flows through a series of
zones of varying transference properties. This model
applies to clays but it should also apply to other materials
like ion exchange resins and membranes   Usually the
term "membrane" is used to describe all of these materials
and we will use this general term in our discussion.

The details of the model are indicated in Figure 3.1

where two zones only are shown. We assume that the distribu-
tion of zones is actually periodic with a great number of
these zone pairs in series. The cationic and anionic
concentrations within each zone are assumed to be identical
and equal to those in the adjoining zone. In general this
will not be the case for most membranes of the type we
are considering have a fixed charge on their matrix. In
clays, this fixed charge is due to isomorphous substitution
within the clay lattice which results in a net negative
charge on the lattice. Attracted to this fixed charge are
counterions which are rather weakly bonded to the lattice
and, in the presence of fluid, some of these counterions can
dissociate from the lattice and become mobile ions in the
pore fluid. This will result in a greater number of cations
than anions in the pore solution. In addition to the
cationic and anionic concentrations being different within
the clay zone, they will also differ from the concentrations
in the adjoining zone, due to a Donnan equilibrium being
set up between the two phases (Kruyt, 1952). The case of
membranes with a fixed charge is very important and after
we have considered the simple model we will consider the
influence of the fixed charges in more detail.

1: Uncharged Membranes

The transference properties of the individual zones
are specified by the quantity σ_i which was defined in
Chapter II.
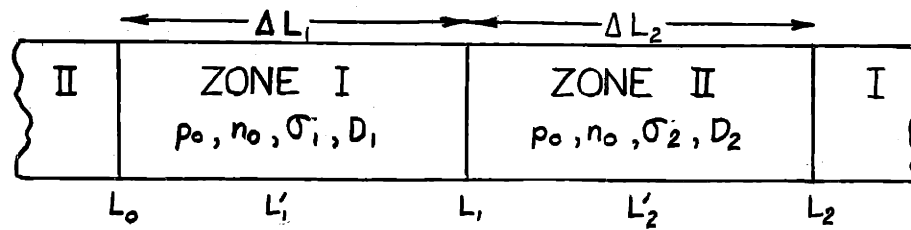
Figure 3.1: Membrane Model used in analysis of diffusion coupling in uncharged membranes.

Differential Equations of Motion

The differential equations describing the flow of ions in our model are obtained from the flow equations (2.2.34, 2.2.35). For the present we neglect all off-diagonal terms and also assume that ∇P, $\nabla T = 0$. The first assumption is valid only for dilute solutions in the same range that Einstein's relation is valid. The second assumption is justified by our previous evaluation of the maximum effect of the pressure and temperature coupling processes.

The flow equations are, with these assumptions,

$$J_p = -L_{11}\nabla \mu_p - L_{11}F\nabla\Phi = -L_{11}RT\frac{\nabla p}{p} + L_{11}FE \qquad 3.1.1$$

$$J_n = -L_{22}\nabla \mu_n + L_{22}F\nabla\Phi = -L_{22}RT\frac{\nabla n}{n} - L_{22}FE \qquad 3.1.2$$

We assume that our current densities and the resulting concentration changes are so small that the coefficients of ∇p, ∇n, E do not change appreciably within the zones

during the current flow. We will examine the limits of the validity of this assumption after the final solution is obtained. If we let

$$L_{11}\frac{RT}{p} = D; \quad L_{22}\frac{RT}{n} = \sigma D \qquad 3.1.3$$

and use Einstein's relation, our equations assume a more familiar form

$$J_p = -D\frac{\partial p}{\partial x} + \mu p E \qquad 3.1.4$$

$$J_n = -\sigma D\frac{\partial n}{\partial x} - \mu \sigma n E \qquad 3.1.5$$

Applying these equations to a small element dx and making a material balance we find

$$\frac{\partial p}{\partial t} = D\frac{d^2 p}{\partial x^2} - \mu\frac{\partial}{\partial x}(pE) \qquad 3.1.6$$

$$\frac{\partial n}{\partial t} = \sigma D\frac{\partial^2 n}{\partial x^2} + \mu\sigma\frac{\partial}{\partial x}(nE) \qquad 3.1.7$$

where we have assumed that a concentration change within the element compensates for the difference between the inflow and outflow. It is also possible in some systems to have an increase or decrease in dissociation which would partially compensate for the flux differences but we neglect this effect because we are primarily interested in strong electrolytes in dilute solutions where dissociation is nearly complete. If this assumption is not valid, it is necessary to add a term proportional to p and to n in

equations 3.1.6, 3.1.7.

In addition to equations 3.1.6 and 3.1.7, there is Maxwell's equation relating the divergence of the electric field to the charge density at any point

$$\frac{\partial E}{\partial x} = \frac{F}{\epsilon}(p-n) \qquad 3.1.8$$

In spite of the fact that we have made several simplifying assumptions, the system of differential equations, 3.1.6-3.1.8, is non-linear and coupled. This can easily be seen by substituting for E from 3.1.8 into 3.1.6 and 3.1.7 and noting that product terms of the form p^2, pn, n^2 appear in the equations.

The analytical treatment of non-linear equations is still in its infancy and the only satisfactory methods of obtaining solutions are approximate methods. Most of these methods have been developed for the treatment of single equations and not for coupled systems. From the physics of our problem we know that the changes in p and n are extremely small for the low current density range in which we are interested and we can make use of this fact to linearize the system. The method we use is to set p, n equal to their equilibrium value, which is independent of time, plus a small perturbation term which is a function of x and t.

$$p = p_0(x) + p_1(x,t) \qquad 3.1.9$$

$$n = n_0(x) + n_1(x,t) \qquad 3.1.10$$

Similarly we let

$$E = E_o(x) + E_1(x,t) \qquad\qquad 3.1.11$$

The perturbation terms, p_1, n_1, E_1 are assumed small enough so that their products can be neglected in comparison with the terms $p_o p_1$, $p_o E_1$ and so forth.

Carrying out this substitution we obtain

$$\left[\frac{\partial p_1}{\partial t} - D\frac{\partial^2 p_1}{\partial x^2} + \mu\frac{\partial}{\partial x}(p_o E_1 + p_1 E_o)\right] + \left[\mu\frac{\partial}{\partial x}p_o E_o - D\frac{\partial^2 p_o}{\partial x^2}\right]$$

$$+ \left[\mu\frac{\partial}{\partial x}p_1 E_1\right] = 0 \qquad\qquad 3.1.12$$

$$\left[\frac{\partial n_1}{\partial t} - D\sigma\frac{\partial^2 n_1}{\partial x^2} - \mu\sigma\frac{\partial}{\partial x}(n_o E_1 + n_1 E_o)\right] - \left[\mu\sigma\frac{\partial}{\partial x}n_o E_o + D\sigma\frac{\partial^2 n_o}{\partial x^2}\right]$$

$$- \left[\mu\sigma\frac{\partial}{\partial x}n_1 E_1\right] = 0 \qquad\qquad 3.1.13$$

In the third bracket of each of the above equations are the terms which we drop in the linearization. The first bracket is dependent on x and t and the second bracket is a function of x only. Therefore, these brackets must be separately equal to zero and we end up with two sets of coupled equations, one for the static or D.C. case and one for the time dependent case.

$$\frac{\partial p_1}{\partial t} = D\frac{\partial^2 p_1}{\partial x^2} - \mu\frac{\partial}{\partial x}(p_o E_1 + p_1 E_o) \qquad\qquad 3.1.14$$

$$\frac{\partial n_1}{\partial t} = D\sigma\frac{\partial^2 n_1}{\partial x^2} + \mu\sigma\frac{\partial}{\partial x}(n_o E_1 + n_1 E_o) \qquad\qquad 3.1.15$$

$$D\frac{d^2 p_0}{dx^2} - \mu\frac{d}{dx} p_0 E_0 = 0 \qquad\qquad 3.1.16$$

$$D\frac{d^2 n_0}{dx^2} + \mu\frac{d}{dx} n_0 E_0 = 0 \qquad\qquad 3.1.17$$

We note that the equations for the static case have not
been linearized but that we now have a coupled linear
system for the time dependent perturbation terms p_1 and n_1.

Even though 3.1.14 and 3.1.15 are linear they still
contain a complication because the coefficients, p_0, n_0, and
E_0, are not constant but functions of x. The reason for
this is that very often when different phases are in contact,
a potential difference exists between them and the charge
density necessary to account for this potential difference
is concentrated in a thin diffuse layer at the boundary. An
exponential type dependence is shown by p_0, n_0, and E_0 in
this diffuse layer region (Kruyt, 1952). In order to
carry through the analysis, we initially neglect this
effect which is consistent with our earlier assumption
where we neglected the fixed charge in the membrane zone.

We are not interested here in the effects of an
applied D.C. bias so we set $E_0 = 0$ and find for the case
of harmonic time dependence

$$jwp_1 = D\frac{d^2 p_1}{dx^2} - \frac{\mu p_0 F}{\epsilon}(p_1 - n_1) \qquad\qquad 3.1.18$$

$$jwn_1 = D\frac{d^2 n_1}{dx^2} + \frac{\mu p_0 F}{\epsilon}(p_1 - n_1) \qquad\qquad 3.1.19$$

$$\frac{dE_1}{dx} = \frac{F}{\epsilon}(p_1 - n_1)$$ 3.1.20

The following combinations of parameters will be useful in simplifying the algebra.

$$K^2 = \frac{2\mu p_0 F}{\epsilon D} \quad ; \quad \gamma = \frac{jw}{D}$$ 3.1.21

$$\theta = \frac{\sigma + 1}{\sigma} \quad ; \quad \Omega = \frac{\sigma - 1}{\sigma + 1}; \quad \Delta = \frac{\gamma}{K^2} \frac{\sigma - 1}{\sigma}$$ 3.1.22

The linear set 3.1.18, 3.1.19 can be solved by assuming exponential solutions of the form

$$p_1 = A_s e^{r_s x}$$ 3.1.23

$$n_1 = B_s e^{r_s x}$$ 3.1.24

In order for non-trivial solutions for A and B to exist, the determinant of their coefficients must vanish

$$\begin{vmatrix} (\gamma - r_s^2 + \frac{K^2}{2}) & -\frac{K^2}{2} \\ -\frac{K^2}{2} & (\frac{\gamma}{\sigma} - r_s^2 + \frac{K^2}{2}) \end{vmatrix} = 0$$ 3.1.25

and this condition leads to the following equation for the eigenvalues

$$r_s^4 - r_s^2(K^2 + \gamma\theta) + (K^2\frac{\gamma\theta}{2} + \frac{\gamma^2}{\sigma}) = 0$$ 3.1.26

The solution of this equation is

$$r_s^2 = \frac{K^2 + \gamma\theta}{2} \pm \frac{K^2}{2}\left\{1 + \Delta^2\right\}^{1/2}$$ 3.1.27

Typical values for K^2 and γ are shown in Table 3.1.

Table 3.1

Kinetic Model Parameters

p_0 moles/liter	K^2	f in cps	γ	$\gamma/K^2, p_0=.001$	$\gamma/K^2, p=.1$
10	10^{16}	1	3×10^5	3×10^{-7}	3×10^{-9}
.1	10^{14}	10	3×10^6	3×10^{-6}	3×10^{-8}
.001	10^{12}	100	3×10^7	3×10^{-5}	3×10^{-7}
.00001	10^{10}	1000	3×10^8	3×10^{-4}	3×10^{-6}

In obtaining this table we have assumed a value for D of 2×10^{-5} cm^2/sec. We have also assumed that $\epsilon/\epsilon_o = 80$ and a temperature of $25°C$.

The quantity Δ is very small over the range in which we are interested so that to a good approximation, the eigenvalues of 3.1.25 are

$$r_1^2 = K^2 + \frac{\gamma\theta}{2} + \Delta\frac{\gamma\Omega\theta}{4} \qquad 3.1.28$$

$$r_2^2 = \frac{\gamma\theta}{2} - \frac{\gamma\Delta\Omega\theta}{4} \qquad 3.1.29$$

If we substitute these eigenvalues back into the determinantal equations we obtain the ratio of A and B

$$A_1/B_1 = -1 + \Delta - \frac{\Delta^2}{2} \qquad 3.1.30$$

$$A_2/B_2 = 1 + \Delta + \frac{\Delta^2}{2} \qquad 3.1.31$$

The eigenfunctions $e^{\pm r_1 x}$ are associated with a

charge separation in the diffuse layer zone. They are
identical to the solutions for a static zeta potential
(Glasstone, 1954) and it appears that the length of the
diffuse layer zone is unchanged up to frequencies of at
least 100,000 cps in .001 Normal solutions. Typical
exponential lengths of the diffuse layer are on the
order of 100 Angstroms and equilibrium is attained very
rapidly in this region. Initially we assumed that no
static diffuse layer is present but the application of
the voltage source has induced one. We suspect that the
static diffuse layer will be strongly coupled to the
induced one so that if we find this term to be important
in our final solution it will be necessary to reinvestigate
the effect of the static solution.

The $e^{\pm r_2 x}$ terms are typical solutions of the
diffusion equation. They are associated with a smaller charge
separation but this separation takes place over a much longer
distance than the diffuse layer charge separation. The
diffusion length is inversely proportional to the square
root of frequency. In the D.C. limit it approaches a linear
concentration gradient if flow is taking place. No such
similar situation exists for the static case.

Summarizing the results to this point, the form of
the solutions within each zone is

$$p_1 = A_1 e^{\pm r_1 x} + A_2 e^{\pm r_2 x}$$

3.1.32

$$n_1 = A_1(-1 + \Delta - \frac{\Delta^2}{2}) \ e^{\pm r_1 x} + A_2(1 + \Delta + \frac{\Delta^2}{2})e^{\pm r_2 x} \quad 3.1.33$$

If we assume that there are a large number of zones in series, the solutions will be periodic with a wavelength equal to the sum of the zone lengths, $\Delta L_1 + \Delta L_2$. Because of this periodicity and the symmetry of the problem, satisfying the boundary conditions at one interface will automatically ensure their satisfaction throughout all the zones. The solutions for p_1 and n_1 must be symmetrical about the center of the zone and this is automatically ensured by choosing, instead of the exponentials $e^{\pm r_1 x}$ and $e^{\pm r_2 x}$, the equivalent solutions

$$p_1 = A_2 \ \text{Sinh} \ r_1(x-L') + A_2 \ \text{Sinh} \ r_2(x-L') \quad 3.1.34$$

$$n_1 = A_1(-1 + \Delta - \frac{\Delta^2}{2}) \ \text{Sinh} \ r_1(x-L^1) +$$

$$A_2(1 + \Delta + \frac{\Delta^2}{2}) \text{Sinh} \ r_2(x-L') \quad 3.1.35$$

These solutions will also satisfy the condition that the integral of p_1 and n_1 over the zone length is equal to zero.

Substituting 3.1.34 and 3.1.35 into Poisson's equation and integrating we find

$$E_1 = -\frac{F}{\epsilon} \frac{A_1}{r_1}(2 - \Delta + \frac{\Delta^2}{2}) \left[\text{Cosh} \ r_1(x - L') - 1 \right] -$$

$$\frac{(\Delta + \Delta^2/2)F}{\epsilon r_2} A_2 \left[\text{Cosh} \ r_2(x - L')-1 \right] + E_\infty \quad 3.1.36$$

where we have evaluated the integration constant by calling the electric field at the center of the zone E_{∞}.

We are now ready to apply the solutions of the differential equations to our physical system shown in Figure 3.1. Solutions of the form 3 1.34 to 3.1.36 apply in each zone but r_1^2 and γ differ because D and σ are not the same for both zone types. We will use the subscripts 1 and 2 to designate quantities in the two zones. When two subscripts are used on the same symbol, the second refers to the zone.

$$\gamma_1 = \frac{jw}{D_1}$$

$$\gamma_2 = \frac{jw}{D_2}$$

3.1.37

$$r_{11}^2 = K^2 + \frac{\gamma_1\theta_1}{2}; \quad r_{21}^2 = \frac{\gamma_1\theta_1}{2}$$

$$r_{12}^2 = K^2 + \frac{\gamma_2\theta_2}{2}; \quad r_{22}^2 = \frac{\gamma_2\theta_2}{2}$$

3.1.38

Listing our final expressions for p_1, n_1 and E in both zones we have

$$p_{11} = A_{11}\text{Sinh } r_{11}(x - L_1')$$

3.1.39

$$n_{11} = A_{11}(-1 + \Delta_1 - \frac{\Delta_1^2}{2})\text{Sinh } r_{11}(x-L_1') + A_{21}(1+\Delta_1+\frac{\Delta_1^2}{2})$$

$$\text{Sinh } r_{21}(x - L_1')$$

3.1.40

$$E_1 = \frac{FA_{11}}{\epsilon r_{11}} (2-\Delta_1+\frac{\Delta_1^2}{2}) \left[\text{Cosh } r_{11}(x-L_1')-1\right] - \frac{\left[\Delta_1+\frac{\Delta_1^2}{2}\right]}{\epsilon r_{21}}FA_{21}$$

$$\left[\text{Cosh } r_{21}(x-L_1')-1\right] + E$$

3.1.41

$$p_{12} = A_{12} \text{Sinh } r_{12}(x-L_2') + A_{22} \text{ Sinh } r_{22}(x-L_2') \qquad 3.1.42$$

$$n_{12} = A_{12}(-1+\Delta_2-\frac{\Delta_2^2}{2}) \text{ Sinh } r_{12}(x-L_2') + A_{22}(1+\Delta_2+\frac{\Delta_2^2}{2})$$

$$\text{Sinh } r_{22}(x-L_2') \qquad 3.1.43$$

$$E_2 = \frac{FA_{12}}{\epsilon r_{12}}\left[(2-\Delta_2+\frac{\Delta_2^2}{2})\right]\left[\text{Cosh } r_{12}(x-L_2')-1\right] -$$

$$\frac{\left[\Delta_2+\frac{\Delta_2^2}{2}\right]}{\epsilon r_{22}} FA_{22}\left[\text{Cosh } r_{22}(x-L_2')-1\right] + E_{2\infty} \qquad 3.1.44$$

These expressions contain a total of six unknowns.

Boundary Conditions

Since this problem has six unknowns, six boundary conditions are necessary for its complete specification. It is not immediately obvious which six conditions will be independent. We choose them in the following manner. At the boundary between zone 1 and 2,

$$p_{11} = p_{12} \qquad 3.1.45$$

$$n_{11} = n_{12} \qquad 3.1.46$$

$$Jp_1 = Jp_2 \qquad 3.1.47$$

$$Jn_1 = Jn_2 \qquad 3.1.48$$

$$E_1 = E_2 \qquad 3.1.49$$

In addition, the total voltage across the system is given by

$$V = -\int_{L_o}^{L_1} E_1 dx - \int_{L_1}^{L_2} E_2 dx \qquad 3.1.50$$

The requirement that $p_{11} = p_{12}$, $n_{11} = n_{12}$ is necessary in order to prevent an infinite gradient in these forces since we have seen that these gradients act as generalized forces. If additional barriers were present, these conditions could be relaxed. Additional barriers might exist due to so called mechanical sieve effects when the pore sizes are of the same size as the ions.

If the electric field were not continuous at the boundary, it would be necessary to have a surface distribution of sources present at the boundary to account for its discontinuity. The only charged particles present, however, are the ions and we have assumed that the differential equations completely describe their motion right up to the boundary. The charge density at any point is given by $\frac{F}{\epsilon}(p_1 - n_1)$. This is a continuous, well-behaved function of position on either side of the boundary. Because of 3.1.45 and 3.1.46, it must also be continuous across this boundary. After we have obtained the final solution we will find that the diffuse layer term looks very much like a surface charge since the charge concentration is contained in such a very small volume. On all but the most detailed scales, E appears to suffer a discontinuity as we pass through the diffuse layer at the boundary.

The insertion of our expressions for p_1, n_1 and E_1 into the boundary conditions results in the set of equations

3.1.55 to 3.1.60. The following abbreviations have been used in these equations.

$$S_{11} = \text{Sinh } r_{11}\Delta L_1/2; \qquad S_{21} = \text{Sinh } r_{21}\Delta L_1/2 \qquad 3.1.51$$

$$S_{12} = \text{Sinh } r_{12}\Delta L_2/2; \qquad S_{22} = \text{Sinh } r_{22}\Delta L_2/2 \qquad 3.1.52$$

$$C_{11} = \text{Cosh } r_{11}\Delta L_1/2 \qquad C_{21} = \text{Cosh } r_{21}\Delta L_1/2 \qquad 3.1.53$$

$$C_{12} = \text{Cosh } r_{12}\Delta L_2/2 \qquad C_{22} = \text{Cosh } r_{22}\Delta L_2/2 \qquad 3.1.54$$

The algebraic solution of this set of six simultaneous equations was carried out. Initially, the eigenvalues 3.1.28, 3.1.29 were determined only to the order Δ which seemed quite reasonable considering the magnitude of this quantity (see Table 3.1). The solution obtained for the impedance looked reasonable but the solution for the space charge concentration term, $A_{11}S_{11}$ did not appear to be correct since it was not symmetric. In carrying out the reduction, small quantities were dropped at various stages in the reduction though care was taken to carry them as far as seemed necessary. This first solution was checked independently by another person. During the reduction it was noted that the set is highly singular and the possibility was considered that, despite the precautions taken, an insufficient number of terms were carried. Therefore, the solution was carried through once more using the next term in the approximation to the eigenvalues. This solution agreed with the previous one for the impedance and, in addition,

$$A_{11}S_{11} + A_{12}S_{12} + A_{21}S_{21} + A_{22}S_{22} = 0 \qquad 3.1.55$$

$$A_{11}S_{11}\left(-1+\Delta_1-\frac{\Delta_1^2}{2}\right)+A_{12}S_{12}\left(-1+\Delta_2-\frac{\Delta_2^2}{2}\right) + A_{21}S_{21}\left(1+\Delta_1+\frac{\Delta_1^2}{2}\right)+A_{22}S_{22}\left(1+\Delta_2+\frac{\Delta_2^2}{2}\right)=0 \qquad 3.1.56$$

$$-\frac{\gamma_1 A_{11}C_{11}D_1}{r_{12}}\cdot\frac{\gamma_2 A_{12}C_{12}D_2}{r_{21}} - \frac{A_{21}C_{21}D_1}{r_{21}}\left[\gamma_1-\frac{k^2}{2C_{21}}\left[\Delta_1+\frac{\Delta_1^2}{2}\right]\right] + \frac{A_{22}C_{22}D_2}{r_{22}}\cdot$$

$$\left[\left(\gamma_2 - \frac{k^2}{2C_{22}}\left[\Delta_2+\frac{\Delta_2^2}{2}\right]\right)\right] + u_1\rho_o E_{1\infty}-u_2\rho_o E_{2\infty} = 0 \qquad 3.1.57$$

$$\frac{\gamma_1 A_{11}C_{11}D_1}{r_{11}}\left(-1+\Delta_1 - \frac{\Delta_1^2}{2} - \frac{\Delta_1^3\Lambda_1\sigma_1\theta_1}{4}\right) - \frac{\gamma_2 A_{12}C_{12}D_2}{r_{12}}\left(-1+\Delta_2-\frac{\Delta_2^2}{2} - \frac{\Delta_2^3\Lambda_2\sigma_2\theta_2}{4}\right)+$$

$$\frac{A_{21}D_1C_{21}\gamma_1}{r_{21}}\left(1+\Delta_1+\frac{\Delta_1^2}{2} - \frac{\Delta_1^3\Lambda_1\sigma_1\theta_1}{8} - \frac{\sigma_1\Lambda_1\theta_1\left(1+\frac{\Delta_1}{2}\right)}{2C_{21}}\right)\cdot\frac{A_{22}D_2C_{22}\gamma_2}{r_{22}}\cdot$$

$$\left(1+\Delta_2+\frac{\Delta_2^2}{2} - \frac{\Delta_2^3\Lambda_2\sigma_2\theta_2}{8}+\frac{\Lambda_2\left(1+\frac{\Delta_2}{2}\right)}{C_{22}}\right)+u_1\sigma_1\rho_o E_{1\infty}-u_2\sigma_2\rho_o E_{2\infty}=0 \qquad 3.1.58$$

$$\frac{FA_{11}C_{11}}{\epsilon\, r_{11}}\left(2-\Delta_1+\frac{\Delta_1^2}{2}\right) - \frac{FA_{12}C_{12}}{r_{12}}\left(2-\Delta_2+\frac{\Delta_2^2}{2}\right) + \frac{FA_{21}}{\epsilon r_{21}}(C_{21}-1)\left(-\Delta_1-\frac{\Delta_1^2}{2}\right)+\frac{FA_{22}}{\epsilon r_{22}}\left(\Delta_2+\frac{\Delta_2^2}{2}\right)(C_{22}-1)$$

$$+ E_{1\infty} - E_{2\infty} = 0 \qquad 3.1.59$$

$$\frac{2FA_{11}S_{11}(2-\Delta_1+\frac{\Delta_1^2}{2})}{\epsilon r_{11}^2}+\frac{2FA_{12}S_{12}(2-\Delta_2+\frac{\Delta_2^2}{2})}{\epsilon r_{12}^2}+\frac{FA_{21}(-\Delta_1-\frac{\Delta_1^2}{2})(2S_{21}-r_{21}\Delta_1)}{r_{21}^2}+\frac{FA_{22}}{r_{22}^2}\cdot$$

$$(-\Delta_2-\frac{\Delta_2^2}{2})(2S_{22}-r_{22}\Delta_2)+E_{1\infty}\Delta L_1+E_{2\infty}\Delta L_2 = -V \qquad 3.1.60$$

$$\frac{A_{11}S_{11}}{A_{21}S_{21}} = \frac{\Delta_1-\Delta_2}{4} \qquad 3.1.61$$

$$\frac{A_{12}S_{12}}{A_{21}S_{21}} = \frac{\Delta_1-\Delta_2}{4} \qquad 3.1.62$$

$$\frac{A_{22}S_{22}}{A_{21}S_{21}} = -(1+\frac{\Delta_1}{2}-\frac{\Delta_2}{2}) \qquad 3.1.63$$

$$A_{21}S_{21} = \frac{V\mu_1 P_0(\sigma_1-\sigma_2)}{4D_1\left[\left(\frac{\sigma_2\theta_2}{\theta_1}+\frac{B\sigma_1}{A}\right)\left(\frac{X_1C_{21}}{S_{21}}+\frac{X_1^2C_{22}}{AX_2S_{22}}\right)+\frac{(\sigma_2-\sigma_1)^2}{\sigma_2\theta_2\sigma_1\theta_1}\right]} \qquad 3.1.64$$

$$E_{1\infty} = \frac{-V}{\Delta L_1}\frac{\left(\frac{\sigma_2\theta_2}{\theta_1}-\frac{(\sigma_2-\sigma_1)}{2C_{21}}\Lambda_1\right)\left(\frac{X_1C_{21}}{S_{21}}+\frac{X_1^2C_{22}}{AX_2S_{22}}+\frac{\sigma_2X_2C_{22}A}{S_{22}B}\right)+\frac{(\sigma_2-\sigma_1)^2}{2\theta_2\sigma_1\theta_1}}{\left(\frac{\sigma_2\theta_2}{\theta_1}+\frac{B\sigma_1}{A}\right)\left(\frac{X_1C_{21}}{S_{21}}+\frac{X_1^2C_{22}}{AX_2S_{22}}\right)+\frac{(\sigma_2-\sigma_1)^2}{\sigma_2\theta_2\sigma_1\theta_1}} \qquad 3.1.65$$

$$E_{2\infty} = \frac{-V}{\Delta L_1}\frac{\left\{\frac{X_1C_{21}B}{S_{21}}+\frac{X_2C_{22}\left[\frac{\sigma_1\theta_1 A}{\theta_2}-\frac{(\sigma_2-\sigma_1)(1-\sigma_2)A}{2\sigma_2\theta_2 C_{22}}\right]}{S_{22}}\right\}}{\left(\frac{\sigma_2\theta_2}{\theta_1}+\frac{B\sigma_1}{A}\right)\left(\frac{X_1C_{21}}{S_{21}}+\frac{X_1^2C_{22}}{AX_2S_{22}}\right)+\frac{(\sigma_2-\sigma_1)^2}{\sigma_2\theta_2\sigma_1\theta_1}} \qquad 3.1.66$$

the intermediate results for the space charge terms are more reasonable and possess the required symmetry. The results of this second solution are listed in equations 3.1.61 to 3.1.66.

The reason that the correct expression was obtained for the impedance in spite of the incorrect value for $A_{11}S_{11}$ is that the space charge term has a very small effect on the impedance, of the order Δ^2. This result may seem unusual but if we refer to the results of T. R. Madden (1958) on the metal electrode-electrolyte case, we note that the diffuse layer impedance goes to zero as the sum of the faradaic current fractions approaches 1. In this system there do not exist the large reaction activation energy barriers that can be present at electrodes and the current can be expected to be almost entirely faradaic.

Check on the Approximations

At this point we can consider the limitations imposed on our solution by the approximations used in obtaining a solution of the differential equations. There are two features involved in the approximation, the dropping of non-linear terms in 3.1.12 and 3.1.13 and the approximate solution for the eigenvalues in 3.1.28, 3.1.29. The first limitation is a limitation on the amplitudes of the perturbation terms and we expect that this can be satisfied by using a sufficiently low current density. The second

limitation is independent of current density and relates to the range of frequencies and concentrations over which the diffuse layer length is independent of frequency and the space charge and diffusion effects are essentially uncoupled.

In the linearization of 3.1.12 and 3.1.13 we dropped terms of the order

$$\frac{\mu p_1}{D} \frac{dE_1}{dx} + \frac{\mu E_1}{D} \frac{\partial p_1}{\partial x} \qquad 3.1.67$$

The validity of this step requires that these terms be small in comparison with the remaining terms in the equation which are

$$\gamma p_1, \quad \frac{\partial^2 p_1}{\partial x^2}$$

Of these terms

$$\gamma p_1 << \frac{\partial^2 p_1}{\partial x^2} \qquad 3.1.68$$

and therefore we require

$$\frac{uF}{\epsilon D \gamma}(p_1 - n_1) + \frac{\mu E_1}{\gamma p_1 D} \frac{dp_1}{dx} << 1 \qquad 3.1.69$$

We will make the comparison for low frequencies at the boundary, $x = L_1$, assuming that σ_1 is approximately equal to 1 and σ_2 is approximately equal to zero. From 3.1.64

$$A_{21} S_{21} \leq \frac{V \mu_1 p_o}{4 D_1}$$

and from 3.1.65

$$E_1 \leq \frac{2V}{\Delta L_1}$$

For a frequency of .1 cps, $r_{21} = 100$ We assume that
$\Delta L_1 = 10^{-3}$cm. and we obtain finally

$$V \ll 1.25 \text{ mv} \qquad 3.1.70$$

Altenatively in terms of current density we find

$$I \ll .05 \text{ma/cm}^2 \qquad 3.1.71$$

In the solution for the eigenvalues, 3.1.28,
3 1.29, we have assumed that

$$\frac{\gamma^2}{K^4}\left(\frac{\sigma-1}{\sigma}\right)^2 \ll 1$$

This assumption has already been checked for the case of σ
= 1 and we found that it is valid up to frequencies of
100,000 cps for concentrations of .001 Normal.   In evaluating
the maximum frequency effects from our model, however, we
let σ in one zone approach zero and we now wish to determine
the minimum size which we can use for σ and still satisfy
the above restriction. We arbitrarily choose to make

$$\left[\frac{\gamma}{K^2}\frac{\sigma-1}{\sigma}\right]^2 \leq 10^{-3} \text{ or } .1\%$$

Practically, solutions more dilute than .001 Normal are
rarely encountered and if we choose this concentration,
our results will be conservative for high concentrations.
We assume that f = 1000 cps, $\gamma = 3 \times 10^8$ and this assumption
will be conservative for lower frequencies. Substituting
these in 3.1.62 we find

$$\sigma \geq .01 \qquad 3.1.72$$

In terms of transference numbers, this corresponds to cation transference numbers less than .99.

Impedance

Since the total current is continuous, we can evaluate the impedance by determining the current at any convenient point and we choose to do this at the center of zone I. Here the current is

$$\frac{-I}{F} = \mu_1 p_0 \sigma_1 \theta_1 E_1 - D_1 r_{21} A_{21} (1 - \sigma_1) \qquad 3.1.73$$

Substituting our solutions for E_1 and A_{21} we obtain the final form for the impedance

$$Z = \frac{\Delta L_1}{\mu_1 p_0 F} \left\{ \frac{1}{\sigma_1 \theta_1} + \frac{B}{A \sigma_2 \theta_2} + \frac{(\sigma_2 - \sigma_1)^2}{\sigma_2^2 \sigma_1^2 \theta_2 \theta_1} \frac{S_{21} S_{22}}{x_1 C_{21} S_{22} \theta_2 + x_2 \theta_1 A C_{22} S_{21}} \right. $$

$$\qquad 3.1.74$$

where $\quad A = \dfrac{\Delta L_1}{\Delta L_2}; \quad B = \dfrac{D_1}{D_2}; \quad x_1 = r_{21} \dfrac{\Delta L_1}{2} ; \quad x_2 = r_{22} \dfrac{\Delta L_2}{2}$

$$\qquad 3.1.75$$

The first two terms are the usual expressions for the high frequency resistances of the separate zones and the third term is the polarization impedance.

It is desirable to have several simple checks on a solution of this much algebraic complexity and there are several such convenient checks on the impedance. One obvious check which is satisfied is that the solution for the impedance is symmetrical in the subscripts 1 and 2. Other checks which are satisfied are that the sign of the

added polarization impedance is always positive and the conduction currents at the centers of the two zones are equal. The absolute check on the original set of equations was also carried through for four of the conditions.

Asymptotic Behaviour of the Impedance

At very low frequencies we can expand the hyperbolic tangents in their power series and the result is that the impedance looks like a parallel RC circuit which is quite reasonable since we do not expect complete blocking at this type of boundary. The frequency range over which it behaves as a simple parallel capacitance, however, is limited to $w \ll \frac{1}{RC}$ so that, practically, this result is not useful since the capacitance has essentially no effect in the frequency range over which this simple equivalent circuit applies.

The nature of the low frequency capacitance is somewhat unusual. It appears to be some sort of chemical capacitance associated with the concentration gradient. It is proportional to the length of the zone. Its value is of the order of 1000 uf/cm. for $\Delta L = 10^{-3}$ cm.

At the higher frequency limit, $\tanh x \to 1$ and the impedance becomes

$$Z = \frac{\Delta L_1}{\mu_1 \rho_0 F} \left\{ \frac{1}{\sigma_1 \theta_1} + \frac{B}{A \sigma_2 \theta_2} + \frac{(\sigma_2 - \sigma_1)^2}{\sigma_2^2 \sigma_1^2 \theta_2 \theta_1 \left[x_1 \theta_1 + \theta_1 x_2 \frac{A}{B} \right]} \right\}$$

$$3.1.76$$

The denominator in the polarization term is proportional to
the square root of jw so the added impedance at high fre-
quencies approaches a typical Warburg impedance which is
characteristic of diffusion controlled impedances. Warburg
impedances were first considered in connection with metal
electrode polarization phenomena where they are very important
(Grahame 1952). The magnitude of a Warburg impedance varies
as $1/\sqrt{w}$ and the phase shift is a constant 45°.

The equivalent circuit at high frequencies is shown
in Figure 3.2 where we have used the symbol proposed by
Grahame for the Warburg impedance.
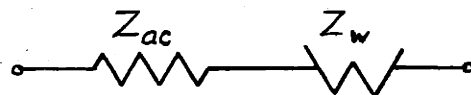
Figure 3.2: Equivalent Circuit for High Frequency Impedance
of Membrane System

Za.c. refers to the sum of the high frequency resistances of
the separate zones.

At intermediate frequencies, no simple circuit
combinations can represent the impedance behaviour and the
general expression must be resorted to.

Mr. T. R. Madden wrote a program for the IBM 704 to
carry out the calculation of the general expression for
several values of A, B, σ_2 assuming $\sigma_1 = 1$. These results
are presented graphically in Figures 3.3 through 3.7. In
plotting these figures, a constant selective zone length
of $\sqrt{10} \times 10^{-4}$ cm. has been assumed. The length of the fluid

FIG. 3.3 FREQUENCY SPECTRA OF MEMBRANE POLARIZATION

SELECTIVE ZONE LENGTH = 3.2×10^{-4} cm.

$B = 1.00$; $\sigma_1 = 1.00$

$\frac{Z\ D.C.}{Z\ A.C.}$

1.60

1.40

1.30

1.20

1.10

A = 11.3

$\sigma_2 = .008$

$\sigma_2 = .031$

$\sigma_2 = .097$

$\sigma_2 = .333$

A = 1.0

$\sigma_2 = .008$

$\sigma_2 = .031$

$\sigma_2 = .097$

$\sigma_2 = .333$

FREQUENCY CPS

10

100

1000

SELECTIVE ZONE LENGTH = 3.2×10^{-4} cm.

$\sigma_2 = .008$ $\sigma_1 = 1.00$

B = 1.00

B = 2.00

B = 4.00

A = 11.3

$\dfrac{Z \ D.C.}{Z \ A.C.}$

1.50

1.30

1.20

1.10

B = 1.00

B = 2.00

B = 4.00

A = 1.0

10

100

1000
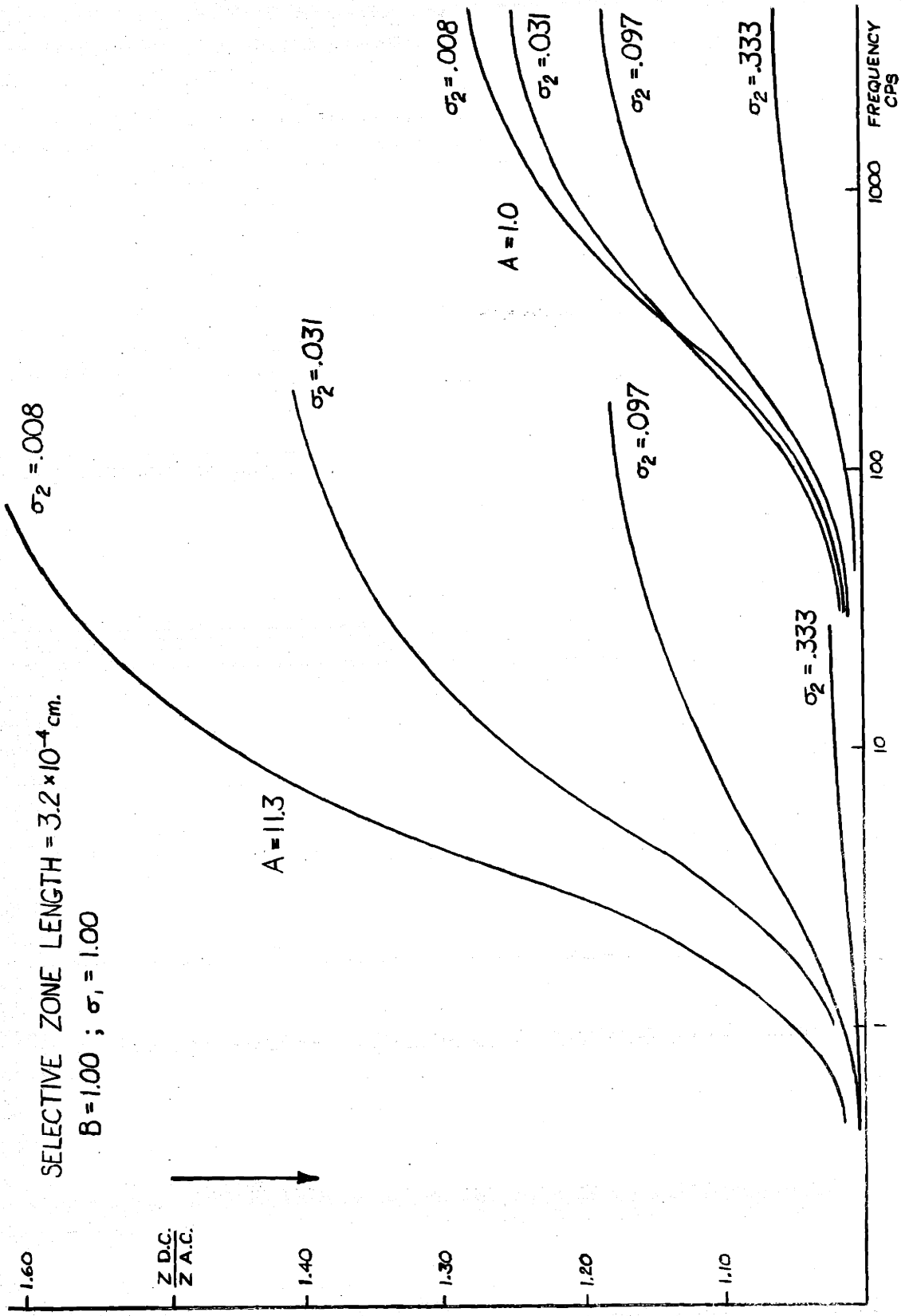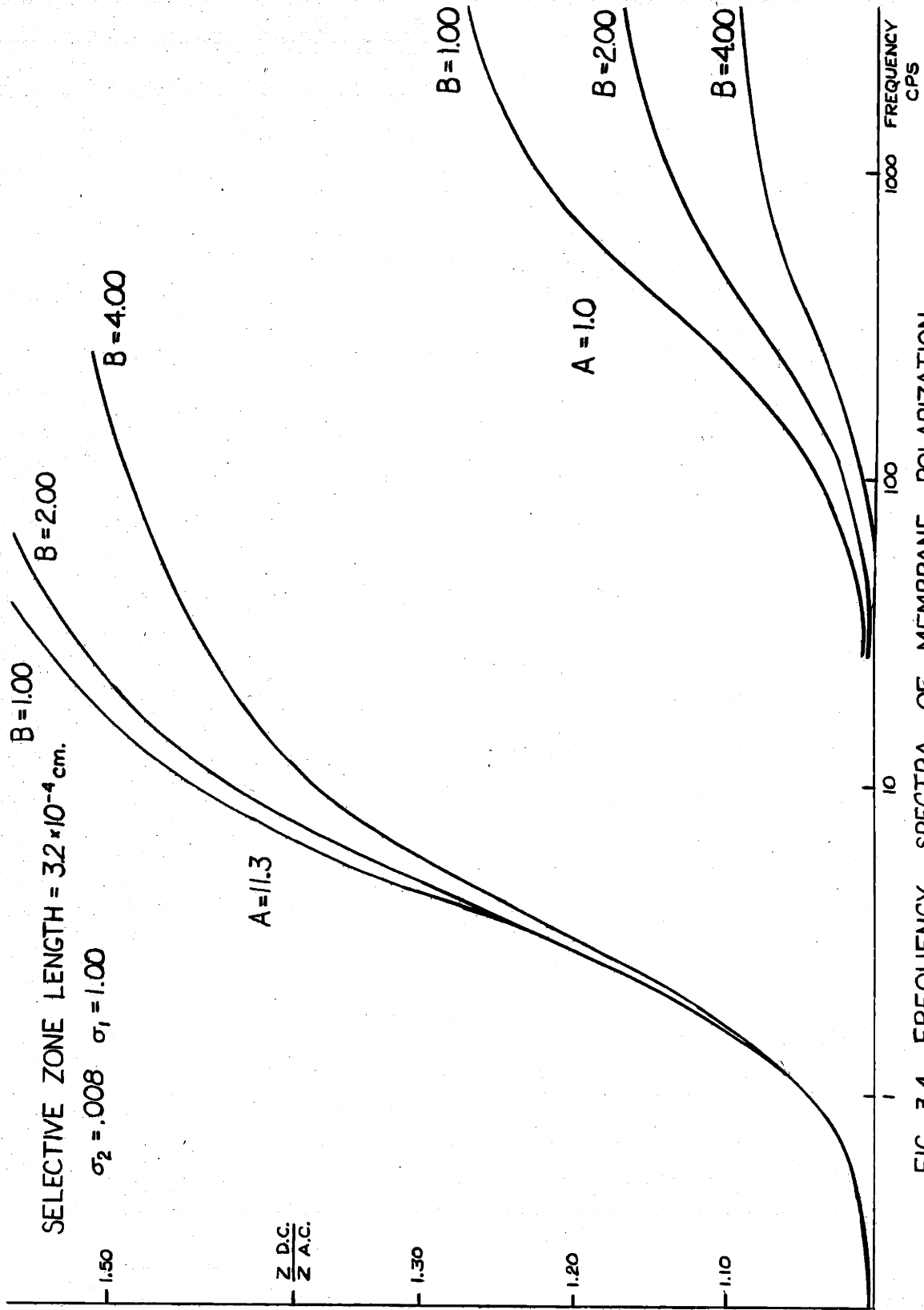
FREQUENCY CPS

FIG. 3.4 FREQUENCY SPECTRA OF MEMBRANE POLARIZATION
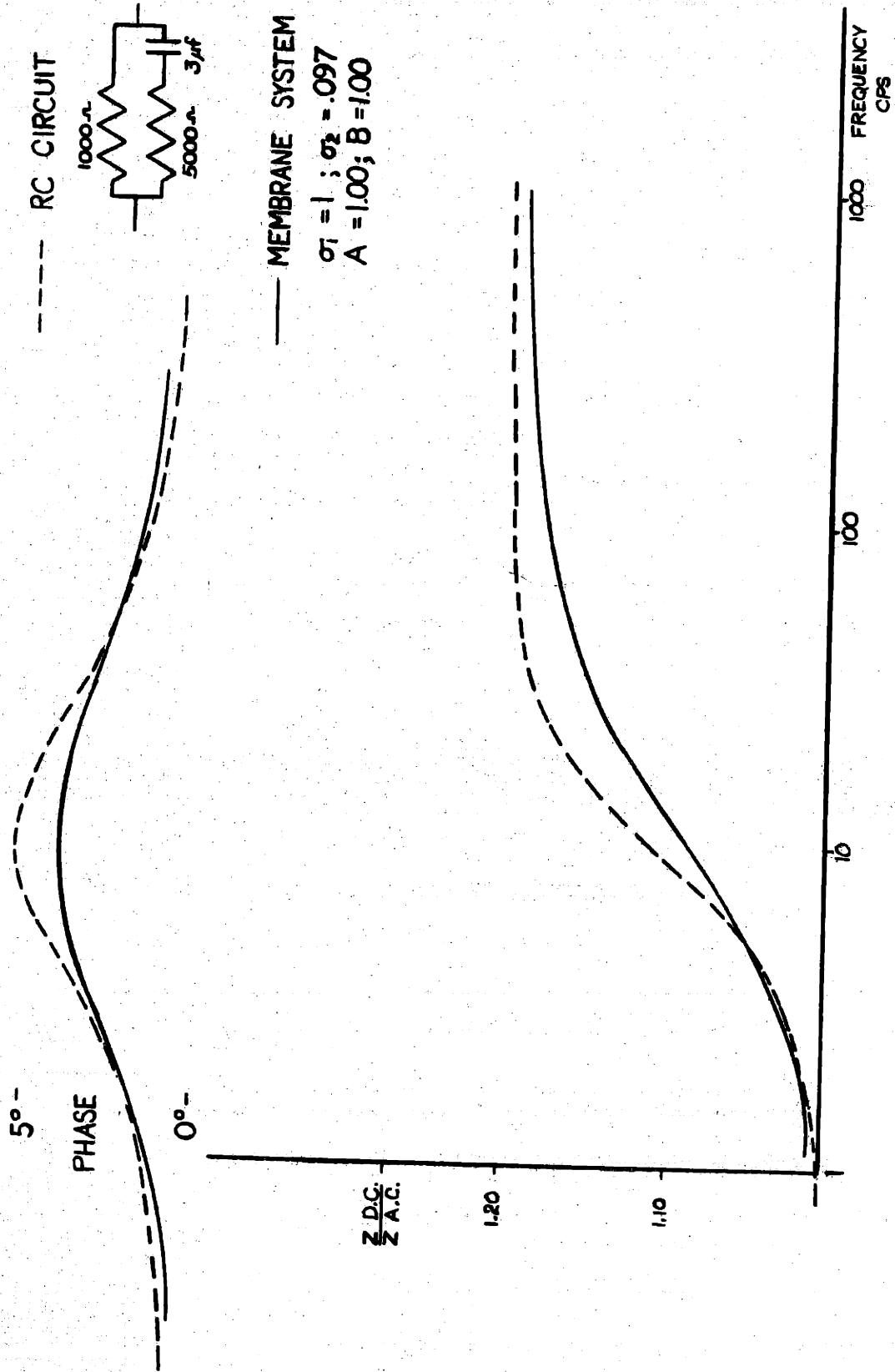
FIG. 3.5 COMPARISON BETWEEN IMPEDANCE OF MEMBRANE SYSTEM AND RC CIRCUIT

FIG. 3.6 FREQUENCY SPECTRA OF MEMBRANE POLARIZATION

SELECTIVE ZONE LENGTH = 3.2×10^{-4} cm

$A = 11.3$; $B = 1.00$; $\sigma_1 = 1.00$

$\sigma_2 = .008$

$\sigma_2 = .031$

$\sigma_2 = .097$

$\sigma_2 = .008$

$\sigma_2 = .031$

$\sigma_2 = .097$

PHASE
10° -

0° -

1000 FREQUENCY
CPS

100

10

1.40

$\frac{Z \text{ D.C.}}{Z \text{ A.C.}}$

1.20

1.10
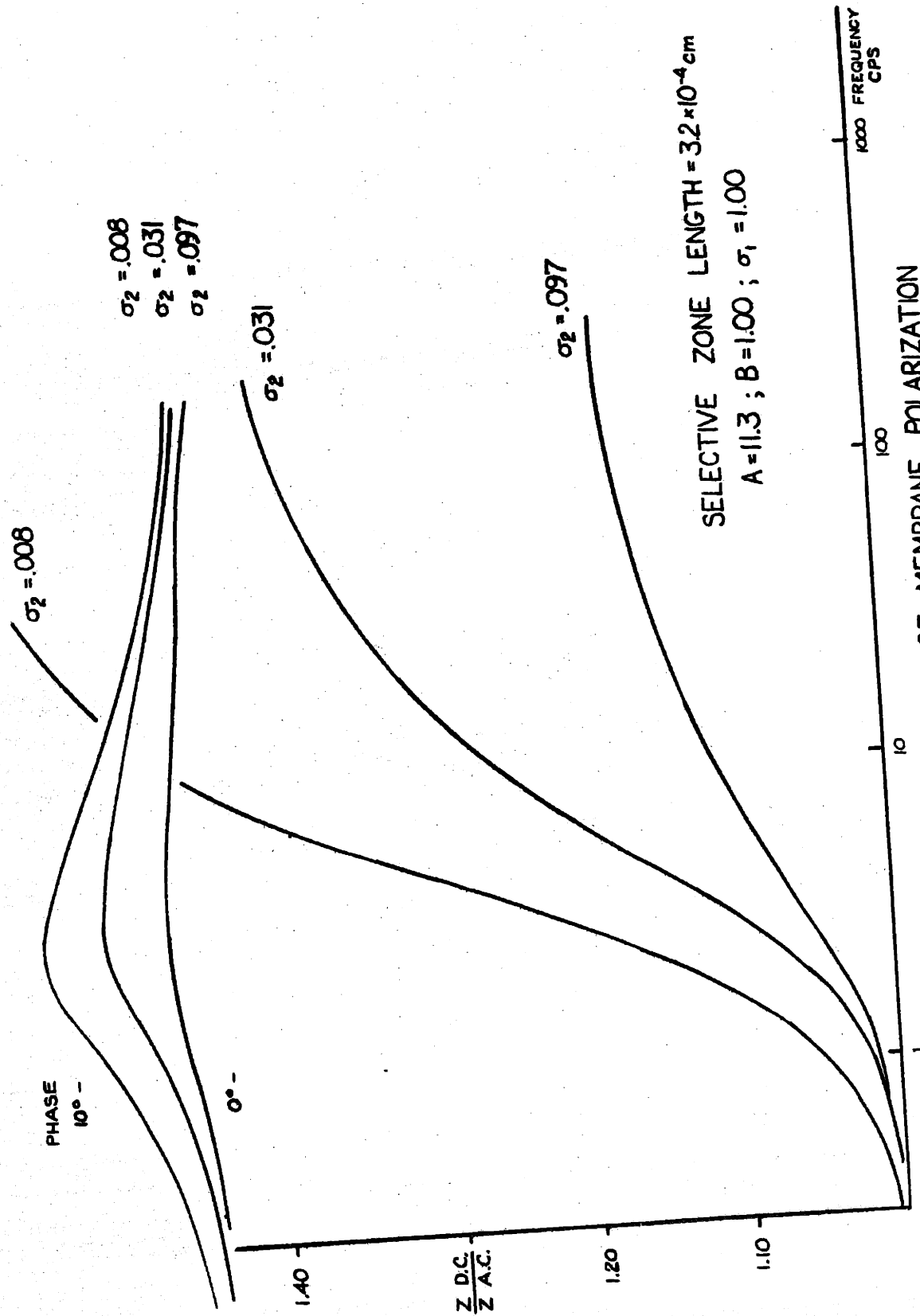
zone, zone 1, varied in accordance with the A value given.
A value of 2×10^{-5} cm/sec. was used for D_1.

In Figure 3.5, a comparison between the membrane
impedance and that of a simple RC circuit with the same
maximum frequency effect is shown. At low frequencies, the
RC circuit does not follow the membrane impedance closely
over any of the range in which the impedance is varying
significantly. The RC circuit has a much sharper character-
istic in the intermediate range and then levels out while
the membrane impedance continues to rise over a long
frequency range. The phase of the membrane impedance of
course remains larger than that of the RC circuit at the
higher frequencies because of this continued slow change in
impedance.

Maximum Frequency Effects

It is interesting to look at the maximum possible
frequency effects exhibited by the model. The maximum effect
occurs when the transference number of the selective zone
approaches unity. Depending on the length ratio and the
ratio of the diffusion coefficients, this maximum varies
between 0 and 100% for $\sigma = 1$ which corresponds closely to
the case for a pore fluid like KC1 where σ is actually 1.02.
For NaCl, t^+ is about .4 and σ_1 equals 1.5. A larger
maximum effect is possible, of the order of 150%. There
are other salts, like LiCl, with even larger σ but they

are not important in the present study though they might
be of use in a theoretical study of membranes.

The maximum effect predicted by this model for
the completely general case of arbitrary A, B, σ_2, σ_1
agrees exactly with the prediction made in Chapter II with
the use of steady state thermodynamics.

The existence of a maximum frequency effect is a
useful model criterion. From Figures 3.3 and 3.4 we
observe, for instance, that for equal zone lengths, the
maximum effect is 33%. In our experimental measurements on
clays and ion exchange resins, to be reported in the next
chapter, we have observed effects of twice this amount and
it appears that these can only be explained by going to a
much larger A value, i.e. a length ratio of 5 to 1 or 10 to
1.

In the IBM calculations, only three length ratios
were used but if we are interested only in the maximum
effects, it is very easy to compute them directly from the
impedance formula and in Table 3.2 these maxima are listed
for the case of σ_2 = .001, B = 1, and σ_1 = 1.

Table 3.2

Maximum Frequency Effects as a Function of the Length Ratio, A

A	Maximum Effect
1	1.332
2	1.496
5	1.705
10	1.814
50	1.871
100	1.814

If the length ratio is < 1, the frequency effect becomes quite small.

In the case of metal electrodes, a similar situation on maximum frequency effects does not exist. Laboratory measurements on well mineralized rock samples have indicated effects of over 1000%. Of course the limiting situtation of an ideal polarized electrode has an infinite frequency effect. The only possibility of obtaining frequency effects of this order in membranes is the unlikely situation of a cationic selective zone in series with an anionic selective zone.

If the membrane is made up of series paths only, the frequency effect is independent of the conductivity of the solution and depends only on the unbalance in the transference numbers, length ratios, etc. If there are parallel paths present, they will act essentially as parallel resistances and will attenuate the maximum effect. This attenuation will be purely a geometrical effect and will be independent of concentration also.

Time Domain

The impedance function, 3.1.74 could not be found in the tables of Fourier Transforms so that it is not possible to write down the step function response of this system directly. This information, which would be useful in studying the great amount of work which has been done in

the time domain by other investigators, could be obtained fairly easily, however, by a break point analysis of the frequency data.

Additional Comments on Model

The kinetic model which we have used is a standard model for describing the motion of ions in solution and in certain other materials, e.g. semiconductors. MacDonald (1953) has applied this model to the study of ac polarization effects in photoconductors, semiconductors, and electrolytes. His mathematical formulation is nearly equivalent to ours, the only difference being that he includes terms to represent dissociation or formation of carriers and therefore takes the concentration of neutral centers into account also. His boundary conditions are too restrictive to apply to electrolytes in general since he assumes perfectly blocking electrodes (ideal polarized electrode). He does not specialize his results for the case of electrolytes but he does consider the case $\sigma = 1$ and $\sigma = \infty$ and arrives at the same form for the diffuse layer capacitance which our solution yields for blocking electrodes. Chang and Jaffé (1952) have considered this model also starting with the linearized equations identical to ours. Their solution is restricted to the case of equal mobilities. The boundary conditions used are that the current flow at the boundary is a first order rate process but they use the same rate

constant for cations and anions which is probably not the
case. The method of solution neglects the inhomogeneity
in the electric field initially (this completely decouples
the equations) and then attempts to correct for it by an
approximate method. This procedure contributes nothing since
his final approximation is only as good as ours yet it does
not satisfy Poisson's equation as it must. Jaffe includes
experimental results on metallic electrodes which he can
explain by his theory only if there are certain very slow
carriers present.

Keilson (1953) considers the solution of the
linearized equations including recombination effects and a
constant E_0. His solutions are carried out in the time
domain using Laplace Transform techniques. The final
solutions are for the concentrations of injected carriers
and he does not consider impedances but only relaxation
times. It does not seem that there is any advantage in
working in the time domain in this case since he is able
to solve only the linearized equations which we have handled
in the frequency domain with no trouble.

The difficulty with this problem lies not in
solving the linearized equations but in justifying the
linearization and the neglect of the static situation.
Solution of the exact set would of course be most desirable
but since this cannot be carried out and the equations must be
linearized, it is important to show that the linearization

is a good first approximation to the exact set. The method used by Chang and Jaffé to linearize the set is to assume the non-linearity causes the first harmonic and all higher harmonics of the forcing voltage to be generated. The class of nonlinearity is very large and it is not at all obvious that all possible types of nonlinearity can be representable in this form. Non-integerial harmonics can be ruled out by stability considerations but subharmonics may be present. In our linearization, we required only that $p_1 << p_0$, $p_1E_1 <<$ $p_0E_1 + p_1E_0$ without specifying any type of non-linearity. This discussion may seem trivial since an identical linear set is arrived at by both approaches but it becomes important when one tries to justify the linearization by studying the differential equations for the higher harmonics.

A more important problem than the linearization procedure is the justification of the neglect of the static solution. None of the authors mentioned have been able to include the static solution except Keilson who includes a constant E_0. Madden (1958) has successfully carried through the problem for the metallic electrode, however, taking the static solution into account.

II. Charged Membranes

In the introduction to this chapter it was pointed out that the important membrane systems including clays are actually more complicated than the simple model which we have

assumed so far in this work. These complications arise from more concentrated solutions where our simple flow equations and the assumptions about complete dissociation are less correct and from the presence of a fixed charge. The more important of these complications is that of the presence of the fixed charge within the membrane zone. This quantity, which we denote by A^-(moles/c.c. of pore fluid), is the charge on the lattices of the crystals themselves. It is fixed in place and does not contribute to the conduction of current, though the counterions attracted to it do. The concentration of mobile anions within this zone is smaller than that of the cations because the fixed charge enters into the overall electroneutrality balance of the solution.

Let us consider a model similar to the one treated previously but the membrane zone is generalized and now contains fixed charges as shown in Figure 3.7.

II	ZONE I $\rho_{o1}, n_{o1}, \sigma_1, D_1$	ZONE II $\rho_{o2}, n_{o2}, A^-, \sigma_2, D_2$	I

L'
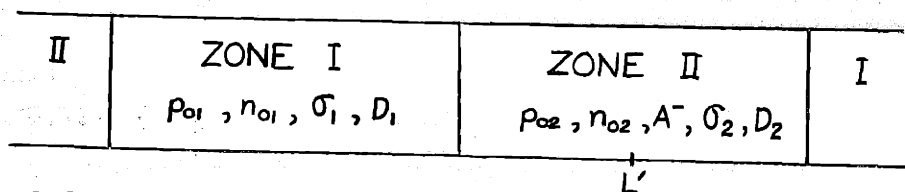
Figure 3.7: Model for Membrane System Including Fixed Charges.

Before treating the time dependent case for this situation, we will apply the kinetic model which we have used so far to the static equilibrium which exists between these two phases. This static problem has been attacked previously using the thermodynamic concept of osmotic equilibrium and is termed a Donnan equilibrium (Kruyt, 1952). The electrochemical potentials of the mobile ionic species and the solvent are equated in the two phases. The effect of the fixed charges is introduced through the electro-neutrality condition within each phase. The osmotic equilibrium strictly applies when the two phases are separated by a thin semipereable membrane. In this system, the boundary between zones I and II is an effective membrane because there is free exchange of the mobile ions across this boundary and no transfer of fixed charge across it. (Kunin and Myers, 1952, pp. 14).

The electrochemical potentials of the components are of the form

$$\mu_i = RT \ln a_i + PV_i + Fz_i \Phi_i \qquad 3.2.01$$

If we equate these expressions and use the electroneutrality condition we can solve for the difference in cation concentration within the phases and we find

$$P_{01} - P_{02} = -\frac{A^-}{2} \qquad 3.2.02$$

For the potential difference we find

$$\Delta V = -\frac{RT}{F} \ln \frac{p_{O2}(p_{O2} - A)}{p_{O1}^2}$$
3.2.03

These results are valid for small values of A^- and low concentrations of p_O, n_O so that the activities are equal to the concentrations. We have also neglected the PV terms in these solutions because they are usually small.

Now we know that if a potential difference exists between the phases, there must be a charge distribution to account for it. We expect that a diffuse layer is formed at the boundary between the phases and that the potential difference occurs across this thin zone. The thermodynamic treatment outlined above, however, gives no hint of the seat of the potential difference.

The kinetic model approach to this problem is completely analogous to the system already considered in Section I of this chapter. Using equations 3.1.18 and 3.1.19 in their D.C. limit and assuming solutions of the form

$$p_1 = A_k e^{r_k x}$$
3.2.04

$$n_1 = B_k e^{r_k x}$$
3.2.05

we find for the eigenvalues in zone II

$$r_k^2 = K_2^2 (1 - \frac{A^-}{2p_{O2}}) \; ; \; 0$$
3.2.06

In zone I the previous solution still holds, and the eigenvalues are

$$r_k^2 = K_1^2 \; ; \; 0$$
3.2.07

The eigenvalues of zero correspond to a constant term plus a term proportional to x. Clearly this latter term can exist only if current is flowing through the system and since we are interested in the static case and not the D.C. case, this term may be set equal to zero. We now follow through the identical steps of the previous problem except that we accept only one exponential solution in each zone, the zones being assumed infinite in length. The following expressions are obtained.

$$p_{11} = A_{11}e^{k_1x} \qquad\qquad 3.2.08$$

$$n_{11} = -A_{11}e^{k_1x} \qquad\qquad 3.2.09$$

$$E_1 = \frac{2FA_{11}}{\epsilon K_1} \qquad\qquad 3.2.10$$

$$p_{12} = A_{12}e^{-k_2x} \qquad\qquad 3.2.11$$

$$n_{12} = -A_{12}\left(\frac{p_{02}-A^-}{p_{02}}\right)e^{-k_2x} \qquad\qquad 3.2.12$$

$$E_2 = \frac{-FA_{12}}{\epsilon K_2}\left(\frac{2p_{02}-A^-}{p_{02}}\right)e^{-k_2x} \qquad\qquad 3.2.13$$

There are three unknowns in this problem, A_{11}, A_{12} and p_{02}. Referring to the boundary conditions, 3.1.45-3.1.49, we note that we have already used the condition that the current is zero in dropping the eigenfunctions for $r_k = 0$. The conditions imposed in this case are on the continuity of total p, total n, and E at the boundary. Substituting into these conditions we have

$$p_{01} + A_{11} = p_{02} + A_{12} \qquad\qquad 3.2.14$$

$$p_{01} - A_{11} = p_{02} - A - A_{12}\left[\frac{p_{02}-A}{p_{02}}\right] \qquad\qquad 3.2.15$$

$$\frac{A_{11}}{K_1} = -\frac{A_{12}}{K_2}\left(\frac{2p_{02}-A^-}{p_{02}}\right) \qquad\qquad 3.2.16$$

This set is not linear since K_1, K_2 depend on p_{0_i}. Let

$$x = p_{01}-p_{02}$$

In terms of x,

$$A_{11} = \frac{(2x + A^-)p_{02}-xA^-}{A^-}$$

$$A_{12} = (2x + A^-)p_{02}/A^-$$

Substituting we find

$$x = -\frac{A^-}{2}\left(\frac{K_1}{K_1+K_2}\right) - \frac{A p_{02}}{(2p_{02}-A)}\frac{K_2}{K_1+K_2} \qquad\qquad 3.2.17$$

Using this expression for x, we obtain

$$A_{11} = \frac{A^-}{2}\frac{K_1}{K_1+K_2} \;;\quad A_{12} = \frac{-A^-K_2}{(K_1+K_2)}\frac{p_{02}}{(p_{02}-A)} \qquad\qquad 3.2.18$$

$$\Delta V = -\frac{RT}{2F}\frac{K_1}{K_2}\frac{A^-}{p_{01}} \qquad\qquad 3.2.19$$

These expressions for x, ΔV are identical to the thermo-dynamic solution for the case of $\frac{A^-}{p_{02}}$ small and this lends further support to our choice of model and boundary conditions.

If we now turn to the time dependent case we find that the appropriate linearized differential equations are

$$\gamma p_1 = \frac{d^2 p_1}{dx^2} - \frac{K^2}{2}(p_1 - n_1) \qquad\qquad 3.2.20$$

$$\frac{\gamma n_1}{\sigma} = \frac{d^2 n_1}{dx^2} + \frac{K^2}{2} \frac{n_0}{p_0}(p_1 - n_1) \qquad\qquad 3.2.21$$

Following the procedure of Section I we assume exponential solutions and find that the eigenvalues are

$$r_1{}^2 = \frac{K^2}{2p_0}(2p_0 - A^-) + \frac{\gamma\theta}{2} \qquad\qquad 3.2.22$$

$$r_2{}^2 = \frac{\gamma}{2}\left(\sigma + 1 - \frac{[\sigma-1]A^-}{2p_0 - A^-}\right) \qquad\qquad 3.2.23$$

Substituting these into the determinantal equations we obtain the ratios of the cationic and anionic concentrations

$$\frac{B_1}{A_1} = -1 + \frac{A^-}{p_0} + \text{terms in } \Delta \qquad\qquad 3.2.24$$

$$\frac{B_2}{A_2} = 1 + \frac{2\gamma}{K^2}\frac{p_0}{p_0 + n_0}\left(\frac{\sigma - 1}{\sigma}\right) \qquad\qquad 3.2.25$$

and therefore the form of the electric field is

$$E_1 = \left(2 - \frac{A^-}{p_0} + \text{terms in } \Delta\right)\frac{FA_1 \sinh r_1(x-L')}{\epsilon r_1} + \frac{2\gamma p_0(1-\sigma)FA_2}{K^2(p_0+n_0)\epsilon r_2}$$

$$\sinh r_2(x-L') + E_\infty \qquad\qquad 3.2.26$$

The voltage drop due to the diffusion term is proportional to $(\sigma - 1)$ as it was before and we conclude therefore that unless the mobilities differ, there will be no polarization voltage developed due to this term. The mere existence of a fixed

charge is not sufficient to guarantee polarization. The primary cause is the mobility differences. If the mobilities are different, the A^- value has an effect on the magnitude of the charge separation term since the denominator is $2p_0-A$ and a larger A^- value increases this term.

The solution for this kinetic model could be carried through for charged membranes exactly as for the previous system where the membranes were not charged. The algebra is even more complicated, however, and probably the results are not significantly different. This algebra has not been worked through.

We have mentioned that the results of the kinetic model are in complete agreement with those from the quasi-steady state analysis of membranes as regards to the maximum possible frequency effect. This quasi-steady state analysis can also be used to study the maximum frequency effects of charged membrane systems.

Quasi Steady State Analysis of Charged Membranes

The system to be analysed is that shown in Figure 3.8. For convenience we will redraw this system in Figure 3.8 and stress the details of the concentration profiles.
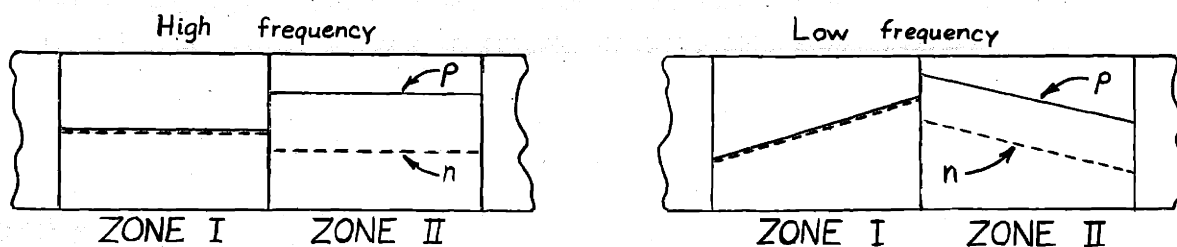
Figure 3.8: Concentration gradients in charged membranes.

Zone I has no fixed charges and p and n are equal in both the static and quasi steady state case.

Zone II contains fixed charges of concentration A^- so p and n differ by this amount in the static case. The changes in p and n brought about in the quasi steady state must be the same however since the fixed charge remains constant. If p and n did not change in the same manner, charge separation would occur.

We denote the change in p and n between these two states by Δp, Δn and in particular use these symbols to represent the charge at the boundary; i.e. Δp and Δn are not functions of x. We also assume that these changes are small.

We further assume that at the common boundary the total concentrations satisfy a Donnan condition even in the quasi-steady state so that

$$(p_1 + \Delta p_1)^2 = (p_2 + \Delta p_2)(n_2 + \Delta p_2) \qquad 3.2.27$$

$$p_1^2 + 2\Delta p_1 = p_2 n_2 + \Delta p_2(p_2 + n_2) \qquad 3.2.28$$

But we have already assumed that the static concentrations satisfy a Donnan condition so that

$$p_1^2 = p_2 n_2 \qquad 3.2.29$$

Therefore

$$\Delta p_1 = \frac{\Delta p_2 (p_2 + n_2)}{2p_1} \qquad 3.2.30$$

The boundary conditions are that the individual currents be continuous and the condition 3.1.50 on the total voltage. The unknowns are Δp_1, E_1, E_2.

When the algebra is worked through we find

$$E_1 = \frac{\Delta p_1 D_1}{u_1 p_1 \Delta L_1} \frac{\sigma_2 n_2 + \sigma_1 p_2 + 2p_1 A \frac{\sigma_2}{B}}{\sigma_2 n_2 - \sigma_1 p_2} \qquad 3.2.31$$

$$E_2 = \frac{2\Delta p_1 D_1}{u_2 \Delta L_1} \frac{\left\{\sigma_1 + \frac{(\sigma_2 + \sigma_1)A p_1}{B(p_2 + n_2)}\right\}}{\sigma_2 n_2 - \sigma_1 p_2} \qquad 3.2.32$$

$$\Delta p_1 = \frac{FV}{RT} \frac{\sigma_1 p_2 - \sigma_2 n_2}{\frac{\sigma_2[3p_1^2 + n_2^2] + \sigma_1[3p_1^2 + p_2^2]}{p_1[p_2 + n_2]} + 2\sigma_2 \frac{A}{B} + 2\sigma_1 \frac{B}{A}} \qquad 3.2.33$$

The low and high frequency impedances are easily found and from them the maximum frequency effect is found to be

$$\frac{Z_{D.C.}}{Z_{A.C.}} = \frac{\theta_1 \left\{\frac{\sigma_2[3p_1^2 + n_2^2] + \sigma_1[3p_1^2 + p_2^2]}{2p_1(p_2 + n_2)} + \sigma_2\frac{A}{B} + \sigma_1\frac{B}{A}\right\}}{\left\{1 + \frac{\sigma_1 \theta_1 p_1 B}{(p_2 + \sigma_2 n_2)A}\right\}\left\{\frac{\theta_1 \sigma_2 A}{B} + \frac{p_2}{p_1} + \sigma_2 \frac{n_2}{p_1}\right\}} \qquad 3.2.34$$

It should be noted that this solution reduces to the previous one if we let the fixed charge go to zero.

If the mobilities do not differ in both zones, the solution predicts no frequency effect regardless of the fixed charge concentration. This result is readily understood if we think in terms of diffusion potentials for these cannot be set up unless the ions diffuse at different rates.

If the mobilities differ, the solution predicts

rather small effects ($\approx 1\%$) until the mobility difference is quite large.

It appears, therefore, that the primary cause of polarization must be mobility differences and not fixed charges.

Admittedly there are many unsatisfactory aspects of these analyses. For the uncharged case the model assumptions are reasonable but the restriction which we have been forced to impose in the charged case, that of small fixed charge, is not so reasonable and it is difficult to estimate just how much relaxing this constraint would affect the result. It appears, however, that the generalization we have made above for the case of equal mobilities in each zone must still be valid.

CHAPTER IV

EXPERIMENTAL STUDIES ON POLARIZATION IN MEMBRANE SYSTEMS

The theoretical studies presented in Chapter III have predicted significant polarization effects in membrane systems. Very little experimental data concerning these effects has been reported previously, however.

Vacquier et al (1957) and Henkel and Van Nostrand (1957) have made laboratory measurements on clay systems and found important polarization effects. Vacquier et al made their measurements on sand-clay systems while Henkel and Van Nostrand made their measurements on pure clay masses. These experimental meausrements were made in the time domain.

In spite of the extensive experimental investigations which have been made on artificial membranes such as ion exchange resins, very little mention has been made of polarization effects in these systems. The conductivity measurements made on these systems are usually carried out at 60 cps and 1000 cps, the results usually agreeing within a few percent. This frequency spread is not sufficient to adequately sample the polarization effects of these membrane materials.

In order to better appraise the theory and to determine the importance and character of clay polarization, an experimental study was made of polarization in some pure clay systems. Additional measurements were also made on ion exchange resins.

Section I: CLAY SYSTEMS

The measurements on clays were carried out in co-operation with Mr. H. W. Olsen of the Soil Mechanics Department, M I.T. Mr. Olsen is engaged in a study of the influence of structure on the permeability of clays and his experimental studies involve the compaction of various pure clay systems to pressure ranging from 1 ton/ft^2 to 256 tons/ft^2. Measurements of permeability, void ratio, streaming potential and conductivity are made at each increment in the loading cycle. Through conversations with Mr. Olsen, we became interested in also studying the induced polarization effects of these systems. It was felt that the combination of these several measurements would give quite good control on the structural models which might be used to explain the results. The interpretation of the results will appear in Mr. Olsen's Ph.D thesis. In this discussion, we will present some of the induced polarization results only.

Sample Preparation

Most of the samples tested were kaolinite clays. The kaolinite came from Bath, South Carolina. The powdered kaolinite was mixed with an excess of NaCl in solution to render the clay homoionic to sodium. After this treatment, the supernatant fulid was diluted to a concentration of .0001 Normal. The flocculated samples were prepared by adding this slurry directly to the sample holders and compacting it.

The dispersed samples were prepared by adding .02% by

weight of trisodium polyphosphate per gram of supernatant fluid to a portion of the above material.

One sample was prepared consisting simply of the natural kaolinite in distilled water.

The effective conductivity of the supernatant fluid in the flocculated sample is about 8×10^{-6} mhos/cm and for the dispersed samples supernatant it is about 2×10^{-4} mhos/cm.

In all cases, the supernatant fluid was retained for use as the permeant in the permeability measurements.

Polarization Measurements

The polarization measurements were made using both transient measurements and variable frequency measurements. The equipment and analysis have been described in a report (Madden and Marshall 1958). The transient measurements gave information evaluated at .1, 1, and 10 cps, while the frequency domain measurements covered the range of 10-20,000 cps. The oscillator used was battery operated and could be operated above electrical ground, so that a four electrode system could be used. This was necessary to prevent polarization of the receiving electrodes, as the clay samples were very conductive, and the electrode polarization had to be kept to an absolute minimum.

The clay samples were placed in a plastic cylinder and closed off by porous plugs. The compressive load was applied across the sample by a plastic piston which had provision for allowing the excess water to pass on through. The receiving

FIG. 4.1 FREQUENCY SPECTRA OF KAOLINITE SYSTEMS
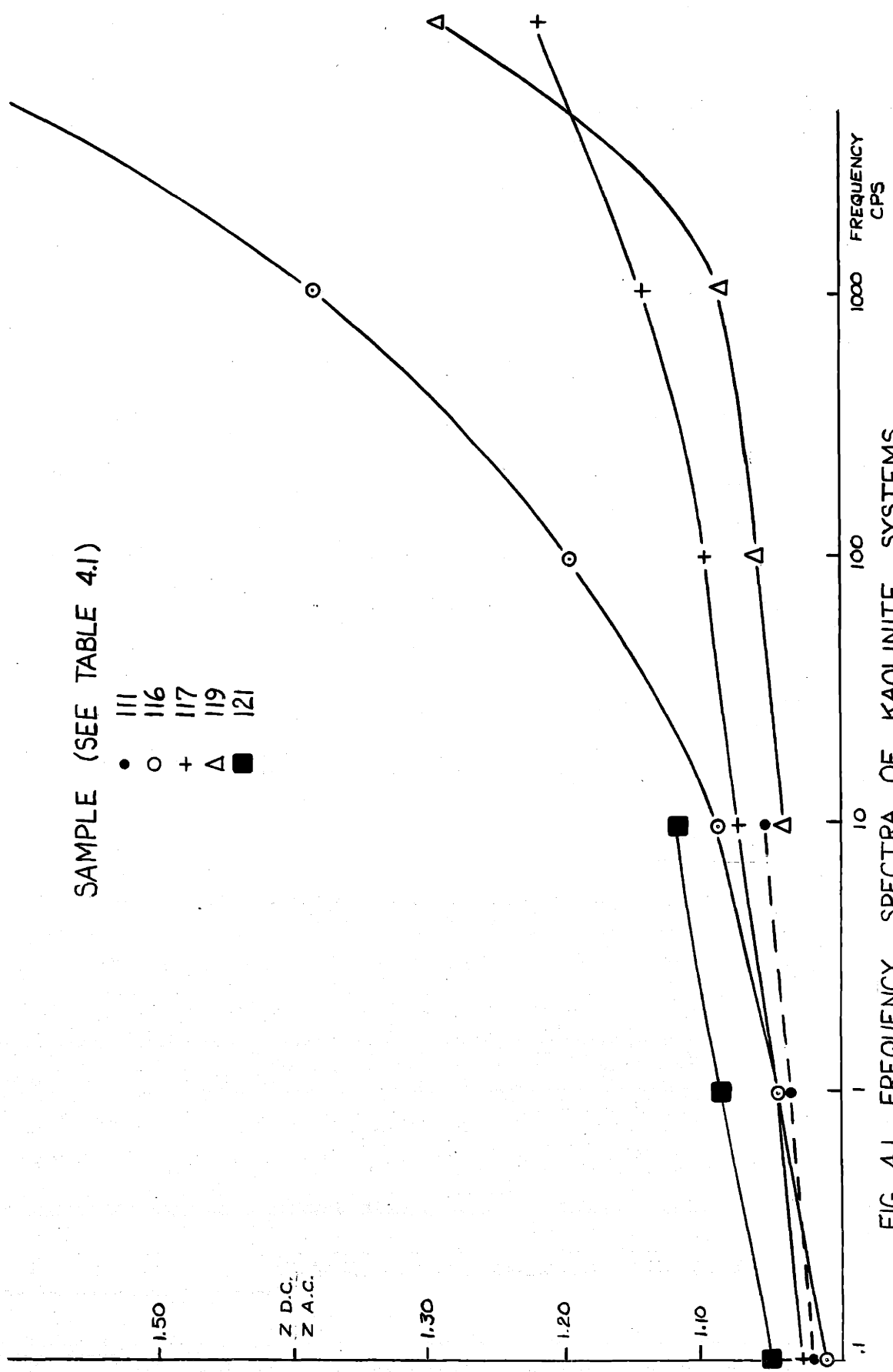
SAMPLE (SEE TABLE 4.1)

●	111
○	116
+	117
△	119
■	121

FREQUENCY CPS

Z D.C.
Z A.C.

98
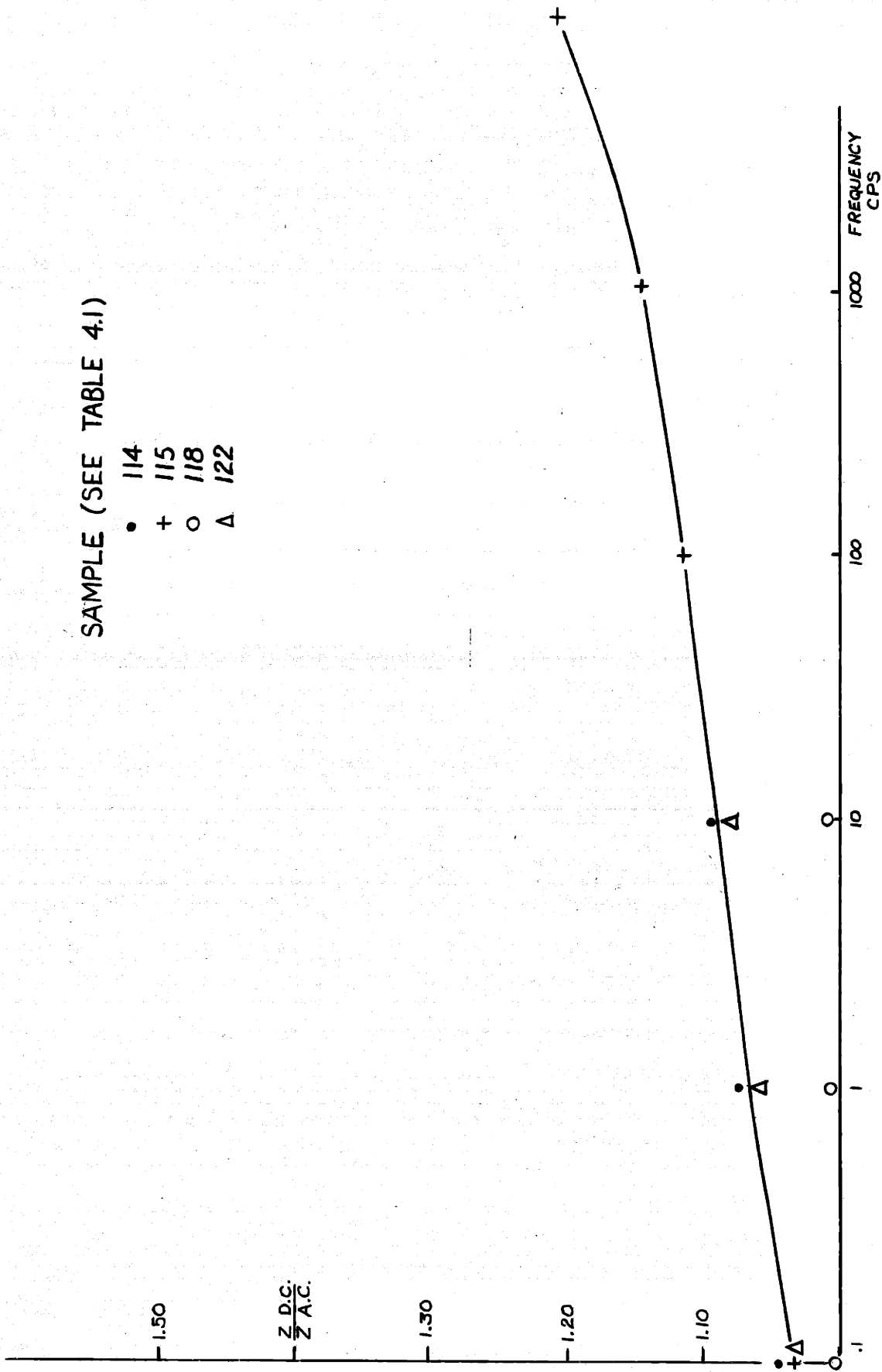
FIG. 4.2 FREQUENCY SPECTRA OF KAOLINITE SYSTEMS

TABLE 4.1

SUMMARY OF INDUCED POLARIZATION MEASUREMENTS ON CLAY SAMPLES

(All results are for load increments of 4 tons/sq.ft. unless otherwise noted.)

Sample	f(10) $\frac{Z(D.C.)}{Z(10cps)}$	mf(10)	in degrees	in ohm. ft.	$\rho/2\pi$ mvs/v	permeability in M.K.S. units
Kaolinites, Na form in .0001 Normal NaCl						
111	1.045	47	18°,25,52	96	63.4	1.06x10^{-13}
117	1.101	144	8,10,17	70	76.5	1.00x10^{-13}
119						.90x10^{-13}
121	1.171				141.5	1.08x10^{-13}
Kaolin, Na form dispersed in .02% NaTP						
115	1.106	279	6,12,22	38	94.7	.90x10^{-13}
118	1.010	43		36		.67x10^{-13}
120						.70x10^{-13}
122	1.113				93.2	.58x10^{-13}
Kaolin, natural form in distilled water						
116	1.096	33	14,29,36	287	48.9	1.64x10^{-13}

TABLE 4.1 (continued)

SUMMARY OF INDUCED POLARIZATION MEASUREMENTS ON CLAY SAMPLES

(All results are for load increments of 4 tons/sq.ft. unless otherwise noted.)

Sample	f(10)	mf(10)	mfθ	ρ/2π	mvs/v	permeability
Kaolin, Na form in .1N NaCl						
112	1.047	1470	15,22,30	3.2	63.	1.06×10^{-13}
*113	1.048	1780	6,10,17	2.7	31.3	$.90 \times 10^{-13}$
Micas, .001 Normal NaCl						
211	1.049				42.	1.05×10
Micas, Dispersed						
212	1.110				123.6	1.92×10
Illite, .0001 Normal NaCl						
312	1.100					

*1 ton/sq. ft. load

electrodes were placed within the porous plugs at the ends of
the clay mass, and remained there during the compression.

Results

      The results of the measurements on kaolinite are pre-
sented in Figures 4.1, 4.2 where the frequency effects only
are plotted. Phase shifts were obtained from the numerical
analysis of the pulse data but they are usually small, of the
order of 1 degree, and are not shown in detail. They are
listed along with the metal factors and various other data in
Table 4.1.

      The parameters referred to in this table are useful
in the geophysical interpretation of induced polarization
measurements and are described elsewhere   (Madden and
Marshall 1958)   The ones of most interest here are simply
the polarization magnitude F (10), which represents the ratio
of the D.C impedance to the 10 cps. impedance of the sample,
the electrical resistivity ρ, and the permeability.

      All the above data were chosen at the load increment
of 4 tons/sq.ft. unless otherwise noted. Surprisingly, there
was no significant trend noted in the dependence of the fre-
quency effects on compression in most of the samples.

      The frequency effects observed are quite important,
some being of the order of 20% at 1000 cycles and still rising.
These effects are apread out over a tremendous frequency range
compared to the theoretical model. This is not too surprising,
however, because the natural system must consist of a distri-

bution of lengths of clay particles and this distribution will tend to destroy the sharper features of the impedance curves.

The curve for natural kaolinite in distilled water is dramatically different from that for the other flocculated samples and the reason for this is not as yet known. The conductivity of this specimen is much less than the others due to a smaller salt concentration but our theoretical results indicate that conductivity should not have any effect on the percentage of the polarization effects. The natural clay is thought to contain a great deal of calcium on the exchange sites and this may result in a significantly different structure being formed (note that the permeability is greater for this sample than for the others). The difference in the salt concentrations between the natural sample and the other samples may also have an influence on the structure

In order to check the possible influence of calcium ions, a system of kaolinite homoionic to calcium and of a .01 normal concentration was prepared. This system was found to have no frequency effect.

On the basis of this result we are forced to conclude either that the salt concentration has an important effect on structure or that there are other influences which we have not considered that are important. We have a very limited amount of evidence, unconfirmed as yet, that polarization properties of flocculated samples change dramatically upon the appli-

cation of a very small amount of shear stress. It is well known, of course, that the mechanical properties of flocculated clays are quite dramatically influenced by shear in the case of the so-called sensitive clays.

Mr. Olsen believes much of the mechanical and electrical data on these clay systems can be explained by an aggregate composition of the clay mass.

We are not primarily interested in pursuing the details of clay structures in this report. Our primary objective has been to determine whether clays have important polarization effects and we have shown that this is so even though a complete understanding of the structural influence has not yet been obtained.

Some of the difficulties with structure are less pronounced in the type of system used by Vacquier et al (1957). They produced artificial dirty sands by circulating clay slurries through a system of sand particles letting the slurry dry so that the clay particles adhered to the surfaces of the sand grains. Then they reintroduced an electroltye and made their measurements. Their structure is controlled primarily by the sand grains and not by the clay properties.

As pointed out earlier, most of the frequency spectra are too spread out to facilitate comparison with the theoretical model curves. The curve for natural kaolinite in distilled water, however, does show a definite inflection which suggests that the majority of the selective zone lengths are

similar. We can compare this experimental curve with those for the theoretical model, Figure 3.3, and make an estimate of the effective zone lengths. We assume that the point of maximum change on the experimental curve is at 1000 cps. If the A value is about 1, this would predict a selective zone length of about 20,000 Angstroms. This is of the order of magnitude of the length of the individual kaolinite particles which, according to Lambe (1958), are approximately 10,000 Angstroms by 1000 Angstroms. This estimate is close to the upper limit on the length also, because any other value of A (which must be greater than 1 in order to explain the large frequency effect) or a decreased value for the diffusion coefficient would decrease the predicted length. In terms of the clay structure, this means that we are sampling the fine details of the clay structure.

Kaolinite particles are the largest among the common clay types, illite and montmorillonite being perhaps 10 times smaller in size. This means that the frequency range in systems of these particles may be pushed even higher, perhaps to as much as 100 KC. This is quite out of the range of practical geophysical interest of course, but measurements may have to be extended to these frequencies to test the validity of this model in clay systems.

Section 11: IMPEDANCE MEASUREMENTS ON SYNTHETIC MEMBRANES

A limited number of experimental impedance studies were carried out on synthetic membrane materials. The

materials used were cation exchange resins of various mesh sizes. These materials are more suitable for these studies than the clays because they are more nearly homogeneous and also approach very closely the ideal behavior of a perfectly selective zone. In addition, the structure factor, which is so serious in the interpretation of the results in clays, is more easily controlled since the beads are all spherical. These materials have been used by Wyllie and his co-workers at Gulf Research and Development Company (Wyllie and Southwick, 1954; McKelvey et al, 1955; Sauer et al, 1955) as electro-chemical models of dirty sands.

EXPERIMENTAL PROCEDURES

The ion exchange resins used were Dowex-50 (cross-linked by 8% divinyl benzene) in the 20-40 mesh size and Dowex-50W, similar to Dowex-50, in the size range less than 400 mesh. The 20-40 mesh size corresponds to a particle diameter between .042 and .084 cm. The 400 mesh size has a diameter of .0037 cm.

The ion exchange resins were wet sieved and then mixed in a beaker with a saturated solution of the chloride of the salt to be used. Several volumes of solution were used and the resin was allowed to remain in each washing for approximately five minutes except in the very fine sizes where of course it took longer for the resin to settle out. This process was repeated with demineralized water and then with a dilute solution of the salt of the concentration de-

sired for the actual run. The resin-solution mixture was then poured into a column and allowed to settle out slowly.

Backwashing of the column was not done but since the column was initially filled with fluid it is unlikely that any air bubbles were entrapped. The resin was poured in slowly enough that it is also unlikely that channeling was serious.

Electrodes were inserted at the ends of the column and the impedance of the column was measured at audio and subaudio frequencies. The current density used was of the order of .03 ma/cm, which, according to the theoretical model, was low enough to insure a linear behaviour for the system. The measurement system is described in a previous report (Madden and Marshall, 1958, pp.10).

Silver chloride electrodes, prepared as described previously (Madden and Marshall, 1958), were used. The contribution of the electrodes to the total measured impedance was evaluated by measuring their impedance after the run was completed. They were removed and placed in a small reservoir filled with the same solution used in the resin column and their impedance measured in exactly the same manner as the resin impedance was measured. Usually the electrode impedances amounted to less than 3 to 4% of the total impedance and the change in their impedance was also about this same percentage of the total impedance change.

Measurements were also made on the resins at higher

temperatures, the resin column being heated by circulating hot water through the jacket in which it is enclosed. This jacket encloses only 65-70% of the total length of the column so that the results indicate only the order of magnitude and the direction of the temperature coefficients of impedance and polarization.

The results of the measurements on resins are shown in Figure 4.3-4.6. Amplitude, phase, and frequency effect data are shown for each sample. The amplitude data is presented in the form of the actually measured impedance values but the high frequency specific conductivity is also listed. The amplitudes of the impedances are probably accurate to within 10% allowing for measurement error and the electrode impedances. The phase data is less accurate because of the small phase shifts encountered and is probably only within 15-20%. The accuracy in both the amplitude and phase is considerably less at the very low frequencies, particularly at .03 and .01 cps.

The frequency effects were computed relative to the .01 reading. In cases where the .01 value was obviously not accurate, an extrapolated value was used as indicated.

RESULTS

These results show that the ion exchange resins are more useful experimental models than the clay systems. The impedance characteristics are somewhat sharper than those for the clays though they are by no means as sharp as the

DOWEX 50, 20-40 mesh

INTERSTITIAL SOLUTION, .012 N NaCl
SPECIFIC CONDUCTIVITY (1000 cps)

.0084 Ω^{-1}cm^{-1} at 25°C
.0121 Ω^{-1}cm^{-1} at 48°C

FIG. 4.3 FREQUENCY SPECTRA OF ION EXCHANGE RESIN IMPEDANCES

DOWEX 50, 20-40 mesh

INTERSTITIAL SOLUTION, .012 N NaCl
SPECIFIC CONDUCTIVITY (1000 cps)
.0084 Ω^{-1}cm^{-1} at 25°C
.0121 Ω^{-1}cm^{-1} at 45°C
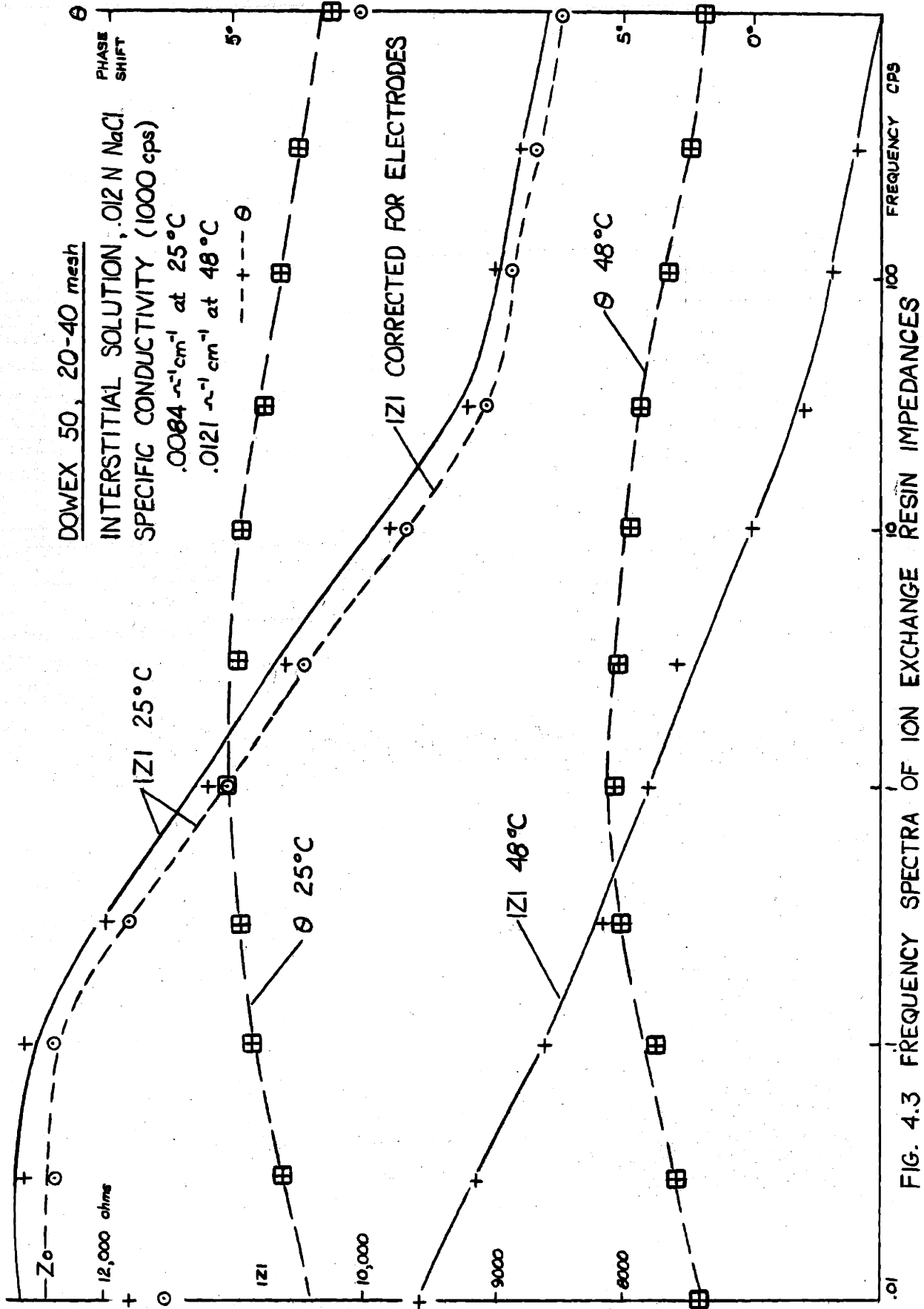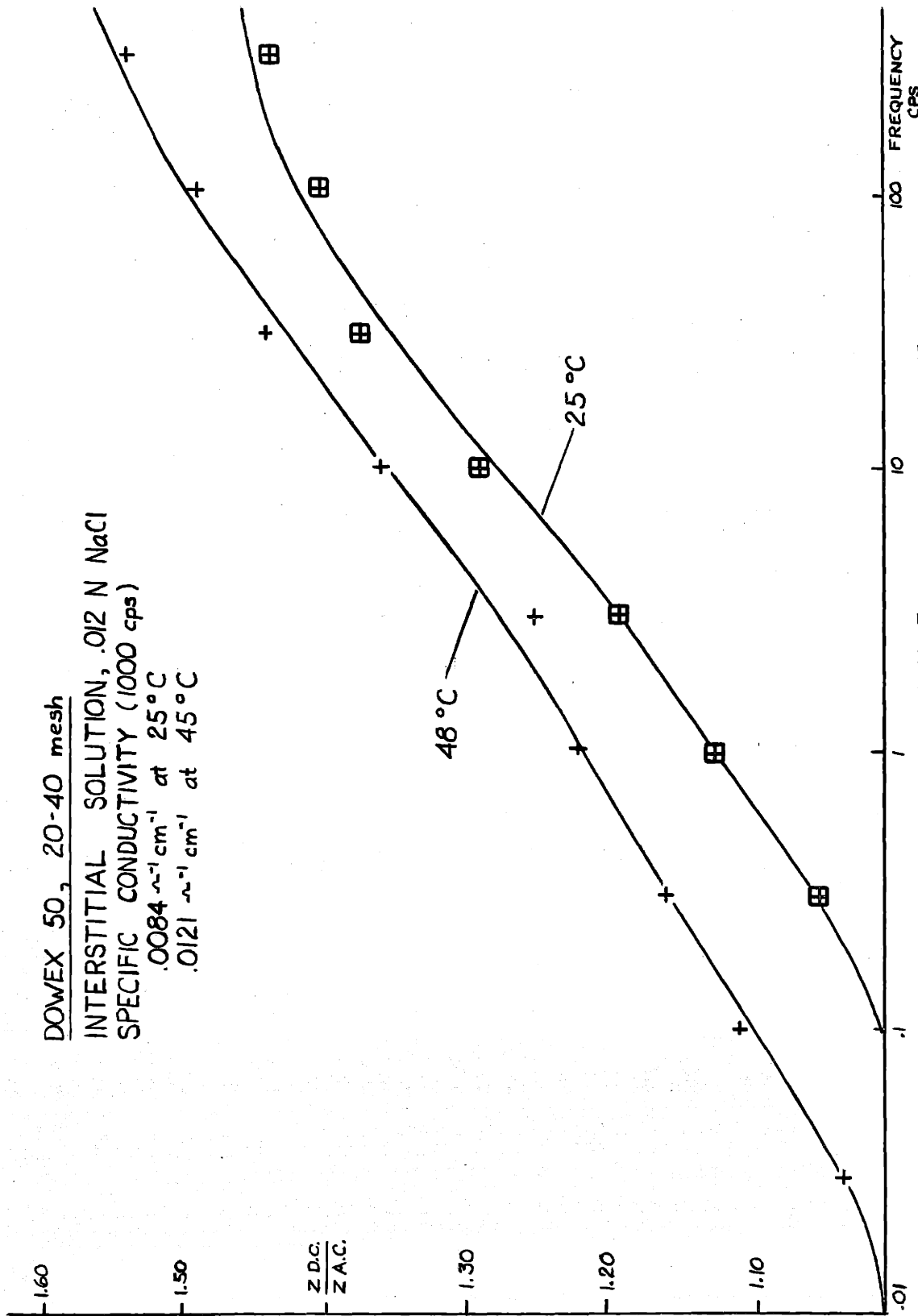
FIG. 4.4   FREQUENCY   SPECTRA   OF   ION   EXCHANGE   RESIN   IMPEDANCE

FIG. 4.5   FREQUENCY SPECTRA OF ION EXCHANGE RESIN IMPEDANCES

DOWEX 50, 20-40 mesh

INTERSTITIAL SOLUTION, .010 N KCL
SPECIFIC CONDUCTIVITY (1000 cps)
.0107 Ω⁻¹ cm⁻¹ at 27.5°C
.0145 Ω⁻¹ cm⁻¹ at 45°C

DOWEX 50, 20-40 mesh

INTERSTITIAL SOLUTION, .010 N KCl
SPECIFIC CONDUCTIVITY (1000 CPS)
.0107 Ω^{-1} cm^{-1} at 27.5°C
.0145 Ω^{-1} cm^{-1} at 45°C
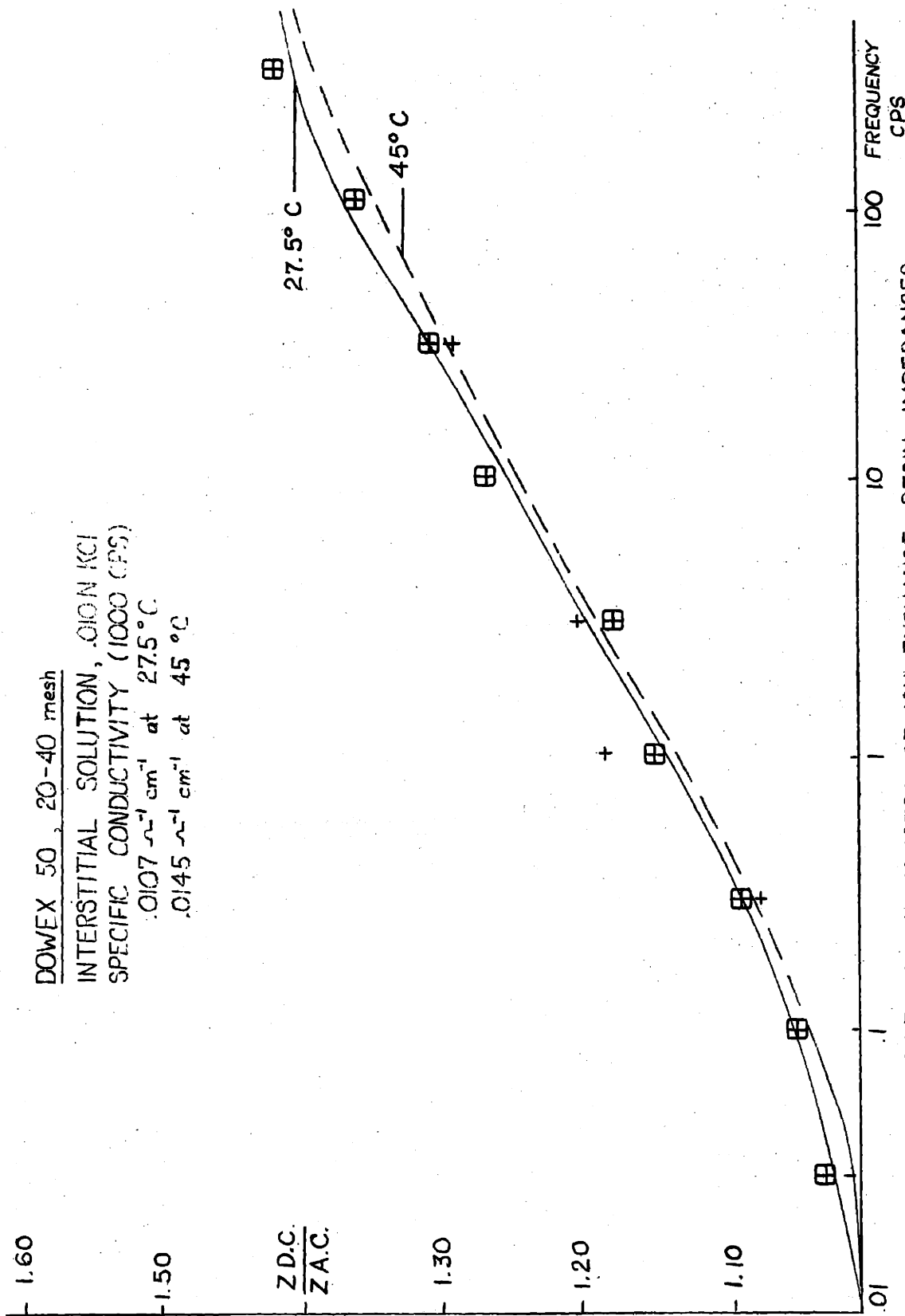
FIG. 4.6   FREQUENCY SPECTRA OF ION EXCHANGE RESIN IMPEDANCES

corresponding curves for the theoretical model. The effective zone length in the resins is more favorable also for both the low and high frequency ends of the impedance curves are fairly well defined in contrast to the clays where it appeared that we were sampling, principally, the low frequency part of the impedance spectra.

The maximum frequency effects do not differ very much between the KCl treated and the NaCl treated resins though they are slightly larger in the Na resin. The theoretical model predicts that, all other things being equal, the Na treated resin should have 1.5 times the frequency effect of the K treated resin. Since we do not observe this great a difference we must look for differences in some of the parameters.

The potassium chloride and sodium chloride solutions which we used had equal conductivites. The potassium-resin system has a larger conductivity, however, so the potassium resin must be the more conductive of the two. This increased conductivity might be attributed to a 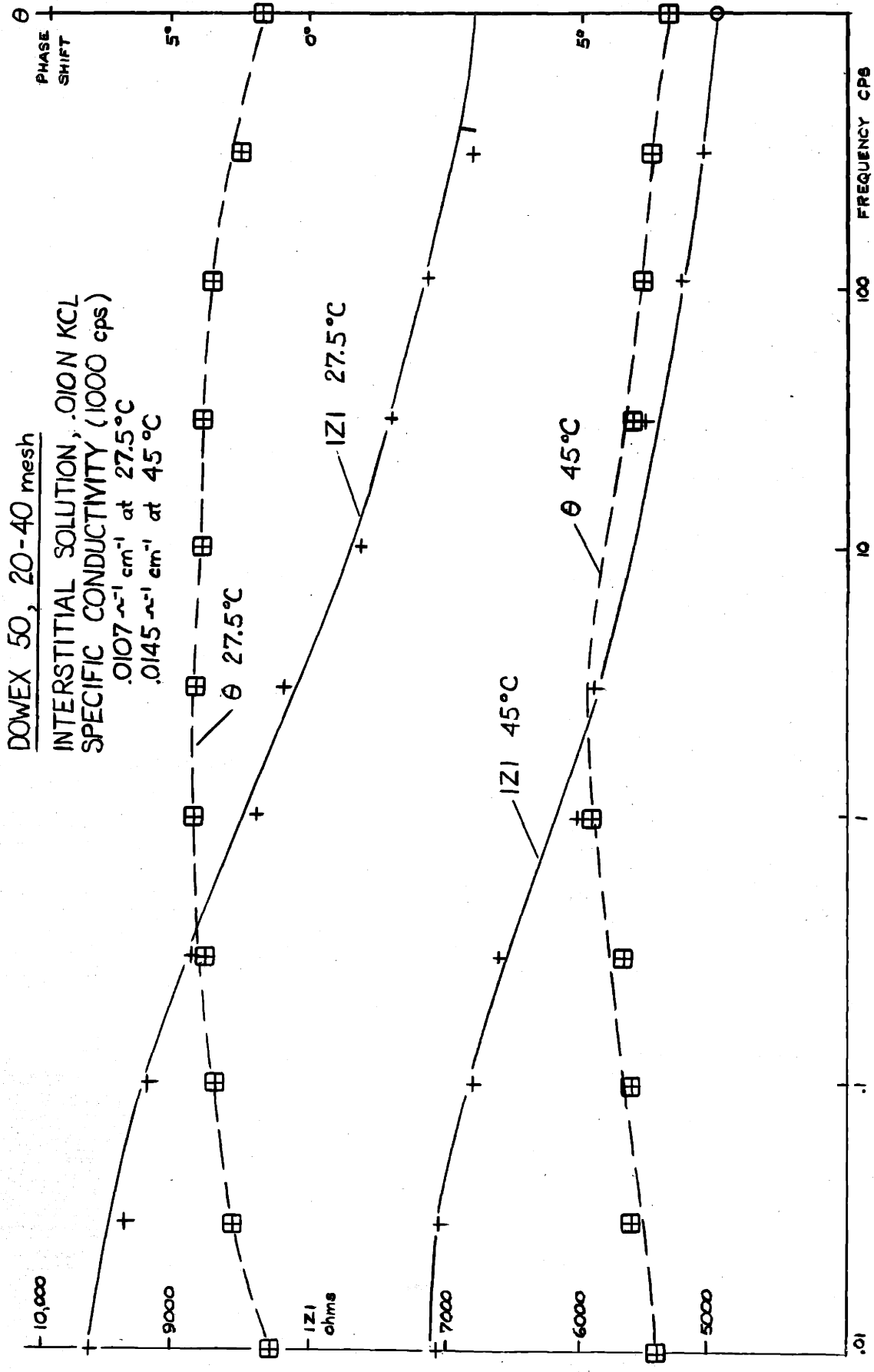larger diffusion coefficient for the potassium or to a larger concentration of potassium within the resin. The first possibility, that is a greater mobility for the potassium than for the sodium, predicts a smaller B value for the potassium resin and this is in the right direction to account for the observed effect. If this possibility existed, the τ values would be smaller for the potassium resin also and this likewise is in the direction

to explain the observed effect.

The impedance measurements can be used to estimate the effective zone length in the resin-fluid system. The maximum effect for the potassium treated resin is about 50%. This requires an A value of 2 to 5 if the diffusion coefficients are equal in both zones and a larger A value if the diffusion coefficient within the selective resin zone is smaller than that in the solution. For the purposes of this estimate, we shall assume that the effective zone length is bracketed between the lengths predicted using A values of 1 and 10. The maximum phase shift in Figure 4.5 is at 3 cps. This is about the same as the corresponding point on the curve for A = 10 in Figure 3.4. This predicts an effective zone length of about .0003 cm. therefore. If we assume that the A value is much smaller and use the curve for A = 1 we find that the effective length is increased to .003 cm. Therefore the effective selective zone length is bracketed between .0003 and .003 cm.

These values for the zone length do not correlate with any apparent property of the resin particles. The particles themselves are much larger than this. It is generally agreed also, on the basis of electron microscopy, X-Ray and other data, (Nachod, 1949) that the individual particles are essentially a homogeneous network of molecules and the irregularities are on the molecular scale. Our results indicate that the resin particles must have inhomogeneities on a larger

scale than this.

A confirmation of this conclusion was obtained when measurements were made with very small resin particles. Measurements were made on Dowex 50W, which is similar to Dowex 50, in the size range smaller than 400 mesh. These particles are smaller than .004 cm, so that the inhomogeneities inferred in the larger resins should be missing in the small particles. Since the particles are in close packing, one could expect the effective A ratio to be very small, most of the conduction path being in the resin zones. This then should result in eliminating any polarization effect in the resin column. The measurements confirmed these ideas, as no impedance variation was observed from .01 to 1000 cps.

This result is of course based on the assumption that the two electrical zones are an anion selective conducting zone, and a neutral or unselective water zone. If cation selective resins were also included, a very strong polarization effect could result from the alternating cation and anion selective zones, even though the individual resins gave no polarization effect. If the current was forced to pass through such alternating zones the polarization effects could in principle become extremely large and virtually prevent any further current flow. In practice, however, the mixture will be in a random arrangement so that the electric current flowing from one resin bead has a possibility of continuing on through another bead of the same properties. Statis-

tically one should expect that 1/4 of the high frequency
current flow would pass through an all anion exchange resin
path, 1/4 through on all cation exchange resin path, and
1/2 through a mixed path. In such a situation the maximum
polarization effect would again be limited to a two fold
increase of the impedance at the low frequencies.

Some measurements were made on just such a system.
The results of these measurements, shown in Figure 4.7, are
very similar to the predictions previously mentioned. The
mixture came very close to attaining the 2:1 maximum expected
impedance ratio. To point out the effect of the mixing on the
polarization, the impedance that would be expected from the
sum of the two resin systems without any mixing effect, is
also shown in the same figure.

The temperature effect in the resin systems is not con-
sistent, sometimes increasing and sometimes decreasing the
frequency effects. This behavior, we believe, can be ac-
counted for by the fact that two variables are being influ-
enced and these operate in different directions on the fre-
quency effect. The first factor which is being influenced
is σ, the selectivity coefficient. We would expect this
quantity to increase towards unity as the temperature is
raised for the energy barriers involved in causing the selec-
tivity become less important. This effect would decrease the
maximum observed frequency effect. The diffusion coefficient
within the membrane is usually smaller than the value in
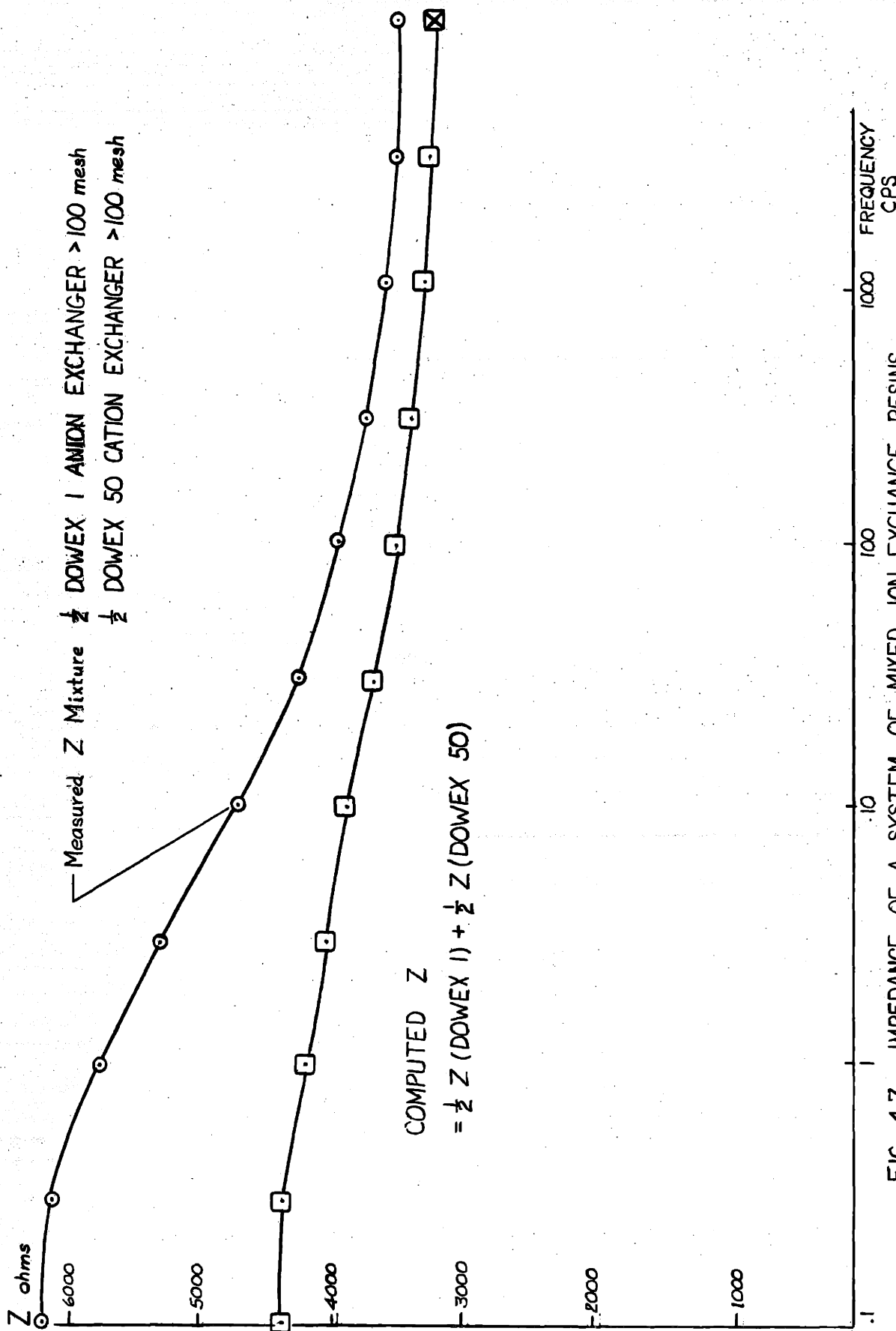
FIG. 4.7   IMPEDANCE OF A SYSTEM OF MIXED ION EXCHANGE RESINS

solution. Using the concept of activation energy, this
means that the activation energy associated with diffusion
in the resin is larger. This in turn means that the tem-
perature coefficient of the diffusion coefficient within the
resin is larger and therefore increasing temperature will
tend to decrease the ratio of the diffusion coefficients
which is the quantity which we have defined as B. As we
have seen, decreased values of B will increase the maximum
frequency effect.

While these studies on ion exchange resin systems
have not been exhaustive they have illustrated several
applications of the diffusion polarization model and reason-
able agreement has been shown between the experimental results
and the model predictions. Unfortunately, as we have noted,
there are several variables operating and this makes it much
easier to obtain a fit with the experimental data. It would
be desirable to have a much more thorough experimental study
made on the ion exchange resin systems. This would put
stricter limits on some of the variables and make a better
test of the theoretical model.

These studies as well as those on the clay systems do
point out the very real contributions to electrical polariza-
tion phenomena that membrane systems can exert.

CHAPTER V

STUDIES ON ANOMALOUS NATURAL ROCK SAMPLES

During the past several years, a great number of induced polarization measurements have been made in this laboratory on natural rock samples of various types. The techniques used in these measurements and a compilation of the results are included in an interim report to the Atomic Energy Commission (Madden and Marshall, 1958)

In the course of these studies, a number of anomalous samples were found. These are the samples with important polarization effects but no apparent metallic mineral content. It is well known, of course, that metallic minerals have predominant polarization effects and rocks containing them can not usually be considered anomalous.

The possibility was considered that the polarization effects in the anomalous samples are due to membrane polarization effects associated with their clay mineral content. In the previous chapter we have shown experimentally that pure clay systems can have significant polarization effects in agreement with the work of Vacquier et al (1957) and Henkel and Van Nostrand (1957). Their importance when they occur in minor amounts as altered material or as depositional components of natural rocks has not been adequately demonstrated. In order to evaluate this possibility it was necessary to investigate the mineralogy of the anomalous specimens in some detail. In particular it was necessary to determine their

119

clay content and their metallic mineral content. Both of these determinations can be difficult analytical problems.

In the following section, a summary of the methods used in the mineralogic investigations is presented. In section2, the detailed results and interpretations of several interesting suites of rocks are presented.

Section I. Mineralogical Analysis

CLAY ANALYSIS

Several techniques are used presently for the analysis of clays and other fine grained materials, each of these methods, of course, having its particular advantages and disadvantages in any given problem. The techniques which we considered are differential thermal analysis (DTA), X-ray diffraction, and ion exchange capacity determinations. Other techniques which are available include electron microscopy, petrographic methods, dye absorption, infra-red methods and chemical analyses.

We felt that for primary orientation purposes, a simple determination of the presence or absence of clay material would be sufficient. Later, if desirable, a more detailed analysis could be made to determine the actual clay mineral present. After helpful discussions with Dr. R. T. Martin of the M.I.T. Soil Technology Laboratory, it was decided that DTA would be the most useful tool for these initial studies.

A fairly complete discussion of the application of DTA to the analysis of clays and other minerals is found in

Mackenzie et al (1957). Lambe (1951) has written an excellent introductory discussion and describes in detail the actual equipment used in our analyses.

Most of the common clay minerals are easily recognizable by DTA analysis. They show an endothermic reaction due to the loss of lattice water, with a peak temperature ranging from $500^{\circ}C$ to $750^{\circ}C$ depending on the clay type. Other reactions are shown at lower temperatures due to the loss of adsorbed water and at higher temperatures due to further structural breakdown. However, the loss of adsorbed water depends strongly on the state of the sample before heating and the higher temperature reactions are near the end of the useful temperature range so these reactions were not considered in the interpretations in general.

The near coincidence of the peak temperatures makes it very difficult to distinguish clay types from the DTA work. Kaolinite can sometimes be diagnosed definitely because it has such a large energy difference, approximately 30% of it being equivalent to 100% of the other types.

The system which we are trying to analyze is of course much more complicated than a simple pure clay system. We must in addition worry about possible thermal effects due to the other common rock forming minerals. Lambe's paper contains an excellent summary listing of the thermal effects of some of the common minerals including the oxides, carbonates, and silicates. It appears that the only common minerals with

important thermal effects besides the clays are quartz, the carbonates, carbon and other organic matter, limonite, the sulfides, and bauxite. Of these, the only ones with effects similar to the clays are the carbonates. In all cases, the samples were tested for carbonates prior to the DTA run.

It must be borne in mind that the above statements refer to systems of a single component. Thermograms of mixed systems are not necessarily additions of the individual thermograms. Many cases of interfering effects occur and a good example is the study of Martin (1958) on the interfering effects of hydrous mica on the carbonate reaction in the presence of a small amount of soluble salt. In a later section we will discuss some of our results on pyrite where apparently just changing the concentration of the reactive material can alter the curve shapes and the peak temperatures.

The techniques used in making the DTA analyses are essentially those described by Lamb. The samples were ground to <140 mesh and run on the single block apparatus at a heating rate of 12 1/2 C per minute to a maximum temperature of 1000 C. After cooling, a rerun was made to determine quartz on some of the samples. No atmosphere control was used during the runs, nor was the moisture content of the samples prior to the run controlled.

One basic problem affecting the DTA ayalyses and all the other analyses is the difficulty of obtaining satisfactory

sampling of the rock specimen. In many cases, the rocks contained inhomogeneities which were not randomly distributed and which were large compared to the total rock sample. When these cases occurred every effort was made to select a portion of the rock which was similar to the portion studied electrically. The most satisfactory procedure would have been to grind up the actual sample used for the electrical measurements after these measurements were completed but we did not wish to destroy the original samples at the present time and in addition it would have been necessary to grind a prohibitive amount of sample. Therefore, we were content to use portions of the original sample from which these were cut.

DIFFERENTIAL THERMAL ANALYSIS OF PYRITE

In the course of running the DTA analyses, one sample was observed to have a large exothermic effect with a peak temperature at about 700 C. An investigation of the reference curves indicated that this could be due to pyrite which was known to be present in the sample (heavy mineral analyses indicated 2-3% pyrite). Very little information is available on the analysis of sulfides by DTA, one reason for this being that the decomposition products are quite corrosive on the thermocouples and the sample block. Recently Kopp and Kerr (1957) have designed a system in which the thermocouples and the block are protected by thin alundum cylinders and with this system they have made studies on several of the sulfides. The concentrations which they used varied from 6% to 20%

pyrite. Pyrite present in this amount in a rock sample is easily recognized by hand specimen examination or binocular inspection however and we are more interested in the anomalous samples where the pyrite may be present in concentrations of less than 1%. Since no information could be found on the DTA behaviour of pyrite in this low concentration range we decided to prepare a set of standards for this range and study the thermal behaviour of pyrite.

The standards consisted of pyrite ground to less than 140 mesh and diluted with either alundum or quartz. The quartz used was Ottawa Sand ground to less than 140 mesh. The alundum used was the standard material used in the sample well containing the reference thermocouple. These samples were analyzed using a heating rate of 12 1/2 C per minute and no atmosphere control. The results of these analyses are shown in Figure 51 and, for comparison, the thermogram obtained with pure Ottawa Sand is also shown.

Several interesting features are observed in these results.

In ideal systems like these, pyrite is readily observable by DTA methods even at concentrations of as little as .2%. In light of this result it is somewhat surprising that so little work has been done previously on pyrite, especially since DTA is used very often for analyzing shales and other materials where it is a fairly common constituent and perhaps an important part of the DTA response.

In the alundum-pyrite mixtures, a broad exothermic peak starts at about 450 C$^{\circ}$ and, depending on the concentration, continues to about 800 C$^{\circ}$. This exothermic peak is attributed to the breakdown of the pyrite to sulfur dioxide and iron oxide The same reaction, with slightly different characteristics, is observed in the quartz-pyrite mixtures also. The differences are undoubtedly associated with the fact that the quartz inversion occurs in the same temperature range.

The exothermic peak temperature exhibits a strong concentration dependence and this is attributed to an influence of the gaseous products formed on the reaction rate, pushing the reaction to higher temperatures with higher concentrations.

A smaller endothermic reaction occurs in the samples with the large pyrite content at about 600 C$^{\circ}$ This peak varies uniformly with concentration and its temperature is affected only slightly by concentration changes. We presume, therefore, that this reaction involves transitions between two solid phases. One of these phases must be the original pyrite. That pyrite (or some sulfide) is still present is indicated by the continuation of the exothermic reaction after this endothermic reaction has stopped. In the samples with smaller pyrite concentrations, the pyrite reaction is completed before 600 C. and this endothermic reaction is not observed.

Unfortunately, little information is available on

phase equilibria of pyrite at higher temperatures since normally it can never be brought to these temperatures, completely decomposing at 450 C (at atmospheric pressure) in a very short time. Therefore, this transient phase could not be identified by comparison with previous work.

Kopp and Kerr(1957) have also observed an endothermic reaction in this temperature range for concentrations of 10% or greater. They suggested that this might be due to two separate exothermic reactions occurring. Their ex otherms were so large that the endotherm did not extend completely to the base line and might be interpreted in this way. In our studies, however, the peak observed is definitely endother-mic.

Near the completion of the present studies on pyrite, the results of similar studies were mentioned in an article by Mangold (1958). He presented DTA curves for pyrite in con-centrations ranging from .2% to 20%. He also observed the endothermic reaction but provided no explanation for it.

In one sample, the quartz used was much coarser (100 mesh) than in the others. The thermogram for this sample is quite different from the others exhibiting a large endotherm and a low, broad exotherm. It is difficult to ex-plain this difference, the only apparent variable being the grain size of the quartz and a larger concentration.

Summarizing the DTA results on pyrite we have:

a. Pyrite can be detected by DTA in concentrations

as low as .2% under favorable circumstances.

b. The nature of the DTA response of pyrite
is, primarily, an exothermic peak at approx-
imately 500 C which is due to decomposition
to iron oxide and sulfur dioxide.

c. The peak characteristics depend strongly
on concentration, possibly because the
evolved gas influences the reaction rate.

d. A transient high temperature (600C°)
solid-solid phase transition has been observed
in some cases. The new phase formed has not
been identified.

CARBON ANALYSES

Dr. Dennen and Mr. H. Linder of the Cabot Spectro-
graphic Laboratory, M.I.T. made spectrographic analyses of
several samples in order to estimate their carbon content.
The technique used has been described in the literature,
(Dennen, 1957). These samples showed no carbonate reaction
with dilute HCl so the measured carbon is in the form of
organic carbon or elemental carbon.

ALUNDUM + .25% PYRITE

ALUNDUM + .7% PYRITE

ALUNDUM +
2.6% PYRITE

QUARTZ +
4.6% PYRITE

EXOTHERMIC
REACTION
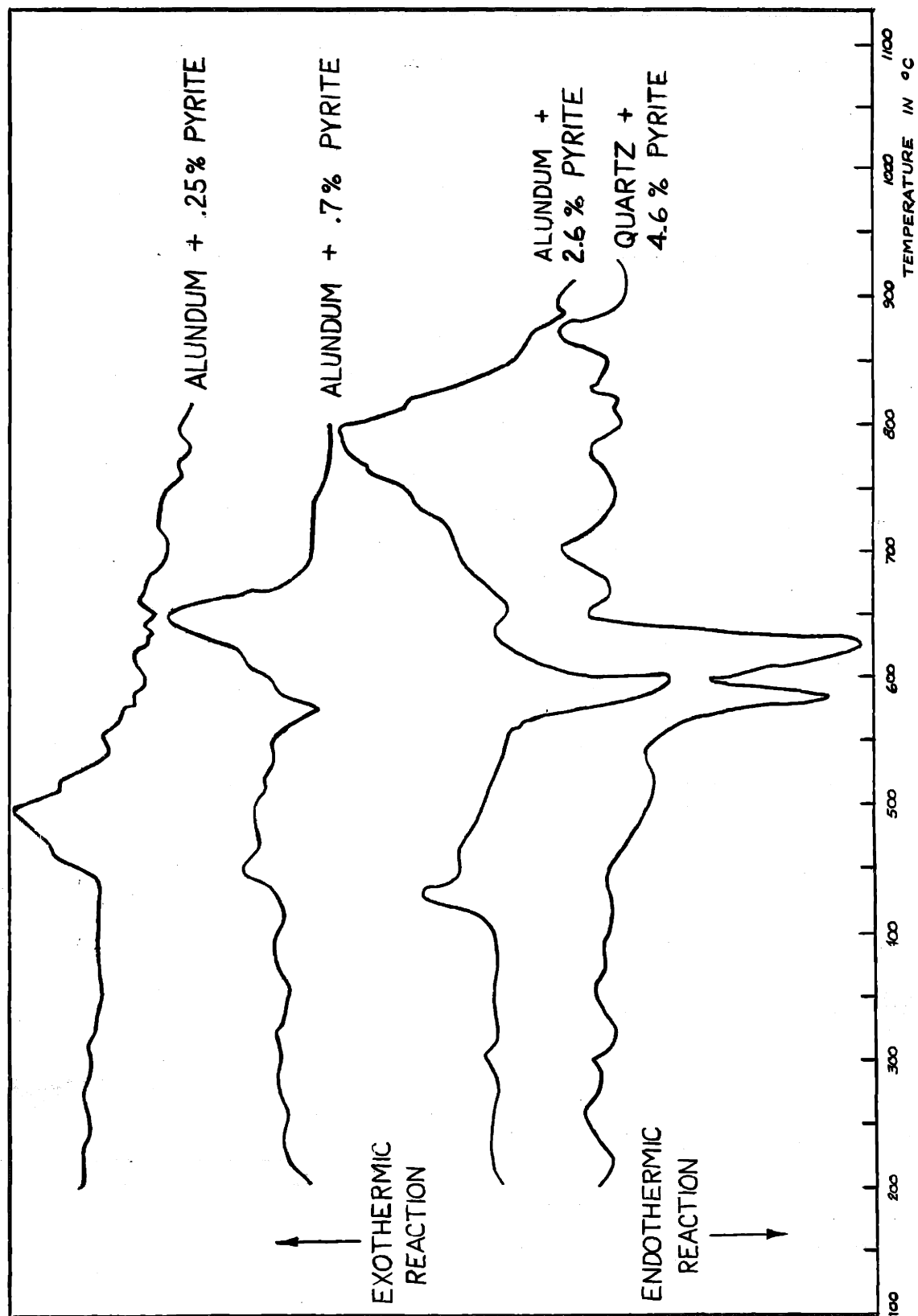
ENDOTHERMIC
REACTION

TEMPERATURE IN °C

FIG. 5.1a   DIFFERENTIAL THERMAL ANALYSIS OF MIXTURES CONTAINING PYRITE
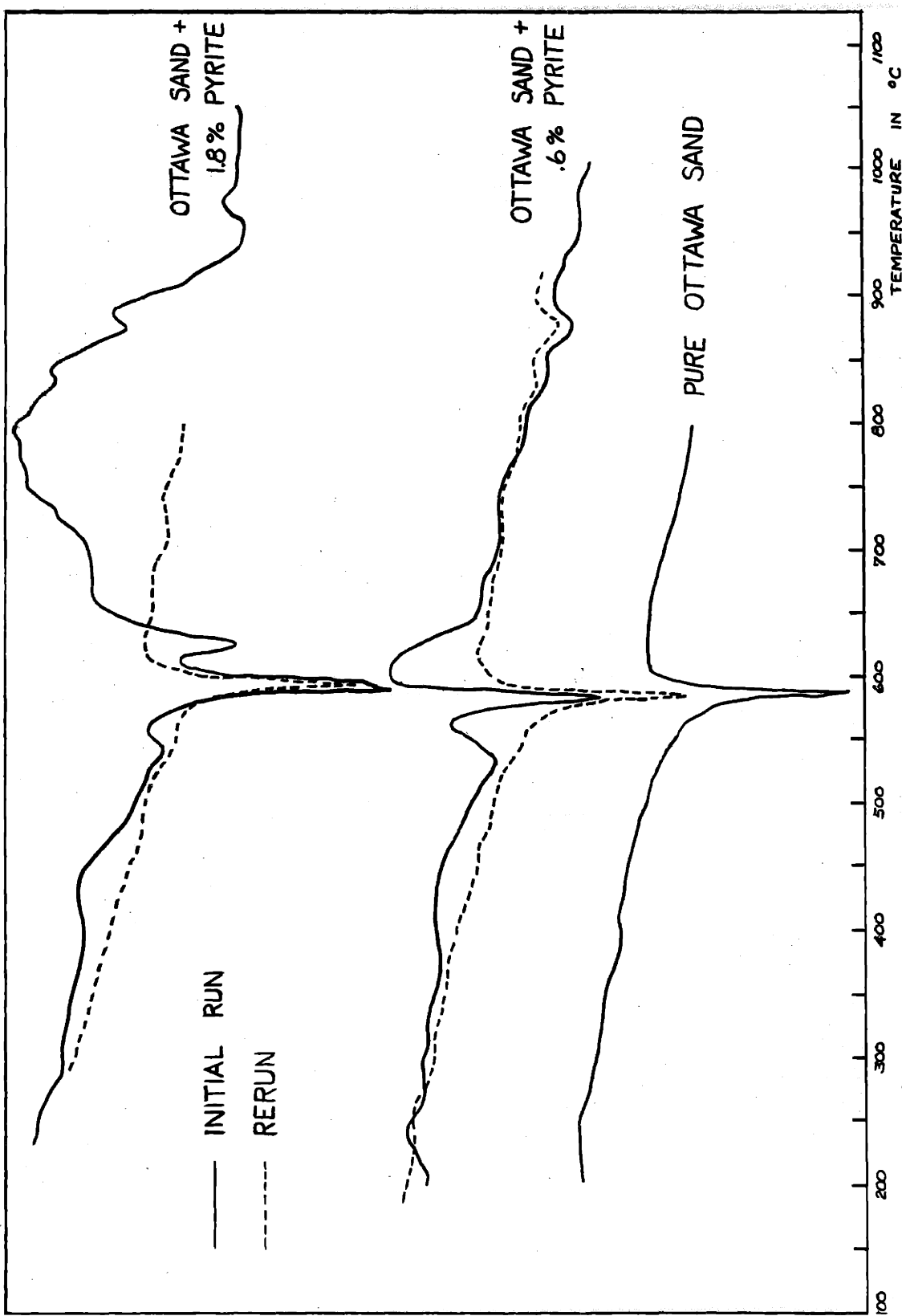
FIG. 5.1b DIFFERENTIAL THERMAL ANALYSIS OF MIXTURES CONTAINING PYRITE

Section II. Results of analysis of natural rock samples.

We now consider some of the experimental results on natural rock samples. As mentioned in the introduction, our primary purpose was to investigate the apparently anomalous samples. Many of the investigated samples turned out not to be anomalous, in the sense we define it, but they are included in the discussion as examples of our experimental approach.

Group I: Sedimentary Samples Containing Carbonaceous Material

This group consists of well core samples from the Muddy Sands, a part of the Dakota Sandstone sequence. They are dirty sands and shales with some carbonaceous material. The sample descriptions and the results of the polarization measurements are listed in Table 5.1. Several of these samples contained appreciable amounts of carbon, readily observed in the hand specimens. Its presence was confirmed by spectrographic analyses kindly carried out by Dr. Dennen and the results of these analyses in weight per cent of carbon are listed in the above table also. No pyrite was visible in samples 7001, 7009, 7010 under the binocular microscope. DTA analyses were made on 7009 and 7010 and these indicated a slight amount of clay in 7009 and no clay in 7010.

In view of their appreciable carbon content, these samples cannot be considered anomalous since carbon is probably a fairly good electronic conductor.

Several samples of this suite contained swelling clays and unfortunately could not be measured using our pre-

TABLE 5.1

GROUP I: SEDIMENTARY SAMPLES CONTAINING CARBONACEOUS MATERIAL

SAMPLE	f(10)	p/2π	mf(10)	mvs/v	mfθ	DESCRIPTION
7001	.5‰			.2	16 69 20	Calcareous silt and shale Swelling clay.
7002	2.5	48	52	25.	14 22 38	Dirty sand. Possible carbon, pyrite.
7003	6.2	22	282	8.8	0 30 31	Alternating sand and shale.
7007	6.6	30	220	68.7	10 10 19	Dirty sand, probably glauconitic. 1.1‰ carbon. No pyrite.
7009	5.0	42	119	57.6	9 19 34	Sand with shale and Carbonaceous material. .48‰ carbon. No pyrite.
7010	11.5	97	119	100.9	9 16 30	Dirty sand, .85‰ carbon. No pyrite.
7012	<.5				9 19 31	Shaly sand. Swelling clay.

Average mf θ of 7002, 3, 7, 9, 10.

sently employed techniques. The two samples containing swelling clay which we could measure, 7001 and 7012, had very small frequency effects. The clay in these samples is not distributed uniformly throughout the samples but instead occurs in distinct pods. Possibly the individual clay particles within these pods are very well connected and no alternating zones are formed. Another possibility is that the clay sizes are so small that the frequency effects are pushed to much higher frequencies than we used.

Group II: Sedimentary Rock Samples

This group of samples, supplied to us by the Atomic Energy Commission, consists of core samples from drill holes in Edgemont, South Dakota.

Several of these samples have important polarization effects. Pyrite was easily identified in sample 9001 but the other samples did not contain obvious pyrite though slight rusting was observed on several of them after soaking. DTA analyses were carried out on several of these samples to determine the clay content.

A summary of the polarization measurements is presented in Table 5.2 and the thermograms are shown in Figure 5.2.

The thermogram for 9001 shows only a pyrite peak and a quartz peak on the rerun. The pyrite in this sample was easily observed in the hand specimen.

Samples 9002 and 9007 show only a quartz peak on their thermograms. There is a slight indication of an exothermic

TABLE 5.2

INDUCED POLARIZATION RESULTS AND MINERALOGICAL ANALYSES OF GROUP II SEDIMENTARY SAMPLES

| SAMPLE	f(10)π	p/2πmf	(10)mfθ	mvs/v	DESCRIPTION	DTA	HEAVY MINERALS
9001	1.242	42	575 1	154	Fine sand, pyrite, iron stains.	Qtz. plus pyrite	2% pyrite
9002	1.061	32	190 6 / 8 / 16	40	Medium grained sandstone.	Qtz. plus .5% pyrite.	.2% pyrite
9007	1.047	54	87 11 / 22 / 35 / 11 / 14	52	Medium grained sand, slight pyrite.	Qtz.; pyrite?	.1% pyrite
9009	1.056	66	85 6 / 9 / 14	35	Medium grained sand, iron stains		.2% pyrite
9010	1.129	153	84 5 / 12 / 22	118	Coarse sand, iron stains	Qtz. plus 1% pyrite	.2% pyrite
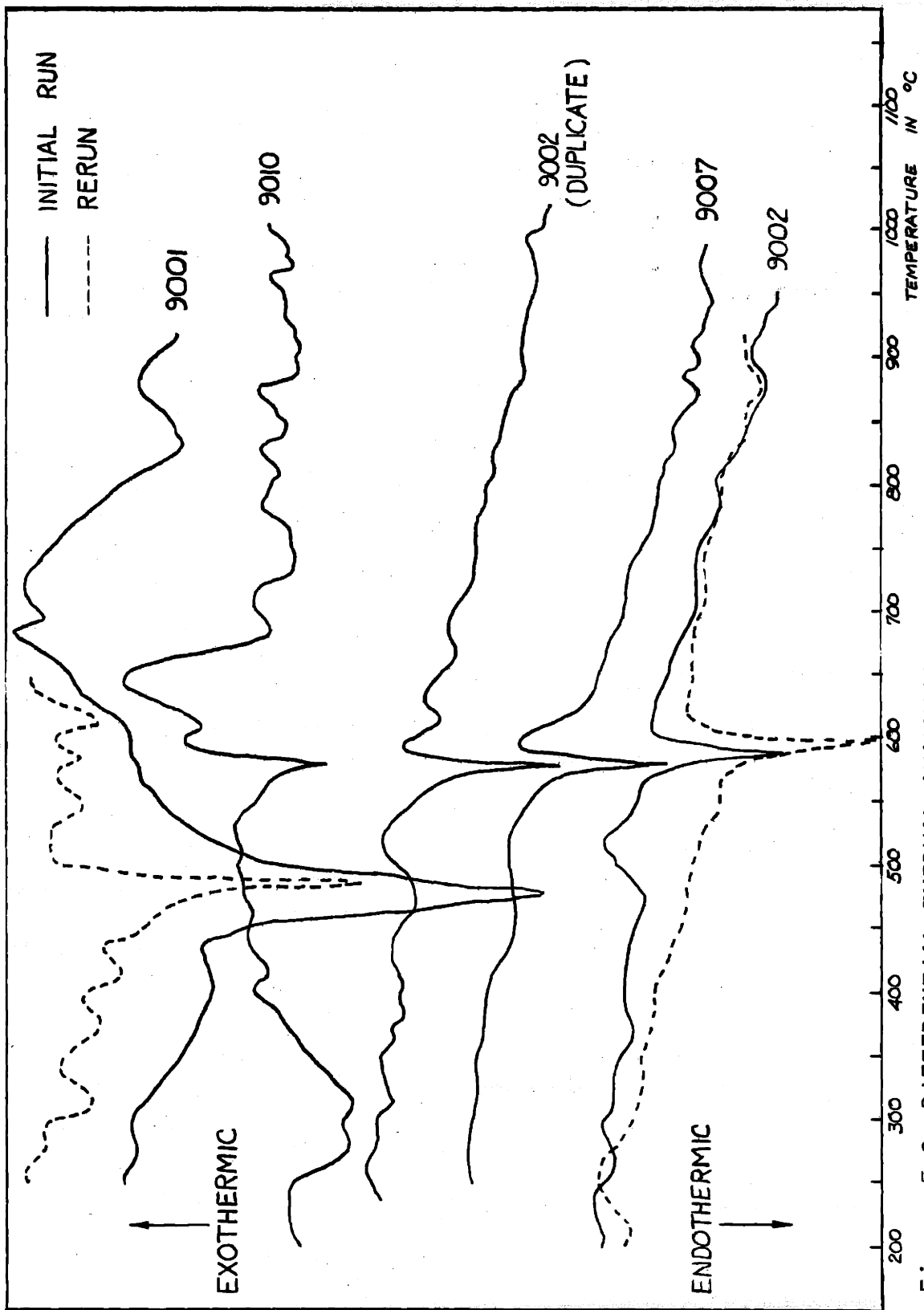
Figure 5.2 DIFFERENTIAL THERMAL ANALYSIS RESULTS OF GROUP II.
SEDIMENTARY SAMPLES.

effect which, if it were due to pyrite, would correspond to less than .5‰.

Sample 9010 shows a much more definite exothermic reaction corresponding to about 1‰ pyrite.

Heavy mineral analyses were attempted on several of these samples. The percentages of heavy minerals found are very similar to those listed above for the pyrite content according to the DTA. Unfortunately, however, an appreciable amount of the sample was lost in the "fines" during the separation. The fractionation occurring in these fines between the pyrite and the quartz is unknown and may be appreciable, the result being that the pyrite content is greater than that measured in the heavy mineral analyses.

None of the above samples show any indication at all of clay mineral content on the thermograms and it must be concluded that their polarization effects are due solely to their pyrite content. It appears that it is possible to obtain metal factors of 100 to 200 with less than .5‰ pyrite by weight. These results are in disagreement with results presented by Anderson and Keller (1958) in an abstract. They found that the polarization effects of pyritic bearing sandstones could be separated from those of non-pyritic bearing sandstones only when the pyrite content approached 10‰ by volume which is nearly 20‰ by weight. The reason for this sharp disagreement is not known and further comment will be withheld until it is possible to compare respective experimental techniques.

The results from this suite illustrate the difficulty which we are going to encounter in proving that pyrite is not responsible for polarization effects observed in a given sample. In order to do this we must be able to detect the presence of pyrite at concentrations of .2 to .5‰.

Group III: Altered Volcanic Rocks

This group consists of samples of several igneous rock types from a southwestern porphyry copper district. The major rock types included are basalts, andesite, quartz latite, and tuffs. Most of these rocks have undergone some alteration.

The majority of these rocks show little apparent mineralization though there are occasional traces of pyrite and native copper in some of them in amounts difficult to find in the hand specimens, even under the binocular microscope.

The most interesting rocks in this group are the crystal lithic tuffs. These rocks have extremely minor amounts of mineralization apparent but their polarization effects are quite important, some metal factors being as much as 500. The assembled data on the crystal lithic tuffs is listed in Table 5.3. Observe that the conductivities are rather high, accounting in part for the high metal factors, but in addition the frequency effects are also large, some being as much as 20-30‰.

DTA were run on several of the samples in order to investigate their clay content. The thermograms are shown in

TABLE 5.3

SAMPLE	p/2π	f(10)	mf(10)	mfθ	t⁺	%Cu	%Fe	%S	DESCRIPTION
7111	145	19	132	9 24 38		.015	1.2	0.13	Fragments of basalt in tuffaceous matrix. Not mineralized. Reworked by water.
7117	164	8	47	12 26 34 38	.51	.01	1.3	.06	Fragments of andesite in tuffaceous matrix.
7120	870	5	5	2 12 18					Tuff, crystal, silicifed, sericitized, partially welded. Minor fragments. Fractures stained with limonite. Minor specularite. Very slightly mineralized.
7124	38	9	240	13 23		.005	1.6	0.14	Fragments andesite and basalts of various shapes and sized in fine grained tuffaceous matrix. No mineralization, reworked by water.
7129	44	20	455	13 23 35 46	.72	.01	1.3	.04	Andesite fragments in tuffaceous matrix. Partially reworked by water.
7130	35	21	600	13 21 32		.01	1.5	.05	Same as 7129.
7131	137	5	36	11 26 45					Crystal Lithic Tuff. Slightly magnetic.
7132	133	6	45	13 24 33		.02	1.0	.09	Same as 7131.
7133	28	3	107	15 19 22		.01	1.1	.14	Fragments of light and dark, fine grained to aphanitic andesite.

TABLE 5.3 (Continued)

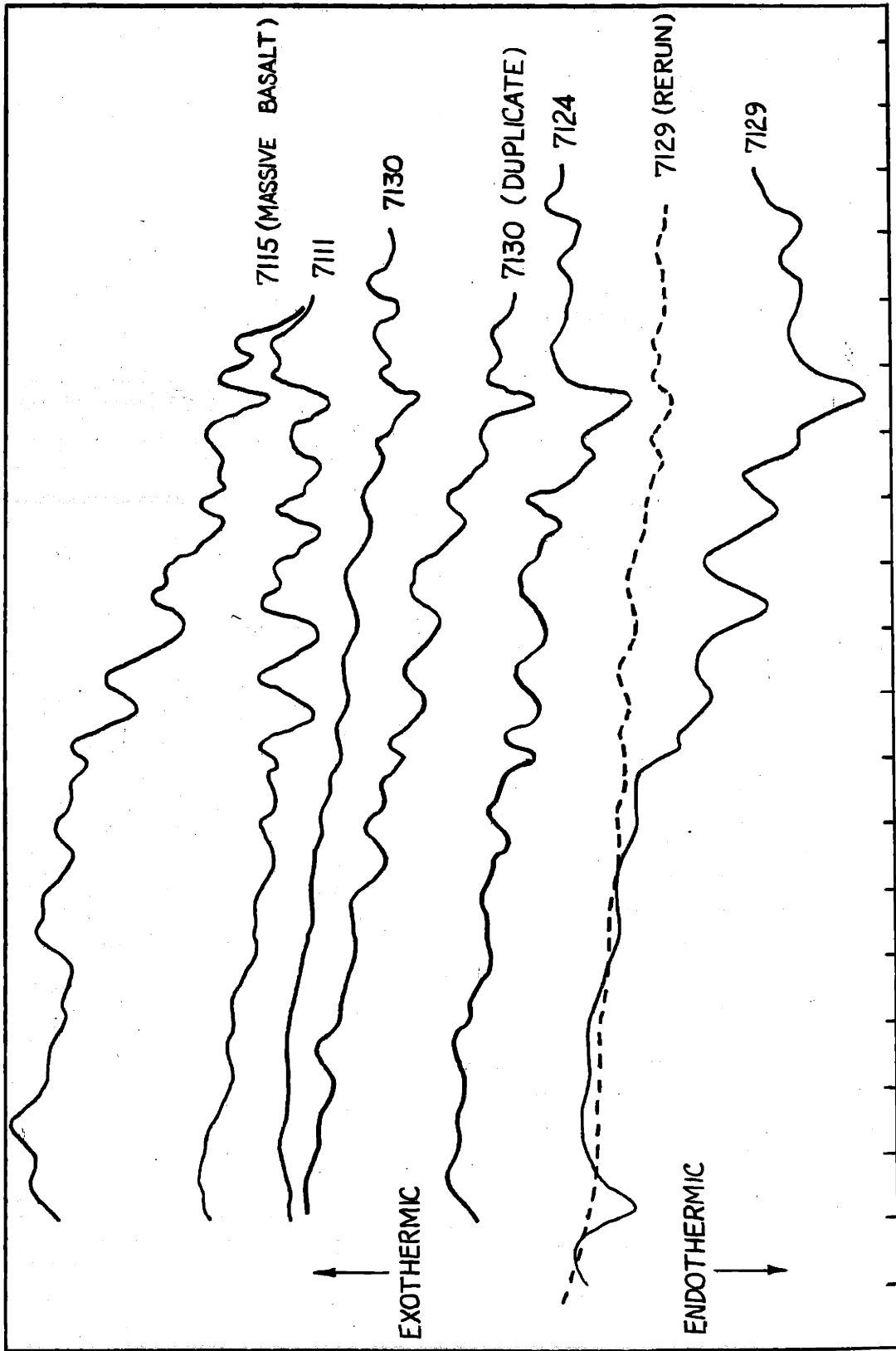| Sample	p/2π	f(10)	mf(10)	mfθ	t+	%Cu	%Fe	%S	DESCRIPTION
7134	30	2	67	11 22 32					Same as 7133
7136	59	8	136	6 17 28		.01	.8	.13	Andesite fragments in tuffaceous
7138	140	5	36	14 23 34		.01	1.3	.07	Brownish mottled andesite and light brown-grey andesite fragments in tuffaceous matrix.
7139	193	8	41	13 20 27					Same as 7138

FIGURE 5.3 DIFFERENTIAL THERMAL ANALYSIS RESULTS OF GROUP III.
ALTERED VOLCANIC ROCKS

Figure 5.3.   These thermograms exhibit no obvious clay peaks though there are some small indications that may correspond to 5-10‰ clay content if they are real peaks and not noise. All the thermograms exhibit these same features so it seems quite possible that they are real clay peaks.

For comparison, the thermogram for another rock from this suite which is not a crystal lithic tuff but rather a massive basalt is shown. This sample had very small polarization effects (frequency effect = 1‰, m.f. = 24) yet its thermogram is quite similar to the others indicating about the same clay content. These results are quite puzzling. It is known from the theoretical studies that the distribution of the clay minerals is much more important than the actual concentration and this may be the determining factor in these samples. Increasing the length ratio, A, and hence decreasing the concentration of clay material leads to increased maximum effects over quite a range of A.

There is also a possibility that there may be selective properties in these samples which are due to the presence of fine grained material which is not a true clay mineral. The presence of these selective properties should be revealed by transference measurements and therefore we made these measurements on some of the tuff samples. The method used for these measurements has been discussed in a report from this project (Madden et al, 1957) and will not be entered into here. The results of the transference measurements are listed in Table

5.3 also. Because of errors in the experimental work, there may be errors of .05 in these values.

The transference values obtained are much too small to account for the measured frequency effects. In fact the transference measurements for 7117 gives $t^+ = .5$. From the results of Chapter II (Figure 2.2) we see that this would predict no effect at all, while, actually, 7117 has a large effect ($f(10) = 8$‰.mf (10)=47). This result rules out membrane effects unless we have the very unlikely situation existing wherein zones with anionic selective properties are in series with cationic selective zones. This situation cannot be detected by a steady state measurement and cannot be ruled out on this basis therefore. One way of obtaining information on this would be to study the anionic and cationic exchange capacities of the same sample. High values for both these exchange capacities would exist if such a situation were present. Anion exchange capacity data is rather scarce and to our knowledge no simultaneous measurements of both exchange capacities of the same sample have been made on this type of material. We did not have sufficient time to pursue this approach any further.

Assays were made on some of these samples for Cu, Fe and S content and these results are listed in Table 5.3 . If all the S is in the form of pyrite, the content of pyrite is less than .2‰ by volume or .4‰ by weight in all these samples. This ties in with the fact that pyrite peaks were not observed

on the DTA results either. The iron content cannot be accounted for solely by the pyrite content and there must be a certain amount of magnetite and hematite or other iron minerals present also. Simple magnetic measurements revealed that these samples are slightly magnetic but the magnetite content must be quite small.

Other samples from this suite were found to be much more magnetic than the crystal lithic tuffs even though they had much smaller polarization response so we cannot simply attribute these effects to the magnetite content.

In light of these facts we are forced to conclude either that the alternating membrane property situation exists or that the small amounts of pyrite and magnetite are responsible for the polarization effects. If the latter answer is accepted, we must accept as a corollary the tremendous variation in polarization effects of metallic minerals depending on their mode of incorporation in the rock. This variation is especially significant in the concentration range of about 1‰.

These samples must still be considered anomalous.

Other Samples

Various other samples suspected of containing clays were studied but in all cases where large effects were present it could not be shown that the metallic mineral content was appreciably less than 1‰ and therefore, because of our previously mentioned results, we could not rule them out as the

source of the measured effects.

In natural samples where clays were definitely present, we very rarely measured frequency effects of more than 5‰ which is far from the theoretical maximum for membrane effects. Most of these effects were studied at low frequencies (less than 10 cps) but on checks made at higher frequencies on some samples less than 5‰ change was found between 100 and 1000 cycles per second which is the upper limit of the equipment which we used. A conservative upper estimate for the actually observed frequency effects in clay bearing rocks is therefore about 10 to 15‰.

CHAPTER VI

CONCLUSIONS

In the introductory chapter of this thesis, three problems relating to polarization in clays were posed. We will now review these questions and the answers which we have found for them.

With regard to the existence of polarization effects in clays, the experimental work reported in Chapter IV on artifically compacted clay systems has shown that significant polarization effects do exist in these materials. The frequency effects can be quite large. The metal factors also can be quite large in some cases, though they never reach the values found in well mineralized rocks. They can cause considerable trouble as a background effect when, because of geometrical considerations, they constitute an important part of the total area sampled in an investigation.

Great difficulty has been experienced in showing, conclusively, that clays are responsible for polarization effects in natural rock samples. The major difficulty is that almost all the samples studied contained metallic minerals in concentrations of at least .2 to .5‰ and often more and these concentrations of metallic minerals have been found to be sufficient to produce significant polarization effects in many cases.

The problem of the variation of polarization with the distribution and mode of incorporation of metallic minerals in rocks remains quite puzzling. We have noted that sedimentary

144

rocks often seem to be most efficiently polarized by small amounts of metallic minerals but notable exceptions occur. The problem is no doubt tied up with the series resistance of the blocked paths which varies with the tightness of the sediment, but other factors must be important also. This problem is worth pursuing in more detail and might very well lead to some interesting results regarding the mechanisms of deposition of metallic ores and native metals in sedimentary rocks.

A physical model for polarization in membrane systems has been proposed. This model assumes the membrane to be made up of zones of alternating transference properties in series. The mathematical formulation for this model is simple and straightforward though the details of carrying out the solution are tedious. The solution yields an impedance of a type characteristically associated with diffusion processes. This impedance is characterized by dependence on the inverse square root of frequency. It is usually referred to as a Warburg impedance. The model predicts a maximum frequency effect of about 100% depending on the particular salt in the solution. This theoretical limit has been approached but never exceeded in the experimental investigations made on natural and artificial membrane systems.

This leads us finally to the most important question of whether or not there are any diagnostic parameters which will permit us to separate membrane caused polarization effects from metallic mineral caused polarization

effects. By diagnostic parameters we mean characteristics of the polarization phenomena which can be observed in actual measurements. Our early hopes centered about the study of details in the frequency spectra of the different mechanisms. It was for this reason that the theoretical model study was initiated for it was hoped that the results of this theoretical study would point to the diagnostic parameters. Simultaneously with the theoretical study on membranes, Mr. T.R. Madden made a study of the frequency behaviour of the impedance of metallic electrodes in electrolyte solutions also through use of a kinetic model. His study led to the postulation of several different equivalent circuits which would apply to this situation depending on the particular phenomena at the boundary. The experimental results on several pure metal electrodes and some well mineralized rock samples were fitted to the theoretical circuits and in most cases it was found that one of the most important elements in the circuit was associated with the diffusion phenomena occurring at the electrode in the presence of a well catalyzed reaction. We have already seen that the diffusion phenomena is the important one in membrane polarization. Thus from a theoretical standpoint it does not seem too hopeful that the effects will be distinguishable, especially in natural samples where we always have a distribution of parameters which tend to decrease the sharpness of the overall response.

For an empirical approach to the problem, the laboratory and field data obtained on a large number of samples was studied in an effort to determine whether there were significant differences in the polarization effects. The actual paramemter which was chosen for comparison is the metal factor phase shift at the frequencies of .1, 1, and 10 cycles per second.

The metal factor phase was chosen rather than the phase shift of the total rock impedance because this avoids the problems associated with the dilution effects of the un-blocked parallel paths.

In Table 6.1 we have listed this data for several different rock types. Each listing is the result of an averaging over at least four and usually more samples of the given rocktypes.

TABLE 6.1

METAL FACTOR PHASE DATA FOR NATURAL ROCK SAMPLES

Sample	MFθ		
	10 cps	1 cps	.1cps
Altered quartz latites, some pyrite	18	26	38
Quartz latite porphyry, altered, slightly mineralized.	6	17	24
Gabbro, altered, serpentine, tremolite, magnetic, slight sulfides.	10	15	22
Ultrabasics, very conductive, very magnetic	46	45	50
Rhodesian copper ore.	18	27	41
Dakota sandstone, carbon, minor pyrite.	11	17	30
Crystal lithic tuffs, altered, very little mineralization.	11	22	33
Siltstone with native copper	12	18	19
Sandstone with about 1% pyrite	6	13	20
Mica	8	12	19
Kaolinite	9	14	22

There are significant differences in the metal factor phase between different rock types but, as yet we do not know what to make of the differences. Note that the samples containing clay have generally low values of the metal factor phase, but that some samples continaing pyrite also have low values.

It does not appear, on the basis of our experimental evidence obtained so far, that the effects of the different sources can be distinguished.

A more extended frequency range might show greater differences but the above range is that of practical interest and usefulness in field applications.

On the basis of the experimental results obtained in this research we can expand the table of typical metal factor values which was given in Chapter I.

TABLE 6.2

TYPICAL METAL FACTOR VALUES (10 cps.)

Granite	2
Basalt	2 - 20
Tuff	5 - 500
Slight Sulfides	1 - 300
Porphyry Coppers	100 - 10,000
High Magnetite	10 - 20,000
Heavy Sulfides	1000 - no limit
Dirty Sandstone and Limestone	2 - 100
Graphitic Sandstone and Limestone	15 - 300
Sandstones with sulfides < 2%	10 - 1000
Shales with sulfides	20 - 2000
Natural clays	0 - 1500
Kaolinite, artificially compacted	40 - 1800

From these results we observe that, with regard to
the metal factor parameter, clays may interfere with the
interpretation of metal factor results in the case of slight
sulfides, and some porphyry coppers but they cannot be mis-
taken for the high sulfides which are the usual targets of
induced polarization exploration. The metal factor still
appears to be the best diagnostic parameter of polarization
effects.

BIBLIOGRAPHY

Anderson, L.A., and Keller, G. V., 1958, Induced polarization effects in pyrite-bearing sandstones: Abstract only, A.I.M.E. Feb. 1958 Meeting. No. 5820P7.

Bleil, D.F., 1953, Induced polarization: A method of geophysical prospecting: Geophysics, v.18, p. 636-661.

Bull, H. B., 1935, A critical comparison of electrophoresis, streaming potential, and electroosmosis: Jour. Phys. Chem., v. 39, p. 577.

Casagrande, L., 1952, Electro-osmotic stabilization of Soils: Jour. Boston Soc. Civil Eng., v. 39, p. 51.

Chang, H.C., and Jaffe, G., 1952, Polarization in electrolytic solutions, part1. theory: Jour. Chem. Phys., v. 20, p. 1071-1077.

Dakhnov, V. N., Latishova, M. G., and Hyapolov, V.A., 1952, Well logging by means of induced polarization (electrolytic logging): Promislovaya Geofizika, p. 46-82.

DeGroot, S.R., 1952, Thermodynamics of irreversible processes: New York, Interscience Publishers, Inc.

Denbigh, K. G., 1951, The thermodynamics of the steady state: London, Methuen and Co. Ltd.

Dennen, W.H., 1957, Spectrographic determination of carbon in sedimentary rocks using direct current arc excitation: Spectrochimica Acta, v. 9, p. 89.

Eckart, C., 1940, The thermodynamics of irreversible processes, II fluid mixtures: Phys. Rev. v. 58, p. 269-275.

Faraday Society, 1956, Membrane phenomena, A General Discussion of the Faraday Society: 288 pages.

Glasstone, S., 1954, An introduction to electrochemistry: New York, D. Van Nostrand Co. Inc.

Grahame, D.C., 1947, The electrical double layer and the theory of electrocapillarity: Chem. Rev., v. 41, p.441.

Grahame, D.C., 1952, Mathematical theory of the faradaic admittance: Jour. of Electrochemical Society, v. 99, p. 370C-385C.

Henkel, J.H., 1958, Some theoretical considerations on induced polarization: Geophysics, v. 23, p. 299-304.

Henkel, J.H., and Van Nostrand, R.G., 1957, Experiments in induced polarization: Mining Engineering, March 1957. AIME Trans, v. 9, p. 355-359.

Juda, W., and McRae, W.A., 1953, U. S. patent 2,636,851.

Keilson, J., 1953, More exact treatment of the equations describing dielectric relaxation and carrier motion in semiconductors: Jour. of Applied Physics, v. 24, p. 1198-1200.

Kermabon, A.J., 1956, A study of some electro-kinetic properties of rocks: M.S. Thesis (unpublished) M.I.T. Dept. of Geology and Geophysics.

Kopp, O.C., and Kerr, P.F., 1957, DTA of Sulfides and Arsenides: The American Mineralogist, v. 42, p. 445.

Kruyt, H.R., editor, 1952, Colloid science: Amsterdam, Elsevier Publishing Company.

Kunin, R., and Myers, R.J., 1952, Ion exchange resins: New York, Wiley.

Lambe, T.W., 1951, Differential thermal analysis: Proceedings Highway Research Board, p. 621.

Lambe, T.W., 1958, The structure of compacted clay: Journal of the Soil Mech. and Foundation Division, Proc. of the Amer. Soc. of Civil Engineer, SM2 p. 1854-1.

Macdonald, J.R., 1953, Theory of ac space charge effects in photoconductors, semiconductors, and electrolytes: Physical Review, v. 92, p. 4-17.

Mackenzie, R.C., editor, 1957, The differential thermal investigation of clays: London, Mineralogical society.

Madden, T.R., Marshall, D.J., Fahlquist, D. A., and Neves, A.S., 1957, Background effects in the induced polarization method of geophysical exploration: Annual Progress Report, U.S. Atomic Energy Commission, Division of Raw Materials, Contract AT(05-1)-718.

Madden, T.R., and Marshall, D.J., 1958, A laboratory investigation of induced polarization: Interim Report, U.S. Atomic Energy Commission, Division of Raw Materials, Contract AT(05-1)-718.

Madden (1959) (Thesis, M.I.T. Department of Geology and
    Geophysics to be presented).

Mangold, G.B., 1958, Subsurface geology in petroleum explora-
    tion. A symposium edited by J.D. Haun and L.W. LeRoy,
    Colorado School of Mines.

Martin, R.T., 1958, Clay-carbonate-soluble salt interaction
    during differential thermal analysis: (in press).

McKelvey, Southwick, Spiegler, and Wyllie, 1955, The
    application of a three element model to the s.p. and
    resistivity phenomena evinced by dirty sands: Geophysics,
    20, 913.

Nachod, F.C., editor, 1949, Ion exchange: New York, Academic
    Press Inc.

Olsen (1959) (Thesis, M.I.T. Department of Soil Mechanics,
    to be presented).

Sauer, Southwick, Spiegler, and Wyllie, 1955, Electrical con-
    ductance of porous plugs, ion exchange resin-solution
    systems: Industrial and Eng. Chem., 20, 2187.

Staverman, O.J., 1952, Non-Equilibrium thermodynamics of
    membrane processes: Trans. Far. Soc., v. 48, p. 176-185.

Uhri, D., (personal communication 1958).

Vacquier, V., Holmes, C.R., Kintzinger, P.R., and Lavergne, M.,
    1957, Prospecting for ground water by induced electrical
    polarization: Geophysics, v. 22, p. 660-687.

Wirtz, K., 1948, Platzwechselprozesse in flussigkeiten,
    Zeit. f. Naturforschung Band 3A, p. 672-690.

Wirtz, K., 1948, Kinetische theorie der thermoosmose: Zeit. f.
    Naturforschung, Band 3A, p. 380-386.

Wyllie, M.R.J., and Southwick, P.F., 1954, An experimental
    investigation of the S.P. and resistivity phenomena in
    dirty sands: Jour. Petroleum Technology, 6, 44.

BIOGRAPHY

The author, Donald James Marshall, was born in
Marlboro, Massachusetts on April 14, 1933. He attended
grammar school and high school in Marlboro. In September,
1950, he enrolled at M.I.T. and was graduated in 1954 with
a B.S. in geophysics. In September, 1954, he enrolled at
California Institute of Technology and received an M.S.
degree in geophysics in June 1955. Since then he has been
a candidate for a Ph.D. degree in the Department of Geology
and Geophysics at M.I.T.

During the academic year 1957-1958 he was the re-
cipient of the Standard Oil Co. of California Fellowship.

The author's experience in geophysics includes one
summer with Phelps Dodge Corporation carrying out gravity
surveys, two summers with Bear Creek Mining Company per-
forming electromagnetic surveying, and one summer with the
Geophysics Branch of the U S. Geological Survey.

The author is a member of the Society of Exploration
Geophysicists.

In September, 1954, he was married to Barbara S.Allen.
A son, Allen, was born in 1955.

In October, 1958, the author accepted a position with
Nuclide Analysis Associates in State College, Pennsylvania.

153